2011

Lasing behavior of an active NIM-PIM directional coupler

Riffat Ara

Rochester Institute of Technology

College of Applied Sciences and Technology

Electrical Computer and Telecommunications Engineering Technology (ECTET)

Lasing Behavior of an Active NIM-PIM Directional Coupler

Riffat Ara

May 13, 2011

Rochester, NewYork, USA

A Research Thesis Submitted in Partial Fulfillment of the Requirements

for the degree of

Masters of Science in Telecommunications Engineering Technology (MSTET)

Thesis Supervisor

Professor Dr.Drew Maywar

Department of Telecommunications Technology

College of Applied Sciences and Technolgy

Rochester Institute of Technology

Rochester, NewYork

Approved by:

Dr. Drew N. Maywar

Thesis Advisor, Department of Electrical and Telecommunications Engineering Technology.

Dr. Warren L. Koontz

Program Chair, Department of Electrical and Telecommunications Engineering Technology.

Professor Ron G. Fulle

Committee Member, Department of Electrical and Telecommunications Engineer-

ing Technology.

Professor William P. Jhonson

Committee Member, Department of Electrical and Telecommunications Engineering Technology.

Professor Mark J. Indelicato

Committee Member, Department of Electrical and Telecommunications Engineering Technology.

Dedicated to my parents

Abstract

Negative index materials are a subclass of metamaterials which are materials having properties that are not found in nature. Present day research regarding metamaterials indicates that they possess remarkable behavior. This thesis is focused on a metamaterial-based photonic directional coupler employing a negative index material (NIM) in one of its waveguides while the other waveguide consists of a positive index material (PIM). A NIM-PIM directional coupler (DC) exhibits optical feedback even without any actual traditional resonator structure. This feedback exists because of the NIM employed in one of the structure's waveguides. The ability of a NIM-PIM DC to propagate light in the backward direction indicates the possible use of NIM-PIM DC for any optical component requiring optical feedback.

We seek to study, for the first time, a laser based on a NIM-PIM DC. Coupled-mode equations and corresponding solutions have been devised for an active NIM-PIM DC in which optical gain is introduced. An analysis of the transmittivity and

reflectivity for the case of a resonator-type optical amplifier has been carried out. Lasing behavior of an active NIM-PIM directional coupler has also been investigated for the first time. We do so using two approaches: the transmittivity and the transcendental eigenvalue equation which we derive for the first time. Throughout the thesis, a distributed feedback (DFB) resonator and standard PIM-PIM DC have been detailed for comparison.

Our equations and solutions are general enough to consider a range of optical gain configurations. In particular, we study three important cases of NIM optical gain: 1) equal to PIM gain; 2) zero gain; 3) negative gain, i.e. loss. The results show that that it is possible to achieve lasing with a NIM-PIM DC similar to that of an a DFB laser if the same amount of gain is introduced in both of its waveguides. It is also possible for the device to lase in the case of gain in the PIM waveguide and no gain in the NIM waveguide. The more practical case involving loss in the NIM waveguide has also been investigated and found to naturally exhibit the much sought-after case of single mode lasing operation. Thus, this research lays the foundation for a new kind of single-mode laser.

Acknowledgments

First and foremost, I thank God, the almighty for making me capable of accomplishing all the major milestones of my life with honor and success.

I would like to express my gratitude for all the assistance and guidance that was offered by different people through the course of this project.

I, sincerely appreciate the help and supervision from my thesis advisor professor D.N.Maywar. Without constant encouragement, patience and support from him, it would have been really impossible to sail through towards the completion of this thesis.

Special thanks to professor G.P.Agrawal (University of Rochester, NY) and professor Natalia Litchinister (University at Buffalo, NY) for their insightful help with the subject matter.

I want to thank all the staff, faculty members of ECTET and my fellows; they were always there to assist and guide, from course work to thesis completion. Finally, a special thanks to my ever loving and supporting parents and family. Thank

you for always believing in me and bringing me to where I am today.

Contents

List of Figures

CHAPTER 1

INTRODUCTION

1.1 METAMATERIALS

Metamaterials is a field with many exciting possibilities and can be rightly termed as one of the hottest areas of present day optical research.

Metamaterials are artificial materials having properties that are pre-fabricated and are not found in naturally occurring materials. "Meta" is a Greek term which means, "beyond" hence, the term meta-material indicates something that does not occur naturally i.e. man-made. These materials are very small structures and allow for manipulation of the trajectory of light or acoustic waves through a material [1].

In the laboratory, metamaterials are fabricated as periodic structures. Each such structure is a meta atom or meta molecule. Each structure is carefully lined up to alter the object's properties and provide custom features. These may include

properties like permeability and permittivity, affecting how waves are transmitted across the material. The size of each structure depends on the electromagnetic radiation it interacts with. Thus materials employed for microwave applications will have a structure size on the millimeter scale while photonic metamaterials will have a structure size smaller than the wavelength of light i.e. in the nano meter range [2]. Since the structure size is very small, metamaterials may appear as homogeneous to the interacting wavelength [1].

Metamaterials are used in the research fields of imaging and lithography. They are also being studied for more efficient data storage, computer chips and much lighter, faster and durable microprocessors. Their special features may be exploited to produce special antennas and enhanced transmission lines etc [3].
Some of the challenges encountered in fabricating metamaterials include the fact that the period of the material has to be in the sub wavelength region. Current lithographic techniques are usually insufficient to satisfy this condition. However, advancement in some of the fabrication procedures has greatly helped in overcoming such limitations. Modern fabrication methods like direct laser writing and nano imprint lithography can also be employed [3]. Metamaterials usually exhibit high optical losses [2]. Such limitations maybe reduced by the introduction of gain medium or through some other novel approaches [3].

Among the various classes of metamaterials, negative index materials (NIMS)

have received considerable importance both from researchers and engineers.

1.2 NEGATIVE INDEX MATERIALS (NIMs)

Refraction is one of the most important behaviors of light and can be described as the bending of light. Refraction explains certain phenomena like how a small coin placed in a pond of water appears closer to the surface than it actually is to an observer standing near the pond.

Every medium has an index of refraction. When light travels from one medium to another, a change in its trajectory can occur due to difference in the refractive indexes of the two mediums. If the light enters from a rarer medium to a denser medium, it bends towards the normal. The reverse is true when traveling from denser to a rarer medium. The normal can be defined as an imaginary line perpendicular to the interface. Naturally occurring materials possess a positive index of refraction. This fact however, does not mean that a material cannot possess a negative index of refraction. A medium with a negative index of refraction results in bending light the 'wrong way'. Such materials are known as negative index materials (NIM) and have negative permittivity and negative permeability.

The phenomenon of negative permittivity and permeability was investigated by a Russian scientist Victor Veselago around four decades back [5]. Veselago reported that such materials possess anti parallel Poynting vector and phase veloc-

ity. Thus it can be stated that in a negative index material energy flows in the same direction as the conventional positive index materials. However, their phase velocities are oppositely directed. Negative index materials (NIMs) do not occur in nature and are a classified as a subclass of metamaterials.

The concept of NIMs having negative 'n' has a revolutionary impact on present day optical research. The fact that index of refraction can be negative, has made researchers consider revising basic formulae of optics. More recent contributions are from John Pendry who predicted the famous NIM based superlens, besides making other significant contributions to this field [6]. Some of the interesting applications of negative index materials include invisibility cloaks, optical nanolithography, super lens, antennae with advanced properties of reception and range and enhancing MRI.

1.3 NIM-PIM DIRECTIONAL COUPLERS

The proposed research for this thesis aims at understanding the performance of a photonic directional couplern(DC) in which one of its waveguides is a NIM and the other waveguide is a positive index material (PIM), which we call a NIM-PIM DC. Such couplers with opposite index materials result in backward propagation of light, establishing a behavior similar to that of fiber Bragg grating, where light is reflected back. Thus a NIM-PIM DC acts like a resonator, which is remarkable

since there is no resonator structure in the DC.

The ability of a NIM-PIM photonic coupler to propagate light in the backward direction indicates the possible use of NIM-PIM waveguides in enhanced optical components. NIMs can be used for generating certain linear and non-linear optical phenomena including optical parametric amplification (OPA) and optical bi-stability [4] [8] [9]. Directional couplers with negative index material (backward coupling) have been reported by Alu, Engheta and Litchinitser. While Alu and Engheta reported on the linear performance of a NIM-PIM directional coupler [7], Litchinitser focused on its non-linear performance [8]. Present day research regarding optical NIM-PIM coupling phenomena indicate that it could result in optical components with capabilities such as optical signal processing, optical memory, buffering and optical switching and routing.

1.4 OVERVIEW OF THESIS

Chapter two concentrates on solving equations and analyzing the behavior of different types of passive directional couplers. Section one introduces the coupled-mode equations which have been developed describing the propagation of light through the linear optical DC. These equations are solved for the conventional PIM-PIM DC. Expressions for power exchange at the output ports are calculated and analyzed with the help of matlab plots. Section two focuses upon a linear

DC comprised of a NIM-PIM waveguide structure. The dispersion relation along with a solution for the transmitted and reflected spectrum using the coupled-mode equations for NIM-PIM DC is analyzed in the same section. Section three explores a conventional distributed feedback (DFB) resonator structure along with its governing equations and solutions, which are found to be quite like the NIM-PIM DC case.

Chapter three concentrates on solving equations and analyzing the behavior of an *active* NIM-PIM DC for the first time. This chapter also demonstrates the effect of introducing equal and variable amount of gain in the two waveguides. Expressions for transmittivity and reflectivity are derived using the coupler boundary conditions. Variation in the gain in one or both the waveguides and its effect on the transmittivity peaks is investigated. Section three deals with the addition of gain to the conventional DFB resonator and derives the solutions accordingly.

Chapter four investigates and analyzes the lasing behavior of an active NIM-PIM DC. Coupled-mode equations including gain are solved and investigated using the lasing boundary conditions. The well-known transcendental eigenvalue equation for an active DFB resonator is derived. A numerical solution is obtained in order to determine the values of gain and detuning at lasing. All of this analysis is modeled in Matlab. Section two of this chapter involves solving the coupled-mode equations using the lasing boundary conditions for the active NIM-PIM DC

for the first time. Lasing behavior of the coupler for the case when both the waveguides have equal gain is modeled and compared with the lasing behavior of the active DFB resonator. Section three addresses unequal amounts of gain in NIM and PIM waveguides. In particular, we study the conditions for single-mode operation of a NIM-PIM DC laser.

CHAPTER 2

PASSIVE NIM-PIM DIRECIONAL COUPLER

2.1 OPTICAL WAVEGUIDES AND COUPLED-MODE THEORY

An optical waveguide constitutes the basic physical structure in integrated photonics. A waveguide guides the optical waves by essentially confining it within its boundaries. This confinement is achieved by the principle of total internal reflection of light where a high index medium is surrounded by a medium with lower index of refraction.

A set of modes can be used to represent the electromagnetic waves travelling in a waveguide. A mode can be defined as the transverse distribution of the electro-

magnetic field intensity passing through the waveguide. Optical waveguides can be classified on the number of supported modes i.e. single mode or multimode, the refractive index (gradient, step-index) and the geometry of the waveguide, i.e. the number of dimensions in which the light is confined [10].

Structures that confine light in a single dimension are classified as the planar waveguides. Channel waveguides confine light in two dimensions [10].The structure that we consider in this thesis are comprised of channel waveguides.

Coupled-mode theory explains the energy transfer between modes of a waveguide. As mentioned earlier, a waveguide structure can support a number of modes. These modes are independent of each other while propagating across the structure. However, if some sort of perturbation is introduced, then the modes are no longer independent and may be mutually coupled i.e. exchanging energy. In order to understand the propagation of such coupled waveguide modes, Maxwell's equations along with exact boundary conditions can be employed. Though this method is more accurate and provides an exact solution, it is fairly tedious and complicated [11].

Perturbation theory is another approach to explain the mentioned phenomena. It may provide approximate but fairly accurate results and is much simpler and more widely used. If an isolated waveguide is replaced by a system of waveguides i.e. two or more waveguides placed close to each other, their mode structure

is disturbed. The new modes generated by the perturbation are different from the original modes and exhibit modified propagation constants. These modes propagate along the waveguide and interact with each other to exchange energy. This exchange of power is more significant when the interacting modes have the same phase velocity.

This phenomenon of exchange of power between a coupled waveguide system has led into the design of many components of optical communication systems. Such components include optical couplers, optical filters, optical modulators and switches.

2.2 PASSIVE PIM-PIM DIRECIONAL COUPLER

2.2.1 Directional Coupler

A directional coupler (DC) is a device that couples or splits several optical inputs. A 3dB photonic directional coupler as shown in Figure 2.1, allows light from one side to split equally and exit the opposite side. In Figure 2.1 two identical and single mode waveguides A and B are placed parallel to each other. Both these waveguides are composed of conventional positive index material and have forward propagating modes. Waveguide A has input energy introduced at $\zeta = 0$ which results in out1 and out2 at $\zeta = 1$. Such directional optical couplers are very

important in-line, passive components of modern fiber optic systems [12].

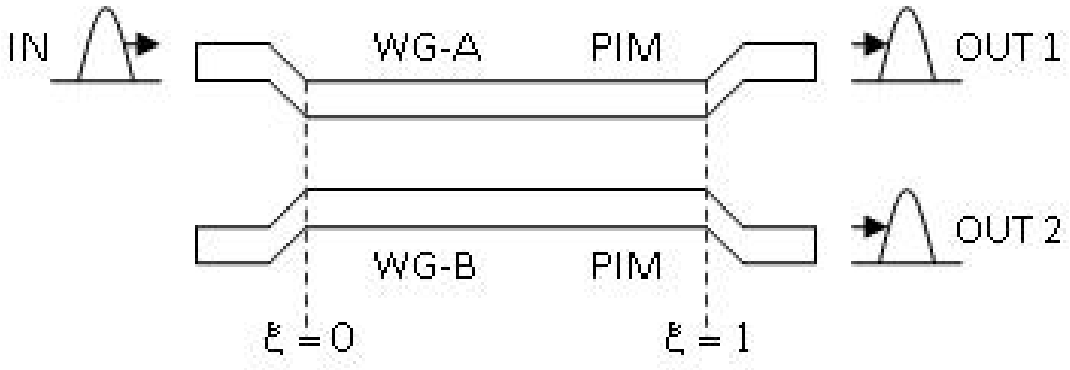

Figure 2.1: *PIM-PIM Directional Coupler*

Couplers can be symmetric or asymmetric depending upon the core of the two waveguides. In case of symmetric couplers, the two cores must be identical in all respects. The amount of coupling that takes place can be controlled by the diameter of the cores in the coupling region, the distance between the two cores in the coupling region, the length of the coupler, and the operating wavelength.

When two waveguides are placed close to each other, a coupling region is created between them. Within this coupling region, the mode fields of these waveguides overlap each other and create coupled modes which facilitates the exchange of power between the two waveguides at periodic intervals.

Optical couplers, currently in commercial use use the conventional positive index material (PIM-PIM) for each waveguide. In case of PIM-PIM DC the two modes are co-directional, resulting in forward coupling.

2.2.2 Coupled-Mode Equations and Generalized Solution

The coupled-mode equations for the passive PIM-PIM DC are [13]:

$$\frac{dE_a(z)}{dz} = i\kappa e^{-2i\Delta\beta z} E_b(z) \tag{2.2.1}$$

$$\frac{dE_b(z)}{dz} = i\kappa e^{+2i\Delta\beta z} E_a(z) \tag{2.2.2}$$

where κ is the coupling co-efficient, $\Delta\beta$ is the detuning between the two waveguides $\Delta\beta = \beta_1 - \beta_2$, $\beta_1 = \frac{2\pi}{\lambda_0} n_1$ is the wavenumber of light wave in the first waveguide, and $\beta_2 = \frac{2\pi}{\lambda_0} n_2$ expresses the wavenumber of light in the second waveguide. E_a and E_b represent the field in the forward and backward traveling modes respectively. Normalizing the equations above by introducing the quantity 'L' yields:

$$L\frac{dE_a(z)}{dz} = i\kappa L e^{-2i\Delta\beta \frac{L}{L} z} E_b(z) \tag{2.2.3}$$

$$L\frac{dE_b(z)}{dz} = i\kappa L e^{+2i\Delta\beta \frac{L}{L} z} E_a(z). \tag{2.2.4}$$

Introducing $\zeta = z/L$, equations (2.2.3) and (2.2.4) become:

$$\frac{dE_a(\zeta)}{d\zeta} = i\kappa L e^{-2i\Delta\beta L\zeta} E_b(\zeta)$$

$$\frac{dE_b(\zeta)}{d\zeta} = i\kappa L e^{+2i\Delta\beta L\zeta} E_a(\zeta)$$

$$\frac{dE_a(\zeta)}{d\zeta} = i\overline{\kappa} e^{-2i\overline{\Delta\beta}\zeta} E_b(\zeta) \tag{2.2.5}$$

$$\frac{dE_b(\zeta)}{d\zeta} = i\overline{\kappa} e^{+2i\overline{\Delta\beta}\zeta} E_a(\zeta). \tag{2.2.6}$$

where $\overline{\kappa} = \kappa L$ and $\overline{\Delta\beta} = \Delta\beta L$ represent the normalized coupling coefficient and normalized waveguide detuning respectively.

The two electromagnetic modes with amplitudes A and B respectively, are assumed as:

$$E_a(z) = Ae^{-i\Delta\beta z}$$

$$E_b(z) = Be^{+i\Delta\beta z}.$$

The normalized form for E_a and E_b becomes:

$$\begin{aligned} E_a(z) &= Ae^{-i\Delta\beta\frac{z}{L}L} \\ E_a(\zeta) &= Ae^{-i\Delta\beta L\zeta} \\ E_a(\zeta) &= Ae^{-i\overline{\Delta\beta}\zeta}. \end{aligned} \tag{2.2.7}$$

$$\begin{aligned} E_b(z) &= Be^{+i\Delta\beta\frac{z}{L}L} \\ E_b(\zeta) &= Be^{+i\Delta\beta L\zeta} \\ E_b(\zeta) &= Be^{+i\overline{\Delta\beta}\zeta}. \end{aligned} \tag{2.2.8}$$

Solving equation (2.2.5) with the help of equations (2.2.7) and (2.2.8) yields:

$$\begin{aligned} \frac{d(Ae^{-i\overline{\Delta\beta}\zeta})}{d\zeta} &= i\overline{\kappa}e^{-2i\overline{\Delta\beta}\zeta}(Be^{+i\overline{\Delta\beta}\zeta}) \\ A\frac{d}{d\zeta}e^{-i\overline{\Delta\beta}\zeta} &= i\overline{\kappa}Be^{-2i\overline{\Delta\beta}\zeta+i\overline{\Delta\beta}\zeta} \\ \frac{dA}{d\zeta} + A(-i\overline{\Delta\beta}) &= i\overline{\kappa}B \\ \frac{dA}{d\zeta} &= i\overline{\Delta\beta}A + i\overline{\kappa}B. \end{aligned} \tag{2.2.9}$$

Solving equation (2.2.6) with the help of equations (2.2.7) and (2.2.8) yields:

$$\begin{aligned}
\frac{d(Be^{i\overline{\Delta\beta}\zeta})}{d\zeta} &= i\overline{\kappa}e^{+2i\overline{\Delta\beta}\zeta}(Ae^{-i\overline{\Delta\beta}\zeta}) \\
B\frac{d}{d\zeta}e^{+i\overline{\Delta\beta}\zeta} &= i\overline{\kappa}Ae^{+2i\overline{\Delta\beta}\zeta - i\overline{\Delta\beta}\zeta} \\
\frac{dB}{d\zeta} + B(+i\overline{\Delta\beta}) &= i\overline{\kappa}A \\
\frac{dB}{d\zeta} &= -i\overline{\Delta\beta}B + i\overline{\kappa}A. \qquad (2.2.10)
\end{aligned}$$

Equations (2.2.9) and (2.2.10) are the main equations that we will be solving for PIM-PIM coupling.

A general solution to the equations can be assumed as:

$$A(z) = A_1e^{iqz} + A_2e^{-iqz}$$

$$B(z) = B_1e^{iqz} + B_2e^{-iqz}$$

where q is the unknown eigenvalue of the solutions. Normalizing the general solution outlined above yields:

$$A(\zeta) = A_1e^{i\overline{q}\zeta} + A_2e^{-i\overline{q}\zeta} \qquad (2.2.11)$$

$$B(\zeta) = B_1e^{i\overline{q}\zeta} + B_2e^{-i\overline{q}\zeta} \qquad (2.2.12)$$

where $\overline{q} = qL$ is the normalized eigenvalue.

2.2.3 Dispersion Relation and Eigenvalue

Substituting equations (2.2.11) and (2.2.12) in (2.2.9) yields:

$$\frac{d}{d\zeta}(A_1 e^{i\overline{q}\zeta} + A_2 e^{-i\overline{q}\zeta}) = (i\overline{\Delta\beta})(A_1 e^{i\overline{q}\zeta} + A_2 e^{-i\overline{q}\zeta}) + i\overline{\kappa}(B_1 e^{i\overline{q}\zeta} + B_2 e^{-i\overline{q}\zeta})$$

$$A_1(i\overline{q})e^{i\overline{q}\zeta} + A_2(-i\overline{q})e^{-i\overline{q}\zeta} = (i\overline{\Delta\beta})(A_1 e^{i\overline{q}\zeta} + A_2 e^{-i\overline{q}\zeta}) + i\overline{\kappa}(B_1 e^{i\overline{q}\zeta} + B_2 e^{-i\overline{q}\zeta}).$$

Equating coefficients of $e^{i\overline{q}\zeta}$ yields:

$$A_1(i\overline{q})e^{i\overline{q}\zeta} = (i\overline{\Delta\beta})A_1 e^{i\overline{q}\zeta} + i\overline{\kappa}B_1 e^{i\overline{q}\zeta}$$

$$(\overline{q} - \overline{\Delta\beta})A_1 = \overline{\kappa}B_1. \tag{2.2.13}$$

Equating coefficients of $e^{-i\overline{q}\zeta}$ yields:

$$A_2(-i\overline{q})e^{-i\overline{q}\zeta} = (i\overline{\Delta\beta})A_2 e^{-i\overline{q}\zeta} + i\overline{\kappa}B_2 e^{-i\overline{q}\zeta}$$

$$(\overline{q} + \overline{\Delta\beta})A_2 = -\overline{\kappa}B_2. \tag{2.2.14}$$

Substituting equations (2.2.11) and (2.2.12) in (2.2.10) yields:

$$\frac{d}{d\zeta}(B_1 e^{i\overline{q}\zeta} + B_2 e^{-i\overline{q}\zeta}) = -(i\overline{\Delta\beta})(B_1 e^{i\overline{q}\zeta} + B_2 e^{-i\overline{q}\zeta}) + i\overline{\kappa}(A_1 e^{i\overline{q}\zeta} + A_2 e^{-i\overline{q}\zeta})$$

$$(B_1(i\overline{q}e^{i\overline{q}\zeta} + B_2 - (i\overline{q}e^{-i\overline{q}\zeta}) = -(i\overline{\Delta\beta})(B_1 e^{i\overline{q}\zeta} + B_2 e^{-i\overline{q}\zeta}) + i\overline{\kappa}(A_1 e^{i\overline{q}\zeta} + A_2 e^{-i\overline{q}\zeta}).$$

Equating coefficients of $e^{i\overline{q}\zeta}$ yields:

$$B_1(i\overline{q})e^{i\overline{q}\zeta} = -(i\overline{\Delta\beta})B_1 e^{i\overline{q}\zeta} + i\overline{\kappa}A_1 e^{i\overline{q}\zeta}$$

$$(\overline{q} + \overline{\Delta\beta})B_1 = \overline{\kappa}A_1. \tag{2.2.15}$$

Equating coefficients of $e^{-i\overline{q}\zeta}$ yields:

$$B_2(-i\overline{q})e^{-i\overline{q}\zeta} = -(i\overline{\Delta\beta})B_2e^{-i\overline{q}\zeta} + i\overline{\kappa}A_2e^{-i\overline{q}\zeta}$$

$$(\overline{q} - \overline{\Delta\beta})B_2 = -\overline{\kappa}A_2. \tag{2.2.16}$$

Equations (2.2.13), (2.2.14),(2.2.15) and (2.2.16) relate the constants A_1, A_2, B_1, and B_2. Substituting (2.2.15) in (2.2.13) allows us to defines the unknown eigenvalue $\overline{q}$ in terms of the known $\overline{\kappa}$ and $\overline{\Delta\beta}$.

$$\begin{aligned}(\overline{q} - \overline{\Delta\beta})A_1 &= \overline{\kappa}B_1 \\ (\overline{q} - \overline{\Delta\beta})A_1 &= \overline{\kappa}\frac{\overline{\kappa}A_1}{\overline{q} + \overline{\Delta\beta}} \\ \overline{q}^2 &= \overline{\Delta\beta}^2 + \overline{\kappa}^2 \\ \overline{q} &= \pm\sqrt{\overline{\Delta\beta}^2 + \overline{\kappa}^2}.\end{aligned} \tag{2.2.17}$$

2.2.4 Boundary Conditions and Specific Solution

Suppose we are transferring energy from waveguide A to waveguide B. This means that initially at $\zeta = 0$, all energy is in A and $B(\zeta = 0) = 0$. Using these values in equation (2.2.12) yields:

$$B(\zeta) = B_1e^{i\overline{q}\zeta} + B_2e^{-i\overline{q}\zeta}$$

$$0 = B_1 + B_2$$

$$B_2 = -B_1.$$

Substituting the above expression in equation (2.2.12) yields:

$$B(\zeta) = B_1 e^{i\overline{q}\zeta} + B_2 e^{-i\overline{q}\zeta}$$

$$B(\zeta) = B_1 e^{i\overline{q}\zeta} - B_1 e^{-i\overline{q}\zeta}.$$

Using the identity $e^{i\alpha} - e^{-i\alpha} = 2i\sin(\alpha)$ yields:

$$B(\zeta) = 2iB_1 \sin(\overline{q}\zeta).$$

We can now find $A(\zeta)$ as follows:

$$\begin{aligned}
\frac{dB}{d\zeta} &= -(i\overline{\Delta\beta})B + i\overline{\kappa}A \\
\frac{d(2iB_1\sin(\overline{q}\zeta))}{d\zeta} &= -(i\overline{\Delta\beta})2iB_1\sin(\overline{q}\zeta) + i\overline{\kappa}A \\
\frac{2B_1 d(\sin(\overline{q}\zeta))}{d\zeta} &= -(i\overline{\Delta\beta})2B_1\sin(\overline{q}\zeta) + \overline{\kappa}A \\
2B_1\overline{q}\cos(\overline{q}\zeta) &= i\overline{\Delta\beta}2B_1\sin(\overline{q}\zeta) + \overline{\kappa}A \\
\overline{\kappa}A &= 2B_1\overline{q}\cos(\overline{q}\zeta) - i\overline{\Delta\beta}2B_1\sin(\overline{q}\zeta) \\
A(\zeta) &= \frac{2B_1}{\overline{\kappa}}\{\overline{q}\cos(\overline{q}\zeta) - i\overline{\Delta\beta}\sin(\overline{q}\zeta)\}. \qquad (2.2.18)
\end{aligned}$$

2.2.5 Power Exchange (Output ports)

As shown in Figure 2.1, waveguide A is excited at $\zeta = 0$. Hence, the initial power P_0 pumped into waveguide A at $\zeta = 0$ can be determined as follows:

$$A(\zeta) = \frac{2B_1}{\overline{\kappa}}\{\overline{q}\cos(\overline{q}\zeta) - i\overline{\Delta\beta}\sin(\overline{q}\zeta)\}$$
$$A(\zeta = 0) = \frac{2B_1}{\overline{\kappa}}\overline{q}$$
$$P_0 = |A(\zeta = 0)|^2 = (\frac{2B_1}{\overline{\kappa}})^2|\overline{q}|^2.$$

The power in waveguide A, P_A is:

$$P_A = |P_A(\zeta)|^2$$
$$P_A = P_0|\cos(\overline{q}\zeta) + \frac{\overline{\Delta\beta}}{\overline{q}}\sin(\overline{q}\zeta)|^2.$$

The field in waveguide B at $\zeta = 1$ is:

$$B(\zeta) = 2iB_1\sin(\overline{q}\zeta)$$
$$B(\zeta = 1) = 2iB_1\sin(\overline{q}).$$

The power in waveguide B, P_B is:

$$P_B = |P_B(\zeta)|^2 = P_0\overline{\kappa}^2|\frac{\sin(\overline{q}\zeta)}{\overline{q}}|^2.$$

The expression for transmittivity T at out1 in Figure 2.1 [13]:

$$T_1 = \frac{P_A(\zeta = 1)}{P_A(\zeta = 0)} = \frac{|\overline{q}\cos\overline{q} + i\overline{\Delta\beta}\sin\overline{q}|^2}{|\overline{q}|^2}.$$

Expression for transmittivity at out2 in Figure 2.1 [13]:

$$T_2 = \frac{P_B(\zeta = 1)}{P_A(\zeta = 0)} = \frac{|\overline{\kappa} \sin \overline{q}|^2}{|\overline{q}|^2}.$$

Neither T_1 nor T_2 depend on the sign of $\overline{q}$.

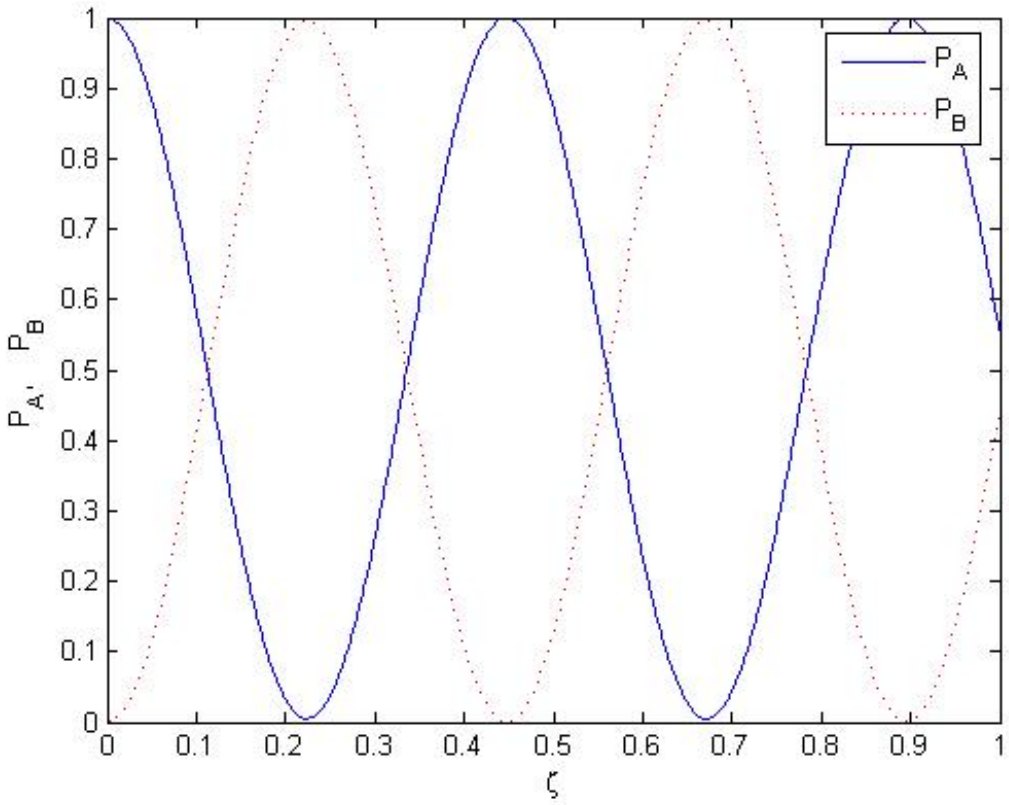

Figure 2.2: *The well-known exchange of power between the two waveguides for a PIM-PIM DC.* $\overline{\kappa} = 7$ and $\overline{\Delta\beta} = 0.5$

Figure 2.2 shows the sinusoidal exchange of normalized power between the singlemode waveguides A and B. It is fairly evident from the plot that at $\zeta = 0$ all the power is in input waveguide A and the power in $B(\zeta) = 0$ is minimum.

For this plot, we have selected coupling coefficient $\overline{\kappa} = 7$. Propagation constants for the two modes are not the same, resulting in a phase difference as the fields propagate. This phase difference of π and 2π leads to the periodic exchange of power between the two waveguides. Generally, a significant amount of power exchange occurs when the two propagation constants are close to each other.

2.3 PASSIVE NIM-PIM DIRECIONAL COUPLER

2.3.1 Directional Coupler

A NIM-PIM DC is a two waveguide structure just like the conventional PIM-PIM DC. However, as opposed to the conventional coupler, one of the waveguides employs a negative index material (NIM). NIM waveguides can guide its modes in a direction opposite to that of PIM waveguides. Thus a negative index of refraction can act as a key component in providing feedback and in coupling the forward and backward propagating modes of the optical waves which may result in exchange of power between the forward and backward propagating modes.

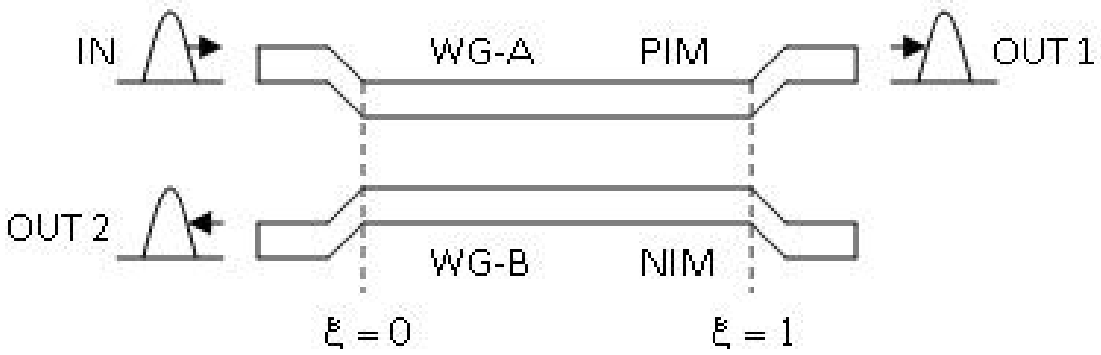

Figure 2.3: *NIM-PIM Directional Coupler*

In Figure 2.3 two single mode waveguides A and B are placed parallel to each other. Waveguide A is composed of conventional positive index material (PIM) and guides its mode in forward direction. Waveguide B is composed of negative index material (NIM) and has a backward propagating mode. Input energry is transferred to waveguide A at $\zeta = 0$. Once the waveguides are brought sufficiently close to each other, a coupling region is created and exchange of power between the oppositely directed modes takes place.

2.3.2 Coupled-Mode Equations and Generalized Solution

The coupled-mode equations for the passive NIM-PIM DC are [14][15]:

$$\frac{d}{d\zeta}E_a(\zeta) = +i\overline{\kappa}e^{-2i\overline{\Delta\beta}\zeta}E_b(\zeta) \tag{2.3.1}$$

$$\frac{d}{d\zeta}E_b(\zeta) = -i\overline{\kappa}e^{+2i\overline{\Delta\beta}\zeta}E_a(\zeta) \tag{2.3.2}$$

where κ is the coupling co-efficient, $\Delta\beta$ is the detuning between the two waveguides $\Delta\beta = \beta_1 - \beta_2$, $\beta_1 = \frac{2\pi}{\lambda_0} n_1$ is the wavenumber of light wave in the PIM waveguide, and $\beta_2 = \frac{2\pi}{\lambda_0} n_2$ expresses the wavenumber of light wave in the NIM waveguide. E_a and E_b represent the forward and backward traveling modes. The two electromagnetic modes with amplitudes A and B along with rotating frames $e^{-i\overline{\Delta\beta}\zeta}$ and $e^{+i\overline{\Delta\beta}\zeta}$ respectively, are defined as:

$$E_a(\zeta) = Ae^{-i\overline{\Delta\beta}\zeta} \tag{2.3.3}$$

$$E_b(\zeta) = Be^{+i\overline{\Delta\beta}\zeta}. \tag{2.3.4}$$

Solving equation (2.3.1) with the help of equations (2.3.3) and (2.3.4) yields:

$$\begin{aligned} d(Ae^{-i\overline{\Delta\beta}\zeta})/d\zeta &= i\overline{\kappa}e^{-2i\overline{\Delta\beta}\zeta}(Be^{+i\overline{\Delta\beta}\zeta}) \\ A\frac{d}{d\zeta}e^{-i\overline{\Delta\beta}\zeta} &= i\overline{\kappa}Be^{-2i\overline{\Delta\beta}\zeta+i\overline{\Delta\beta}\zeta} \\ \frac{dA}{d\zeta} + A(-i\overline{\Delta\beta}) &= i\overline{\kappa}B \\ \frac{dA}{d\zeta} &= i\overline{\Delta\beta}A + i\overline{\kappa}B. \end{aligned} \tag{2.3.5}$$

Solving equation (2.3.2) with the help of equations (2.3.3) and (2.3.4) yields:

$$\begin{aligned} d(Be^{i\overline{\Delta\beta}\zeta})/d\zeta &= -i\overline{\kappa}e^{+2i\overline{\Delta\beta}\zeta}(Ae^{-i\overline{\Delta\beta}\zeta}) \\ \frac{dB}{d\zeta}e^{+i\overline{\Delta\beta}\zeta} &= -i\overline{\kappa}Ae^{+2i\overline{\Delta\beta}\zeta - i\overline{\Delta\beta}\zeta} \\ B\frac{d}{d\zeta} + B(+i\overline{\Delta\beta}) &= -i\overline{\kappa}A \\ \frac{dB}{d\zeta} &= -i\overline{\Delta\beta}B - i\overline{\kappa}A \\ -\frac{dB}{d\zeta} &= i\overline{\Delta\beta}B + i\overline{\kappa}A. \end{aligned} \tag{2.3.6}$$

Equations (2.3.5) and (2.3.6) are the main equations that we will be solving for the NIM-PIM DC. Comparing the mentioned equations to the coupled-mode equations (2.2.9) and (2.2.10) for a standard directional coupler (PIM-PIM DC), a difference of sign is observed for the equation representing the propagation in the second waveguide. This essentially states the fact that the choice of this sign depends on the direction of coupling. In case of codirectional coupling, a positive sign is chosen for both the equations. If the two modes are counter propagating, a negative sign is the valid choice [14]. A general solution can be postulated as:

$$A(\zeta) = A_1 e^{i\overline{q}\zeta} + A_2 e^{-i\overline{q}\zeta} \tag{2.3.7}$$

$$B(\zeta) = B_1 e^{i\overline{q}\zeta} + B_2 e^{-i\overline{q}\zeta} \tag{2.3.8}$$

where $\overline{q} = qL$.

2.3.3 Dispersion Relation and Eigenvalue

Substituting equations (2.3.7) and (2.3.8) in (2.3.5) yields:

$$\frac{d}{d\zeta}(A_1 e^{i\overline{q}\zeta} + A_2 e^{-i\overline{q}\zeta}) = (i\overline{\Delta\beta})(A_1 e^{i\overline{q}\zeta} + A_2 e^{-i\overline{q}\zeta}) + i\overline{\kappa}(B_1 e^{i\overline{q}\zeta} + B_2 e^{-i\overline{q}\zeta})$$

$$A_1(i\overline{q})e^{i\overline{q}\zeta} + A_2(-i\overline{q})e^{-i\overline{q}\zeta} = (i\overline{\Delta\beta})(A_1 e^{i\overline{q}\zeta} + A_2 e^{-i\overline{q}\zeta}) + i\overline{\kappa}(B_1 e^{i\overline{q}\zeta} + B_2 e^{-i\overline{q}\zeta}).$$

Equating coefficients of $e^{i\overline{q}\zeta}$ yields:

$$A_1(i\overline{q})e^{i\overline{q}\zeta} = (i\overline{\Delta\beta})A_1 e^{i\overline{q}\zeta} + i\overline{\kappa}B_1 e^{i\overline{q}\zeta}$$

$$(\overline{q} - \overline{\Delta\beta})A_1 = \overline{\kappa}B_1. \tag{2.3.9}$$

Equating coefficients of $e^{-i\overline{q}\zeta}$ yields:

$$A_2(-i\overline{q})e^{-i\overline{q}\zeta} = (i\overline{\Delta\beta})A_2 e^{-i\overline{q}\zeta} + i\overline{\kappa}B_2 e^{-i\overline{q}\zeta}$$

$$(\overline{q} + \overline{\Delta\beta})A_2 = -\overline{\kappa}B_2. \tag{2.3.10}$$

Substituting equations (2.3.7) and (2.3.8) in (2.3.6) yields:

$$\frac{d}{d\zeta}(B_1 e^{i\overline{q}\zeta} + B_2 e^{-i\overline{q}\zeta}) = -(i\overline{\Delta\beta})(B_1 e^{i\overline{q}\zeta} + B_2 e^{-i\overline{q}\zeta}) - i\overline{\kappa}(A_1 e^{i\overline{q}\zeta} + A_2 e^{-i\overline{q}\zeta})$$

$$B_1(i\overline{q})e^{i\overline{q}\zeta} + B_2(-i\overline{q})e^{-i\overline{q}\zeta}) = -(i\overline{\Delta\beta})(B_1 e^{i\overline{q}\zeta} + B_2 e^{-i\overline{q}\zeta}) - i\overline{\kappa}(A_1 e^{i\overline{q}\zeta} + A_2 e^{-i\overline{q}\zeta}).$$

Equating coefficients of $e^{i\overline{q}\zeta}$ yields:

$$B_1(i\overline{q})e^{i\overline{q}\zeta} = -(i\overline{\Delta\beta})B_1 e^{i\overline{q}\zeta} - i\overline{\kappa}A_1 e^{i\overline{q}\zeta}$$

$$(\overline{q} + \overline{\Delta\beta})B_1 = -\overline{\kappa}A_1. \tag{2.3.11}$$

Equating coefficients of $e^{-i\overline{q}\zeta}$ yields:

$$B_2(-i\overline{q})e^{-i\overline{q}\zeta} = -(i\overline{\Delta\beta})B_2e^{-i\overline{q}\zeta} - i\overline{\kappa}A_2e^{-i\overline{q}\zeta}$$

$$(\overline{q} - \overline{\Delta\beta})B_2 = \overline{\kappa}A_2. \tag{2.3.12}$$

Equations (2.3.9), (2.3.10),(2.3.11) and (2.3.12) relate the constants A_1, A_2, B_1 and B_2. Substituting (2.3.11) in (2.3.9) yields unknown eigenvalue $\overline{q}$ in terms of known $\overline{\kappa}$ and $\overline{\Delta\beta}$.

$$\begin{aligned}(\overline{q} - \overline{\Delta\beta})A_1 &= \overline{\kappa}B_1\\ (\overline{q} - \overline{\Delta\beta})A_1 &= \overline{\kappa}\{\frac{-\overline{\kappa}A_1}{\overline{q} + \overline{\Delta\beta}}\}\\ \overline{q}^2 &= \overline{\Delta\beta}^2 - \overline{\kappa}^2\\ \overline{q} &= \pm\sqrt{\overline{\Delta\beta}^2 - \overline{\kappa}^2}.\end{aligned} \tag{2.3.13}$$

In case of a standard PIM-PIM directional coupler as discussed earlier, the power exchange was always sinusoidal. However, in case of NIM-PIM DC the power exchange is not always sinusoidal. Considering the result obtained above, if we have a relatively small κ as compared to the detuning between the waveguides then $\overline{q}$ is real and power is exchanged sinusoidally. However, if the two waveguides are brought closer enough, κ increases and $\overline{q}$ may decrease to zero. Further increase in κ bears an imaginary $\overline{q}$ which indicates an exponential change in the power exchanged between the waveguides and power is reflected back in the second waveguide.

2.3.4 Boundary Conditions and Specific Solution

There is no backward propagating wave at $\zeta = 1$. This means $B(\zeta = 1) = 0$. Using these values in equation (2.3.8) yields:

$$\begin{aligned} B(\zeta) &= B_1 e^{i\overline{q}\zeta} + B_2 e^{-i\overline{q}\zeta} \\ 0 &= B_1 e^{i\overline{q}} + B_2 e^{-i\overline{q}} \\ B_2 &= -B_1 e^{2i\overline{q}}. \end{aligned} \tag{2.3.14}$$

Substituting the above expression in equation (2.3.8) yields:

$$\begin{aligned} B(\zeta) &= B_1 e^{i\overline{q}\zeta} + B_2 e^{-i\overline{q}\zeta} \\ B(\zeta) &= B_1 e^{i\overline{q}\zeta} - (B_1 e^{2i\overline{q}}) e^{-i\overline{q}\zeta} \\ B(\zeta) &= \frac{B_1}{e^{-i\overline{q}}} (e^{i\overline{q}\zeta - i\overline{q}} - e^{2i\overline{q} - i\overline{q}\zeta - -i\overline{q}}) \\ B(\zeta) &= B_1' \{ e^{i(\overline{q}\zeta - \overline{q})} - e^{-i(\overline{q}\zeta - \overline{q}} \} \\ B(\zeta) &= B_1' \sinh \{ i(\overline{q}\zeta - \overline{q}) \} \end{aligned} \tag{2.3.15}$$

where $B_1' = \frac{B_1}{e^{-i\overline{q}}}$. We can now find $A(\zeta)$ by using:

$$\begin{aligned} -\frac{dB}{d\zeta} &= (i\overline{\Delta\beta})B + i\overline{\kappa}A \\ -\frac{d[B_1' \sinh \{ i(\overline{q}\zeta - \overline{q}) \}]}{d\zeta} &= (i\overline{\Delta\beta})[B_1' \sinh \{ i(\overline{q}\zeta - \overline{q}) \} + i\overline{\kappa}A \\ -B_1'(i\overline{q}) \cosh \{ i(\overline{q}\zeta - \overline{q}) \} &= (i\overline{\Delta\beta})[B_1' \sinh \{ i(\overline{q}\zeta - \overline{q}) \} + i\overline{\kappa}A \\ -B_1'[\overline{q} \cosh \{ i(\overline{q}\zeta - \overline{q}) \}] &= (\overline{\Delta\beta})[B_1' \sinh \{ i(\overline{q}\zeta - \overline{q}) \}] + \overline{\kappa}A. \end{aligned}$$

Solving for $A(\zeta)$ yields:

$$\overline{\kappa}A = -B_1'[\overline{q}\cosh\{i(\overline{q}\zeta - \overline{q})\} - (\overline{\Delta\beta})\sinh\{i(\overline{q}\zeta - \overline{q})\}]$$
$$A(\zeta) = \frac{-B_1'}{\overline{\kappa}}[\overline{q}\cosh\{i(\overline{q}\zeta - \overline{q})\} - \overline{\Delta\beta}\sinh\{i(\overline{q}\zeta - \overline{q})\}]. \tag{2.3.16}$$

2.3.5 Transmittivity and Reflectivity

Power carried by waveguide A and waveguide B can be expressed as:

$$P_A = |A(\zeta)|^2 = |\frac{-B_1'}{\overline{\kappa}}[\overline{q}\cosh\{i(\overline{q}\zeta - \overline{q})\} - \overline{\Delta\beta}\sinh\{i(\overline{q}\zeta - \overline{q})\}]|^2$$
$$P_B = |B(\zeta)|^2 = |B_1'\sinh\{i(\overline{q}\zeta - \overline{q})\}|^2.$$

Transmittivity T at out1 of Figure 2.3 can be expressed as:

$$T = \frac{P_A(\zeta = 1)}{P_A(\zeta = 0)} = \frac{|\overline{q}|^2}{|\overline{q}\cosh(-i\overline{q}) + (\overline{\Delta\beta})\sinh(-i\overline{q})|^2}.$$

Figure 2.4 shows the normalized transmittivity of a passive NIM-PIM DC versus the mismatch between the wave numbers of the two waveguides. We have selected coupling coefficient $\overline{\kappa} = 3$ for this plot. Power is exchanged sinusoidally between the two waveguides as long as $\overline{\Delta\beta} > \overline{\kappa}$. Once the two $\beta's$ are close enough, strongly coupling occurs which results in the entire power being reflected back to out2 and hence, a drop in the transmittivity for this range. This results in formation of a stopband in the transmittivity spectrum.

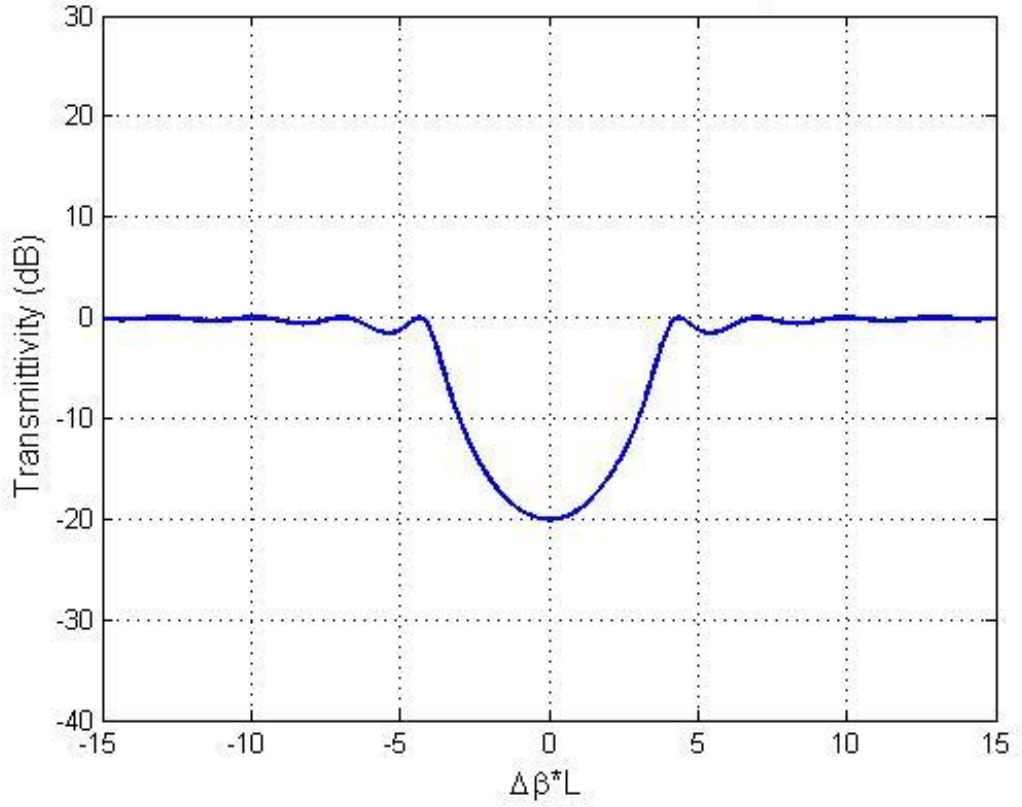

Figure 2.4: *NIM-PIM - Transmittivity at out1* ($\overline{\kappa} = 3$)

Reflectivity R at out2 of Figure 2.3 can be expressed as:

$$R = \frac{P_B(\zeta = 0)}{P_A(\zeta = 0)} = \frac{|\overline{\kappa} \sinh(-i\overline{q})|^2}{|\overline{q} \cosh(-i\overline{q}) + (\overline{\Delta\beta}) \sinh(-i\overline{q})|^2}.$$

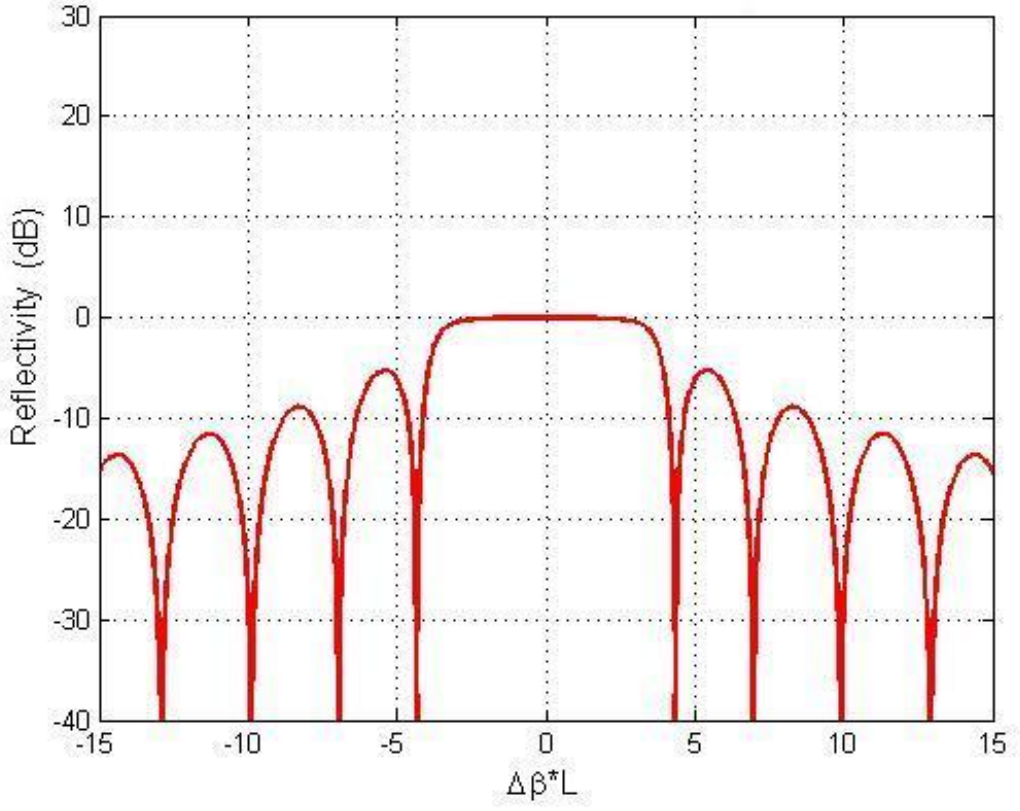

Figure 2.5: *NIM-PIM DC - Reflectivity at out2 ($\overline{\kappa} = 3$). Similar spectrum shown in [14].*

Figure 2.5 shows the normalized reflectivity plot of a passive NIM-PIM DC with coupling coefficient $\overline{\kappa} = 3$. Power is exchanged sinusoidally between the two waveguides as long as $\overline{\Delta\beta} > \overline{\kappa}$. Once the two $\beta's$ are close enough strong coupling occurs, $\overline{q}$ becomes imaginary and the power exchange becomes exponential rather than sinusoidal. This results in the entire power being reflected back to out2.

Both T and R are independent of the sign of $\overline{q}$. We can define the effective re-

flectivity $r_a = \frac{A_1}{B_1}$ and $r_b = \frac{A_2}{B_2}$ using equations (2.3.9), (2.3.10), (2.3.11) and (2.3.12):

$$r_a = \frac{A_1}{B_1} = \frac{\overline{q} - \overline{\Delta\beta}}{\overline{\kappa}}.$$
$$r_b = \frac{A_2}{B_2} = \frac{-\overline{\kappa}}{\overline{q} + \overline{\Delta\beta}}.$$
$$r_a = \frac{B_1}{A_1} = \frac{-\overline{\kappa}}{\overline{q} + \overline{\Delta\beta}}.$$
$$r_b = \frac{A_2}{B_2} = \frac{\overline{q} - \overline{\Delta\beta}}{\overline{\kappa}}.$$

From these expressions obtained for r_a and r_b, it is evident that $r_a = r_b = r$ for the case of a passive NIM-PIM DC. Figure 2.6 shows a matlab plot of $|r|$ versus $\overline{\Delta\beta}$. It is clear from the plot that in order to hold the condition $|r| <= 1$ [16], positive value of $\overline{q}$ is considered when $\overline{\Delta\beta} > 0$ and vice versa.

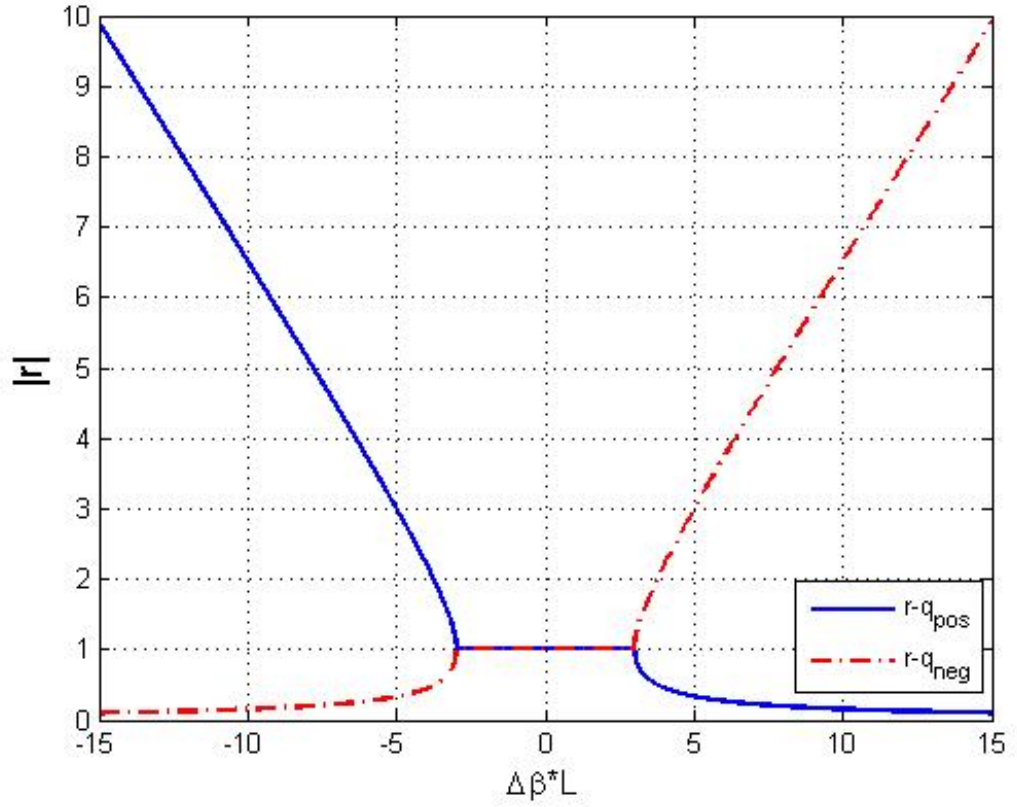

Figure 2.6: *NIM-PIM DC- Effective Reflectivity* ($\overline{\kappa} = 3$).

2.4 PASSIVE DFB RESONATOR

2.4.1 DFB Resonator

Contra directional coupling results from two modes propagating in opposite directions. For coupling to occur within a distributed feedback (DFB) resonator, some

kind of periodic perturbation is introduced in the waveguide e.g. a diffraction grating. Gratings are periodic structures that are normally built on or etched in a waveguide. Unlike a co-directional coupler with two waveguides, a DFB resonator only consists of a single waveguide. The periodic structures introduce a perturbation within the waveguide. Variations in the refractive index act as a key component in providing feedback and in coupling the forward and backward propagating modes of the optical waves inside the waveguide. Thus exchange of power between the forward and backward propagating mode is possible.

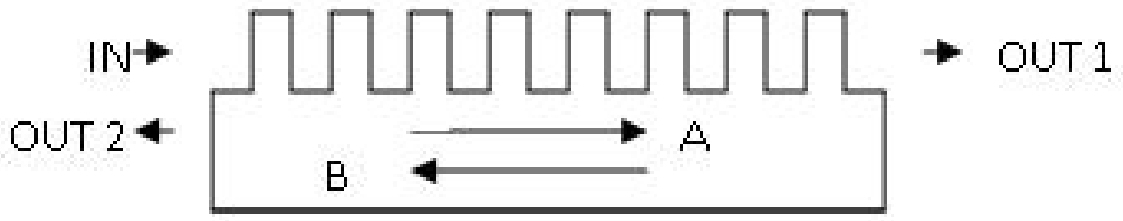

Figure 2.7: *DFB Resonator*

Figure 2.7, shows a DFB waveguide structure with periodic perturbations. These perturbations help in mode coupling in the DFB structure, whose modes would otherwise remain independent. Power is introduced at $\zeta = 0$ and and is reflected back at out2 when the phase mismatch is sufficiently smaller than $\overline{\kappa}$.

2.4.2 Coupled-Mode Equations and Generalized Solution

The coupled-mode equations for the passive DFB resonator are [16]:

$$\frac{dA}{d\zeta} = i\overline{\Delta\beta}A + i\overline{\kappa}B$$
$$\frac{dB}{d\zeta} = -i\overline{\Delta\beta}B - i\overline{\kappa}A$$

where $\overline{\kappa}$ is the normalized coupling coefficient. $\overline{\kappa} = (\pi L/\lambda)\Delta n$, Δn is the index perturbation, $\overline{\Delta\beta} = \overline{\beta_1} - \overline{\beta_2}$ represent the normalized waveguide detuning, β_1 is the wavenumber of light wave in the waveguide, and $\beta_2 = \frac{\pi}{\Lambda}$ represents the wavenumber of the grating structure, Λ is the grating period. A general solution can be postulated as:

$$A(\zeta) = A_1 e^{i\overline{q}\zeta} + A_2 e^{-i\overline{q}\zeta}$$

$$B(\zeta) = B_1 e^{i\overline{q}\zeta} + B_2 e^{-i\overline{q}\zeta}.$$

It is fairly evident that both the passive DFB resonator and NIM-PIM DC are governed by the same system of coupled-mode equations.

2.4.3 Comparison with NIM-PIM DC

The dispersion relation for the passive DFB resonator is expressed as [16]:

$$\overline{q} = \pm\sqrt{\overline{\Delta\beta}^2 - \overline{\kappa}^2}.$$

The transmittivity at output 1 is given by:

$$T = \frac{P_A(\zeta = 1)}{P_A(\zeta = 0)} = \frac{|\overline{q}|^2}{|\overline{q}\cosh(-i\overline{q}) + (\overline{\Delta\beta})\sinh(-i\overline{q})|^2}.$$

While reflectivity at output 2 is calculated as [16]:

$$R = \frac{P_B(\zeta = 0)}{P_A(\zeta = 0)} = \frac{|\overline{\kappa}\sinh(-i\overline{q})|^2}{\overline{q}\cosh(-i\overline{q}) + (\overline{\Delta\beta})\sinh(-i\overline{q})}.$$

Comparing the above three relations with those derived for the passive NIM-PIM DC, we conclude that a passive NIM-PIM DC demonstrates a behavior which is the same as a passive DFB resonator.

2.5 COMPARISON BETWEEN STRUCTURES

Both the DFB structure and NIM-PIM DC evaluates equations similarly, however the physical interpretation is different. The passive DFB resonator is a single waveguide structure whereas a passive NIM-PIM DC consists of two waveguides.

Detuning for both the passive DFB resonator and the passive NIM-PIM DC is expressed as $\Delta\beta = \beta_1 - \beta_2$. In case of passive DFB resonator this may be interpreted as the difference between the wave number of the light wave in the waveguide and the grating structure's wave number. Mathematically, it may be

expressed as:

$$\beta_1 = \frac{2\pi}{\lambda_0} n$$
$$\beta_2 = \frac{\pi}{\Lambda}.$$

In case of passive NIM-PIM DC detuning is interpreted as the difference between the wave number of the light wave in the PIM and NIM waveguide. Mathematically, it may be expressed as:

$$\beta_1 = \frac{2\pi}{\lambda_0} n_1$$
$$\beta_1 = \frac{2\pi}{\lambda_0} n_2.$$

Coupling coefficient κ represents the coupling strength for both passive DFB resonator and passive NIM-PIM DC. In case of a passive DFB resonator κ is interpreted as:

$$\overline{\kappa} = \frac{\pi L}{\lambda} \Delta n$$

In case of passive NIM-PIM DC the interpretation of κ is as follows [14]:

$$C_{km1} = \frac{\omega}{2} \int_{S2} [\Delta\epsilon_2 e^*_{m1}(y).e_{k2}(y) + \Delta\mu_2 h^*_{m1}(y).h_{k2}(y)] \, \mathrm{d}y$$
$$C_{km2} = \frac{\omega}{2} \int_{S1} [\Delta\epsilon_1 e^*_{m2}(y).e_{k1}(y) + \Delta\mu_1 h^*_{m2}(y).h_{k1}(y)] \, \mathrm{d}y.$$

2.6 SUMMARY OF KEY DERIVATIONS

Deriving the Dispersion Relation

1. Consider the normalized coupled-mode equations (2.3.5) and (2.3.6).
2. Postulate the general solution e.g. equations (2.3.7) and (2.3.8).
3. Plug in the general solution in the first coupled mode equation. e.g. equations (2.3.7) and (2.3.8) in (2.3.5).
4. Equate the coefficients of $e^{i\bar{q}\zeta}$, and two sub equations are obtained e.g. equations (2.3.9) and (2.3.10).
5. Equate the coefficients of $e^{-i\bar{q}\zeta}$, and two sub equations are obtained e.g. equations (2.3.11) and (2.3.12).
6. Substitute for the value of B_1 or A_1 in the first pair of sub equations with the value from the second pair of sub equations derived above e.g. equation (2.3.11) in (2.3.9).
7. Dispersion Relation is obtained e.g. equation (2.3.13).
8. Repeat steps 3-8 for the second coupled-mode equation e.g. equation (2.3.6).
9. Same dispersion relation is obtained.

Deriving Transmittivity and Reflectivity

1. Consider the general solution e.g. equation (2.3.8).
2. Apply the boundary condition to the general solution i.e $B(\zeta) = B_1 + B_2$ to

find B_2 e.g. equation (2.3.14).

3. Plug this value of B_2 in the original generalized solution and an expression for $B(\zeta)$ is obtained e.g. equation (2.3.15).
4. Consider the first coupled-mode equation and substitute for the value of B with the expression obtained above e.g. equations (2.3.5) and (2.3.15).
5. An expression for $A(\zeta)$ is derived e.g. equation (2.3.16).
6. Reflectivity is the ratio of output power at $B(\zeta = 0)$ and input power $A(\zeta = 0)$.
7. Transmittivity is the ratio of output power at $A(\zeta = 1)$ and input power $A(\zeta = 0)$.

CHAPTER 3

ACTIVE NIM-PIM DIRECIONAL COUPLER

In this chapter, optical gain is introduced into the waveguide structure. The governing equations for the active system are stated and solved for both the DFB and NIM-PIM waveguide structures. Initially equations for the well known DFB resonator with gain are solved and different attributes like the dispersion relation, transmittivity, and reflectivity are derived and analyzed. Later, the same process is applied to the more complicated case of an active NIM-PIM system for the first time and its corresponding dispersion relation, transmittivity, and reflectivity expressions are derived and analyzed.

3.1 ACTIVE DFB RESONATOR

3.1.1 Coupled-Mode Equations and General Solution

The normalized coupled-mode equations for an active DFB resonator [16] are:

$$\frac{dA}{d\zeta} = i(\overline{\Delta\beta} - i\frac{\overline{g}}{2})A + i\overline{\kappa}B \tag{3.1.1}$$

$$\frac{-dB}{d\zeta} = i(\overline{\Delta\beta} - i\frac{\overline{g}}{2})B + i\overline{\kappa}A, \tag{3.1.2}$$

where $\zeta = z/L$ is the normalized length, $\overline{g} = gL$ is the normalized gain in the DFB structure, κ is the coupling coefficient, $\kappa L = \overline{\kappa}$ represent the normalized coupling strength, $\Delta\beta$ represents the wavenumber detuning, $\overline{\Delta\beta} = \Delta\beta L$ represents the normalized wavenumber detuning. The detuning between two wavenumbers can be expressed as $\Delta\beta = \beta_1 - \beta_2$. $\beta_2 = \frac{\pi}{\Lambda}$ is Bragg's wave number and Λ is the grating period. $A(\zeta)$ and $B(\zeta)$ represent the amplitude of the forward and backward traveling fields respectively. Equations (3.1.1) and (3.1.2) are the main equations that we will be solving for active DFB coupling.

A generalized solution for the active system can be postulated as:

$$A(\zeta) = A_1 e^{i\overline{q}\zeta} + A_2 e^{-i\overline{q}\zeta} \tag{3.1.3}$$

$$B(\zeta) = B_1 e^{i\overline{q}\zeta} + B_2 e^{-i\overline{q}\zeta}, \tag{3.1.4}$$

where $\overline{q} = qL$, represents the unknown eigenvalue for the DFB waveguide structure and, A_1, A_2, B_1 and B_2 are constant coefficients to be solved for.

3.1.2 Dispersion Relation and Eigenvalue

Substituting equations (3.1.3) and (3.1.4) in (3.1.1) yields:

$$\frac{d}{d\zeta}(A_1 e^{i\overline{q}\zeta} + A_2 e^{-i\overline{q}\zeta}) = i(\overline{\Delta\beta} - \frac{\overline{g}}{2})(A_1 e^{i\overline{q}\zeta} + A_2 e^{-i\overline{q}\zeta}) + i\overline{\kappa}(B_1 e^{i\overline{q}\zeta} + B_2 e^{-i\overline{q}\zeta})$$
$$A_1(i\overline{q})e^{i\overline{q}\zeta} + A_2(-i\overline{q})e^{-i\overline{q}\zeta} = i(\overline{\Delta\beta} - i\frac{\overline{g}}{2})(A_1 e^{i\overline{q}\zeta} + A_2 e^{-i\overline{q}\zeta}) + i\overline{\kappa}(B_1 e^{i\overline{q}\zeta} + B_2 e^{-i\overline{q}\zeta}).$$

Equating coefficients of $e^{i\overline{q}\zeta}$ yields:

$$A_1(i\overline{q})e^{i\overline{q}\zeta} = i(\overline{\Delta\beta} - i\overline{g}/2)A_1 e^{i\overline{q}\zeta} + i\overline{\kappa}(B_1 e^{i\overline{q}\zeta})$$
$$(i\overline{q})A_1 = i(\overline{\Delta\beta} - i\overline{g}/2)A_1 + i\overline{\kappa}B_1$$
$$\{\overline{q} - (\overline{\Delta\beta} - i\overline{g}/2)\}A_1 = \overline{\kappa}B_1. \tag{3.1.5}$$

Equating coefficients of $e^{-i\overline{q}\zeta}$ yields:

$$A_2(-i\overline{q})e^{-i\overline{q}\zeta} = i(\overline{\Delta\beta} - i\overline{g_p}/2)A_2 e^{-i\overline{q}\zeta} + i\overline{\kappa}(B_2 e^{-i\overline{q}\zeta})$$
$$(-i\overline{q})A_2 = i(\overline{\Delta\beta} - i\overline{g}/2)A_2 + i\overline{\kappa}B_2$$
$$\{\overline{q} + (\overline{\Delta\beta} - i\overline{g}/2)\}A_2 = -\overline{\kappa}B_2. \tag{3.1.6}$$

Substituting equations (3.1.3) and (3.1.4) in (3.1.2) yields:

$$\frac{-d}{d\zeta}(B_1 e^{i\overline{q}\zeta} + B_2 e^{-i\overline{q}\zeta}) = i(\overline{\Delta\beta} - i\frac{\overline{g}}{2})(B_1 e^{i\overline{q}\zeta} + B_2 e^{-i\overline{q}\zeta}) + i\overline{\kappa}(A_1 e^{i\overline{q}\zeta} + A_2 e^{-i\overline{q}\zeta})$$
$$B_1(-i\overline{q})e^{i\overline{q}\zeta} - B_2(-i\overline{q})e^{-i\overline{q}\zeta} = i(\overline{\Delta\beta} - i\frac{\overline{g}}{2})(B_1 e^{i\overline{q}\zeta} + B_2 e^{-i\overline{q}\zeta}) + i\overline{\kappa}(A_1 e^{i\overline{q}\zeta} + A_2 e^{-i\overline{q}\zeta}).$$

Equating coefficients of $e^{i\overline{q}\zeta}$ yields:

$$-B_1(i\overline{q})e^{i\overline{q}\zeta} = i(\overline{\Delta\beta} - i\overline{g}/2)B_1e^{i\overline{q}\zeta} + i\overline{\kappa}(A_1e^{i\overline{q}\zeta})$$

$$-B_1(i\overline{q}) = i(\overline{\Delta\beta} - i\overline{g}/2)B_1 + i\overline{\kappa}A_1$$

$$\{\overline{q}) + (\overline{\Delta\beta} - i\overline{g}/2)\}B_1 = -\overline{\kappa}A_1. \tag{3.1.7}$$

Equating coefficients of $e^{-i\overline{q}\zeta}$ yields:

$$-B_2(-i\overline{q})e^{-i\overline{q}\zeta} = i(\overline{\Delta\beta} - i\overline{g}/2)B_2e^{-i\overline{q}\zeta} + i\overline{\kappa}A_2e^{-i\overline{q}\zeta}$$

$$-B_2(-i\overline{q}) = i(\overline{\Delta\beta} - i\overline{g}/2)B_2 + i\overline{\kappa}A_2$$

$$\{\overline{q} - (\overline{\Delta\beta} - i\overline{g}/2)\}B_2 = \overline{\kappa}A_2. \tag{3.1.8}$$

Equations (3.1.5),(3.1.6), (3.1.7) and (3.1.8) relate the constants A_1, A_2, B_1 and B_2. Substituting (3.1.7) in (3.1.5) yields:

$$\{\overline{q} - (\overline{\Delta\beta} - i\frac{\overline{g}}{2})\}A_1 = \overline{\kappa}\frac{-\overline{\kappa}A_1}{\{\overline{q}) + (\overline{\Delta\beta} - i\frac{\overline{g}}{2})\}} \tag{3.1.9}$$

$$\{\overline{q} - (\overline{\Delta\beta} - i\frac{\overline{g}}{2})\}\{\overline{q}) + (\overline{\Delta\beta} - i\frac{\overline{g}}{2})\} = -(\overline{\kappa})^2$$

$$(\overline{q})^2 = (\overline{\Delta\beta} - i\overline{g}/2)^2 - (\overline{\kappa})^2$$

$$\overline{q} = \pm\sqrt{(\overline{\Delta\beta} - i\frac{\overline{g}}{2})^2 - (\overline{\kappa})^2}. \tag{3.1.10}$$

This expression defines the unknown eigenvalue $\overline{q}$ in terms of known values of coupling constant $\overline{\kappa}$, detuning $\overline{\Delta\beta}$, and gain $\overline{g}$. The same expression is obtained if we use (3.1.8) in (3.1.6).

3.1.3 Amplifier Boundary Conditions and Specific Solution

Using the DFB resonator as a resonant type amplifier means that there is no backward propagating wave at $\zeta = 1$ i.e. $B(\zeta = 1) = 0$. Applying this condition to (3.1.4) yields:

$$B(\zeta) = B_1 e^{i\overline{q}\zeta} + B_2 e^{-i\overline{q}\zeta}$$

$$B(1) = B_1 e^{i\overline{q}} + B_2 e^{-i\overline{q}}$$

$$0 = B_1 e^{i\overline{q}} + B_2 e^{-i\overline{q}}$$

$$B_2 = -B_1 e^{2i\overline{q}}.$$

Substituting the above relation for B_2 into (3.1.4) yields:

$$B(\zeta) = B_1 e^{i\overline{q}\zeta} + B_2 e^{-i\overline{q}\zeta}$$

$$B(\zeta) = B_1 e^{i\overline{q}\zeta} + (-B_1 e^{2i\overline{q}}) e^{-i\overline{q}\zeta}$$

$$B(\zeta) = B_1 e^{i\overline{q}\zeta} - B_1 e^{2i\overline{q} - i\overline{q}\zeta}$$

$$B(\zeta) = B_1 (\frac{e^{-i\overline{q}}}{e^{-i\overline{q}}})(e^{i\overline{q}\zeta} - e^{2i\overline{q} - i\overline{q}\zeta})$$

$$B(\zeta) = \frac{B_1}{e^{-i\overline{q}}}(e^{i\overline{q}\zeta - i\overline{q}} - e^{-i\overline{q}\zeta + i\overline{q}})$$

$$B(\zeta) = B_1'(\sinh i(\overline{q}\zeta - \overline{q})) \tag{3.1.11}$$

where $B_1' = \frac{B_1}{e^{-i\overline{q}}}$. We can now find $A(\zeta)$ by substituting the expression (3.1.11) for $B(\zeta)$ into (3.1.2):

$$\begin{aligned}
\frac{-dB}{d\zeta} &= i(\overline{\Delta\beta} - i\frac{\overline{g}}{2})B + i\overline{\kappa}A \\
\frac{-d}{d\zeta}\{B_1'(\sinh i(\overline{q}\zeta - \overline{q}))\} &= i(\overline{\Delta\beta} - i\frac{\overline{g}}{2})\{B_1'(\sinh i(\overline{q}\zeta - \overline{q}))\} + i\overline{\kappa}A \\
-B_1'(i\overline{q})(\cosh i(\overline{q}\zeta - \overline{q})) &= i(\overline{\Delta\beta} - i\frac{\overline{g}}{2})\{B_1'(\sinh i(\overline{q}\zeta - \overline{q}))\} + i\overline{\kappa}A.
\end{aligned}$$

Simplifying the above expression yields:

$$\begin{aligned}
-i\overline{\kappa}A &= B_1'(i\overline{q})(\cosh i(\overline{q}\zeta - \overline{q})) + i(\overline{\Delta\beta} - i\frac{\overline{g}}{2})\{B_1'(\sinh i(\overline{q}\zeta - \overline{q}))\} \\
-\overline{\kappa}A &= B_1'(\overline{q})(\cosh i(\overline{q}\zeta - \overline{q})) + (\overline{\Delta\beta} - i\frac{\overline{g}}{2})\{B_1'(\sinh i(\overline{q}\zeta - \overline{q}))\} \\
A(\zeta) &= \frac{-B_1'}{\overline{\kappa}}[\overline{q}\cosh i(\overline{q}\zeta - \overline{q}) + (\overline{\Delta\beta} - i\frac{\overline{g}}{2})\{\sinh i(\overline{q}\zeta - \overline{q})\}]. \qquad (3.1.12)
\end{aligned}$$

3.1.4 Reflectivity and Transmittivity

The transmittivity T at out1 in Figure 2.7 of an active DFB resonator can be expressed using equation (3.1.12) at $\zeta = 1$ and $\zeta = 0$ [16]:

$$T = \frac{|A(\zeta = 1)|^2}{|A(\zeta = 0)|^2} = \frac{|\overline{q}|^2}{|\overline{q}\cosh(-i\overline{q}) + (\overline{\Delta\beta} - i\overline{g}/2)\sinh(-i\overline{q})|^2}.$$

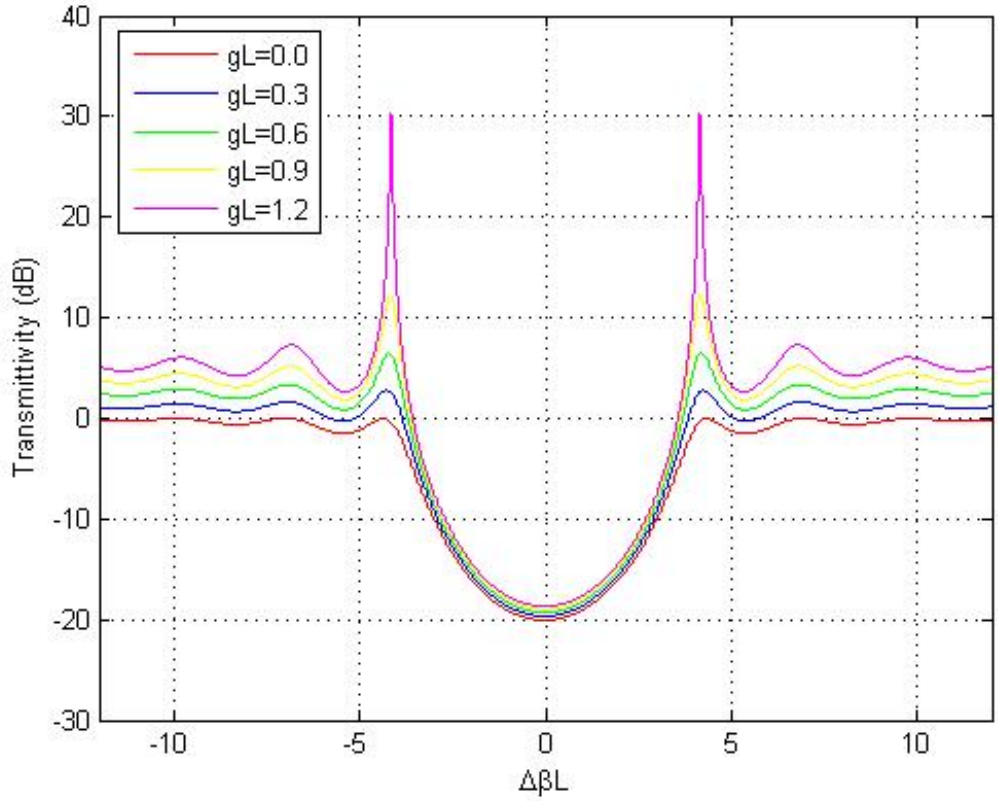

Figure 3.1: *Active DFB - Transmittivity at out1* ($\overline{\kappa} = 3$).

Figure 3.1 depicts the behavior of the transmission peaks of an active DFB resonator with different levels of optical gain versus the normalized detuning. T_{max} on the y-axis represent the highest level of peaks in the spectrum. For this plot, we have chosen the coupling coefficient $\overline{\kappa} = 3$. It is interesting to note that with increasing levels of gain the peaks grow. At a certain detuning and optical gain, the peak may hit infinity even for a very small increase in gain and achieve a lasing action. Such lasing behavior will be studied in more detail in chapter four. Increas-

ing the gain further beyond this point result in a gradual lowering of the peak.

The reflectivity R at out2 in figure 2.7 of an active DFB resonator can be expressed by using equations (3.1.12) and (3.1.11) at $\zeta = 0$ [16]:

$$R = \frac{|B(\zeta = 0)|^2}{|A(\zeta = 0)|^2} = \overline{\kappa}^2 \frac{|\sinh(-i\overline{q})|^2}{|\overline{q}\cosh(-i\overline{q}) + (\overline{\Delta\beta} - i\overline{g}/2)\sinh(-i\overline{q})|^2}.$$

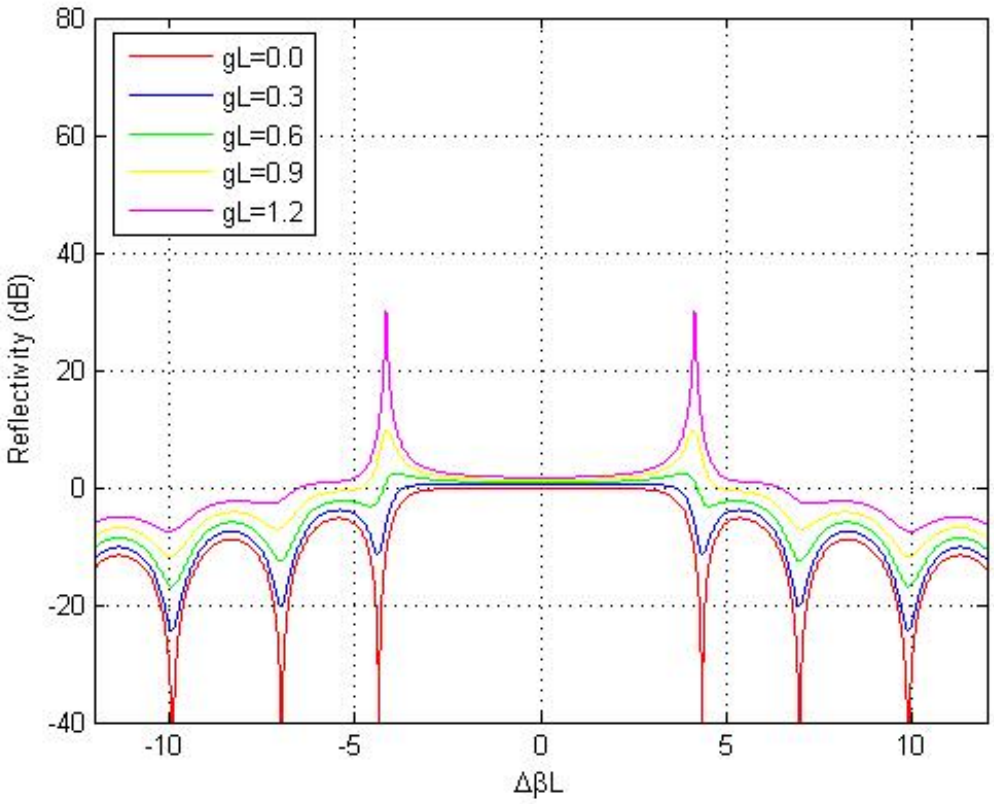

Figure 3.2: *Active DFB - Reflectivity at out2* ($\overline{\kappa} = 3$).

Figure 3.2 depicts the behavior of the reflectivity peaks of an active DFB resonator with different levels of optical gain versus the normalized detuning. For

this plot, we have chosen the coupling coefficient $\overline{\kappa} = 3$. It is interesting to note that with lesser gain the reflectivity dips push downward while with increasing levels of optical gain these peaks grow upward. At a certain detuning and optical gain, the peak may push up and hit infinity even for a very small increase in gain and achieve a lasing action.

3.2 ACTIVE NIM-PIM DC

In this section we study the introduction of optical gain into the NIM-PIM DC for the first time. Contrary to the DFB case, the NIM-PIM structure has two waveguides and the amount of gain in one waveguide can be different from the other. Hence the use of g_p (gain in PIM) and g_n (gain in NIM). A different amount of gain in the waveguides lends an asymmetry to the system which leads to the use of a modified generalized solution for the active NIM PIM DC. The normalized eigenvalue for NIM is expressed as $\overline{q'}$ and the same for PIM can be represented by $\overline{q}$.

3.2.1 Coupled-Mode Equations and General Solution

Normalized coupled-mode equations for active NIM-PIM coupler are:

$$\frac{dA}{d\zeta} = i(\overline{\Delta\beta} - i\overline{g_p}/2)A + i\overline{\kappa}B \tag{3.2.1}$$

$$\frac{-dB}{d\zeta} = i(\overline{\Delta\beta} - i\overline{g_n}/2)B + i\overline{\kappa}A, \tag{3.2.2}$$

where $\zeta = z/L$ is the normalized length, $\overline{g_p} = g_p L$ is the normalized gain in the PIM waveguide, $\overline{g_n} = g_n L$ is the normalized gain in the NIM waveguide, κ is the coupling coefficient, $\kappa L = \overline{\kappa}$ represent the normalized coupling strength, $\Delta\beta$ represents the waveguide detuning, and $\overline{\Delta\beta} = \Delta\beta L$, represent the normalized waveguide detuning. Detuning between two waveguides can be expressed as $\Delta\beta = \beta_1 - \beta_2$. β_1 and β_2 are the respective wavenumbers of light in the PIM and NIM waveguide. $A(\zeta)$ and $B(\zeta)$ represent the amplitude of the forward and backward traveling fields respectively. Equations (3.2.1) and (3.2.2) are the main equations that we will be solving for NIM-PIM coupling.

A modified general solution for the active NIM-PIM system can be postulated as:

$$A(\zeta) = A_1 e^{i\overline{q}\zeta} + A_2 e^{-i\overline{q}\zeta} \tag{3.2.3}$$

$$B(\zeta) = B_1 e^{i\overline{q'}\zeta} + B_2 e^{-i\overline{q'}\zeta} \tag{3.2.4}$$

where $\overline{q}$ and $\overline{q'}$, represents the eigenvalue for the PIM and NIM waveguides as discussed previously. $\overline{q'}$ differs from $\overline{q}$ by an amount x. i.e. $\overline{q'} = \overline{q} + x$. We will

soon arrive at an explicit expression for x later in this chapter. A_1, A_2, B_1 and B_2 are constant coefficients to be solved for.

3.2.2 Dispersion Relation and Eigenvalue

Substituting equations (3.2.3) and (3.2.4) in (3.2.1) yields:

$$\frac{d}{d\zeta}(A_1 e^{i\overline{q}\zeta} + A_2 e^{-i\overline{q}\zeta}) = i(\overline{\Delta\beta} - i\frac{\overline{g_p}}{2})(A_1 e^{i\overline{q}\zeta} + A_2 e^{-i\overline{q}\zeta}) + i\overline{\kappa}(B_1 e^{i\overline{q'}\zeta} + B_2 e^{-i\overline{q'}\zeta})$$

$$A_1(i\overline{q})e^{i\overline{q}\zeta} + A_2(-i\overline{q})e^{-i\overline{q}\zeta} = i(\overline{\Delta\beta} - i\frac{\overline{g_p}}{2})(A_1 e^{i\overline{q}\zeta} + A_2 e^{-i\overline{q}\zeta}) + i\overline{\kappa}(B_1 e^{i\overline{q'}\zeta} + B_2 e^{-i\overline{q'}\zeta}).$$

Equating coefficients of $e^{i\overline{q}\zeta}$ yields:

$$A_1(i\overline{q})e^{i\overline{q}\zeta} = i(\overline{\Delta\beta} - i\overline{g_p}/2)A_1 e^{i\overline{q}\zeta}$$

$$(i\overline{q})A_1 = i(\overline{\Delta\beta} - i\overline{g_p}/2)A_1. \tag{3.2.5}$$

Equating coefficients of $e^{-i\overline{q}\zeta}$ yields:

$$A_2(-i\overline{q})e^{-i\overline{q}\zeta} = i(\overline{\Delta\beta} - i\overline{g_p}/2)A_2 e^{-i\overline{q}\zeta}$$

$$(-i\overline{q})A_2 = i(\overline{\Delta\beta} - i\overline{g_p}/2)A_2. \tag{3.2.6}$$

Equating coefficients of $e^{i\overline{q'}\zeta}$ yields:

$$0 = i\overline{\kappa}(B_1 e^{i\overline{q'}\zeta})$$

$$0 = i\overline{\kappa}B_1. \tag{3.2.7}$$

Equating coefficients of $e^{-i\overline{q'}\zeta}$ yields:

$$0 = i\overline{\kappa}(B_2 e^{-i\overline{q'}\zeta})$$

$$0 = i\overline{\kappa}B_2. \tag{3.2.8}$$

In case of an active DFB resonator we only have to equate the coefficients of $e^{i\overline{q}\zeta}$ and $e^{-i\overline{q}\zeta}$ resulting in two sub equations. The derivation process for an active NIM-PIM DC involves the additional steps of equating coefficients of $e^{i\overline{q'}\zeta}$ and $e^{-i\overline{q'}\zeta}$ which eventually result in four sub equations. Later, we combine these four sub equations into two sub equations. Substituting equations (3.2.3) and (3.2.4) in (3.2.2) yields:

$$\frac{-d}{d\zeta}(B_1 e^{i\overline{q'}\zeta} + B_2 e^{-i\overline{q'}\zeta}) = i(\overline{\Delta\beta} - i\frac{\overline{g_n}}{2})(B_1 e^{i\overline{q'}\zeta} + B_2 e^{-i\overline{q'}\zeta}) + i\overline{\kappa}(A_1 e^{i\overline{q}\zeta} + A_2 e^{-i\overline{q}\zeta})$$

$$B_1(-i\overline{q'})e^{i\overline{q'}\zeta} - B_2(-i\overline{q'})e^{-i\overline{q'}\zeta} = i(\overline{\Delta\beta} - i\frac{\overline{g_n}}{2})(B_1 e^{i\overline{q'}\zeta} + B_2 e^{-i\overline{q'}\zeta}) + i\overline{\kappa}(A_1 e^{i\overline{q}\zeta} + A_2 e^{-i\overline{q}\zeta}).$$

Equating coefficients of $e^{i\overline{q}\zeta}$ yields:

$$0 = i\overline{\kappa}(A_1 e^{i\overline{q}\zeta})$$

$$0 = i\overline{\kappa}A_1. \tag{3.2.9}$$

Equating coefficients of $e^{-i\overline{q}\zeta}$ yields:

$$0 = i\overline{\kappa}(A_2 e^{-i\overline{q}\zeta})$$

$$0 = i\overline{\kappa}A_2. \tag{3.2.10}$$

Equating coefficients of $e^{i\overline{q'}\zeta}$ yields:

$$B_1(-i\overline{q'})e^{i\overline{q'}\zeta} = i(\overline{\Delta\beta} - i\overline{g_n}/2)(B_1 e^{i\overline{q'}\zeta})$$

$$B_1(-i\overline{q'}) = i(\overline{\Delta\beta} - i\overline{g_n}/2)B_1. \tag{3.2.11}$$

Equating coefficients of $e^{-i\overline{q'}\zeta}$ yields:

$$-B_2(-i\overline{q'})e^{-i\overline{q'}\zeta} = i(\overline{\Delta\beta} - i\overline{g_n}/2)(B_2 e^{-i\overline{q'}\zeta})$$

$$-B_2(-i\overline{q'}) = i(\overline{\Delta\beta} - i\overline{g_n}/2)B_2. \tag{3.2.12}$$

Similar to the process followed for the coupled-mode expression for PIM, NIM-PIM waveguides also involve the additional steps of equating coefficients of $e^{i\overline{q'}\zeta}$ and $e^{-i\overline{q'}\zeta}$ which eventually result in four sub equations. This situation is different from an active DFB resonator where we end up with two sub equations. Later, we combine these four sub equations into two sub equations.

Now, we can combine (3.2.5) and (3.2.7). Addition of these two equations yields:

$$(i\overline{q})A_1 = i(\overline{\Delta\beta} - i\overline{g_p}/2)A_1 + i\overline{\kappa}B_1$$

$$\overline{q}A_1 = (\overline{\Delta\beta} - i\overline{g_p}/2)A_1 + \overline{\kappa}B_1$$

$$(\overline{q} - \overline{\Delta\beta} + i\overline{g_p}/2)A_1 = \overline{\kappa}B_1. \tag{3.2.13}$$

Adding (3.2.6) and (3.2.8) yields:

$$
\begin{aligned}
(-i\overline{q})A_2 &= i(\overline{\Delta\beta} - i\overline{g_p}/2)A_2 + i\overline{\kappa}B_2 \\
(-\overline{q})A_2 &= (\overline{\Delta\beta} - i\overline{g_p}/2)A_2 + \overline{\kappa}B_2 \\
(\overline{q} + \overline{\Delta\beta} - i\overline{g_p}/2)A_2 &= -\overline{\kappa}B_2. \qquad (3.2.14)
\end{aligned}
$$

Adding (3.2.9) and (3.2.11) yields:

$$
\begin{aligned}
(-i\overline{q'})B_1 &= i(\overline{\Delta\beta} - i\overline{g_n}/2)B_1 + i\overline{\kappa}A_1 \\
(-\overline{q'})B_1 &= (\overline{\Delta\beta} - i\overline{g_n}/2)B_1 + \overline{\kappa}A_1 \\
(\overline{q'} + \overline{\Delta\beta} - i\overline{g_n}/2)B_1 &= -\overline{\kappa}A_1. \qquad (3.2.15)
\end{aligned}
$$

Adding (3.2.10) and (3.2.12) yields:

$$
\begin{aligned}
-(-i\overline{q'})B_2 &= i(\overline{\Delta\beta} - i\overline{g_n}/2)B_2 + i\overline{\kappa}A_2 \\
(\overline{q'})B_2 &= (\overline{\Delta\beta} - i\overline{g_n}/2)B_2 + \overline{\kappa}A_2 \\
(\overline{q'} - \overline{\Delta\beta} + i\overline{g_n}/2)B_2 &= \overline{\kappa}A_2. \qquad (3.2.16)
\end{aligned}
$$

Equations (3.2.13), (3.2.14), (3.2.15) and (3.2.16) relate the constants A_1, A_2, B_1 and B_2. Substituting (3.2.15) in (3.2.13) yields:

$$
\begin{aligned}
(\overline{q} - \overline{\Delta\beta} + i\overline{g_p}/2)A_1 &= \overline{\kappa}B_1 \\
(\overline{q} - \overline{\Delta\beta} + i\overline{g_p}/2)A_1 &= \overline{\kappa}[-\overline{\kappa}A_1/(\overline{q'} + \overline{\Delta\beta} - i\overline{g_n}/2)] \\
(\overline{q} - \overline{\Delta\beta} + i\overline{g_p}/2)(\overline{q'} + \overline{\Delta\beta} - i\overline{g_n}/2) &= -(\overline{\kappa})^2.
\end{aligned}
$$

The above expression differs from the standard active DFB resonator case as it contains two different variables g_p and g_n. Taking the product yields:

$$\overline{q}\overline{q'} + \overline{q}(\overline{\Delta\beta} - i\frac{\overline{g_n}}{2}) - \overline{q'}(\overline{\Delta\beta} - i\frac{\overline{g_p}}{2}) + \overline{\Delta\beta}(i\frac{\overline{g_p}}{2} + i\frac{\overline{g_n}}{2}) - (\overline{\Delta\beta})^2 + \frac{\overline{g_p g_n}}{4} = -(\overline{\kappa})^2. \tag{3.2.17}$$

Substituting (3.2.16) in (3.2.14) yields:

$$(\overline{q} + \overline{\Delta\beta} - i\overline{g_p}/2)A_2 = -\overline{\kappa}[\overline{\kappa}A_2/(\overline{q'} - \overline{\Delta\beta} + i\overline{g_n}/2)]$$

$$(\overline{q} + \overline{\Delta\beta} - i\overline{g_p}/2)(\overline{q'} - \overline{\Delta\beta} + i\overline{g_n}/2) = -(\overline{\kappa})^2.$$

Taking the product:

$$\overline{q}\overline{q'} - \overline{q}(\overline{\Delta\beta} - i\frac{\overline{g_n}}{2}) + \overline{q'}(\overline{\Delta\beta} - i\frac{\overline{g_p}}{2}) + \overline{\Delta\beta}(i\frac{\overline{g_p}}{2} + i\frac{\overline{g_n}}{2}) - \overline{\Delta\beta}^2 + \frac{\overline{g_p g_n}}{4} = -(\overline{\kappa})^2. \tag{3.2.18}$$

Adding (3.2.17) and (3.2.18):

$$2(\overline{q}\overline{q'}) + 2\overline{\Delta\beta}(i\frac{\overline{g_p}}{2} + i\frac{\overline{g_n}}{2}) - 2(\overline{\Delta\beta})^2 + \frac{\overline{g_p g_n}}{2} + 2(\overline{\kappa})^2 = 0$$

$$\overline{q}\overline{q'} - [(\overline{\Delta\beta})^2 - (\overline{\kappa})^2 - \overline{\Delta\beta}(i\frac{\overline{g_p}}{2} + i\frac{\overline{g_n}}{2}) - \frac{\overline{g_p g_n}}{2}] = 0. \tag{3.2.19}$$

Subtracting (3.2.18) from (3.2.17) yields:

$$
\begin{aligned}
2\overline{q}(\overline{\Delta\beta} - i\frac{\overline{g_n}}{2}) - 2\overline{q'}(\overline{\Delta\beta} - i\frac{\overline{g_p}}{2}) &= 0 \\
\overline{q}(\overline{\Delta\beta} - i\frac{\overline{g_n}}{2}) - \overline{q'}(\overline{\Delta\beta} - i\frac{\overline{g_p}}{2}) &= 0 \\
\overline{q}(\overline{\Delta\beta} - i\frac{\overline{g_n}}{2}) &= \overline{q'}(\overline{\Delta\beta} - i\frac{\overline{g_p}}{2}) \\
(\overline{q'} - x)(\overline{\Delta\beta} - i\frac{\overline{g_n}}{2}) &= \overline{q'}(\overline{\Delta\beta} - i\frac{\overline{g_p}}{2}) \\
\overline{q'\Delta\beta} - \overline{q'}(i\frac{\overline{g_n}}{2}) - x\overline{\Delta\beta} + x(i\frac{\overline{g_n}}{2}) &= \overline{q'\Delta\beta} - \overline{q'}(i\frac{\overline{g_p}}{2}) \\
-\overline{q'}(i\frac{\overline{g_n}}{2}) + \overline{q'}(i\frac{\overline{g_p}}{2}) &= x\overline{\Delta\beta} - x(i\frac{\overline{g_n}}{2}) \\
\overline{q'}(i\frac{\overline{g_p}}{2} - i\frac{\overline{g_n}}{2}) &= x(\overline{\Delta\beta} - i\frac{\overline{g_n}}{2}) \\
x &= \frac{\overline{q'}(i\frac{\overline{g_p}}{2} - i\frac{\overline{g_n}}{2})}{(\overline{\Delta\beta} - i\frac{\overline{g_n}}{2})}.
\end{aligned}
\tag{3.2.20}
$$

Here, we introduce a new quantity $'H'$, defined as $x = \overline{q'}H$, which yields:

$$
H = \frac{(i\overline{g_p}/2 - i\overline{g_n}/2)}{(\overline{\Delta\beta} - i\overline{g_n}/2)}. \tag{3.2.21}
$$

The eigenvalue $\overline{q}$ and $\overline{q'}$ are related by H as follows:

$$
\begin{aligned}
\overline{q'} &= \overline{q} + x \\
\overline{q'} &= \overline{q} + \overline{q'}H \\
\overline{q} &= \overline{q'} - \overline{q'}H \\
\overline{q} &= \overline{q'}(1 - H).
\end{aligned}
\tag{3.2.22}
$$

Using (3.2.22) and substituting for $\overline{q}$ in (3.2.19) yields:

$$\begin{aligned}
\overline{q}\overline{q'} - [(\overline{\Delta\beta})^2 - (\overline{\kappa})^2 - \overline{\Delta\beta}(i\frac{\overline{g_p}}{2} + i\frac{\overline{g_n}}{2}) - \frac{\overline{g_p g_n}}{2}] = 0 \\
(\overline{q'}(1-H))\overline{q'} - [(\overline{\Delta\beta})^2 - (\overline{\kappa})^2 - \overline{\Delta\beta}(i\frac{\overline{g_p}}{2} + i\frac{\overline{g_n}}{2}) - \frac{\overline{g_p g_n}}{2}] = 0 \\
(\overline{q'})^2(1-H) - [(\overline{\Delta\beta})^2 - (\overline{\kappa})^2 - \overline{\Delta\beta}(i\frac{\overline{g_p}}{2} + i\frac{\overline{g_n}}{2}) - \frac{\overline{g_p g_n}}{2}] = 0.
\end{aligned}$$

Applying the quadratic formula yields:

$$\begin{aligned}
\overline{q'} = \pm\sqrt{\frac{-4(1-H)[-(\overline{\Delta\beta})^2 + (\overline{\kappa})^2 + \overline{\Delta\beta}(i\frac{\overline{g_p}}{2} + i\frac{\overline{g_n}}{2}) + \frac{\overline{g_p g_n}}{4}]}{4(1-H)^2}} \\
\overline{q'} = \pm\sqrt{\frac{(\overline{\Delta\beta})^2 - (\overline{\kappa})^2 - \overline{\Delta\beta}(i\frac{\overline{g_p}}{2} + i\frac{\overline{g_n}}{2}) - \frac{\overline{g_p g_n}}{4}}{(1-H)}}.
\end{aligned} \tag{3.2.23}$$

This expression defines the unknown eigenvalue $\overline{q'}$ in terms of $\overline{\kappa}$, H, $\overline{g_p}$, $\overline{g_n}$, and $\overline{\Delta\beta}$. H is defined in terms of $\overline{g_p}$, $\overline{g_n}$, and $\overline{\Delta\beta}$.

3.2.3 Amplifier Boundary Conditions and Specific Solution

Here, we apply amplifier boundary conditions to an active NIM-PIM coupler. Similar to the case of an active DFB resonator, there is no backward propagating wave in the NIM-PIM DC at $\zeta = 1$ i.e. $B(\zeta = 1) = 0$.

$$\begin{aligned}
B(\zeta) &= B_1 e^{i\overline{q'}\zeta} + B_2 e^{-i\overline{q'}\zeta} \\
B(1) &= B_1 e^{i\overline{q'}} + B_2 e^{-i\overline{q'}} \\
0 &= B_1 e^{i\overline{q'}} + B_2 e^{-i\overline{q'}} \\
B_2 &= -B_1 e^{2i\overline{q'}}.
\end{aligned} \tag{3.2.24}$$

Substituting the above expression for B_2 into (3.2.4) yields:

$$
\begin{aligned}
B(\zeta) &= B_1 e^{i\overline{q'}\zeta} + B_2 e^{-i\overline{q'}\zeta} \\
B(\zeta) &= B_1 e^{i\overline{q'}\zeta} + (-B_1 e^{2i\overline{q'}}) e^{-i\overline{q'}\zeta} \\
B(\zeta) &= B_1 e^{i\overline{q'}\zeta} - B_1 e^{2i\overline{q'} - i\overline{q'}\zeta} \\
B(\zeta) &= B_1 (\frac{e^{-i\overline{q'}}}{e^{-i\overline{q'}}})(e^{i\overline{q'}\zeta} - e^{2i\overline{q'} - i\overline{q'}\zeta}) \\
B(\zeta) &= \frac{B_1}{e^{-i\overline{q'}}}(e^{i\overline{q'}\zeta - i\overline{q'}} - e^{-i\overline{q'}\zeta + i\overline{q'}}) \\
B(\zeta) &= B_1'(\sinh i(\overline{q'}\zeta - \overline{q'})) \qquad (3.2.25)
\end{aligned}
$$

where $B_1' = \frac{B_1}{e^{-i\overline{q}}}$. We can now find $A(\zeta)$ by using expression (3.2.25) in equation (3.2.2):

$$
\begin{aligned}
\frac{-dB}{d\zeta} &= i(\overline{\Delta\beta} - i\frac{\overline{g_n}}{2})B + i\overline{\kappa}A \\
\frac{-d}{d\zeta}(B_1' \sinh\{i(\overline{q'}\zeta - \overline{q'})\}) &= i(\overline{\Delta\beta} - i\frac{\overline{g_n}}{2})(B_1' \sinh\{i(\overline{q'}\zeta - \overline{q'})\}) + i\overline{\kappa}A \\
-B_1'(i\overline{q'}) \cosh\{i(\overline{q'}\zeta - \overline{q'})\} &= i(\overline{\Delta\beta} - i\frac{\overline{g_n}}{2})(B_1' \sinh\{i(\overline{q'}\zeta - \overline{q'})\}) + i\overline{\kappa}A.
\end{aligned}
$$

Solving the above expression for A:

$$
\begin{aligned}
-i\overline{\kappa}A &= B_1'(i\overline{q'})(\cosh i(\overline{q'}\zeta - \overline{q'})) + i(\overline{\Delta\beta} - i\frac{\overline{g_n}}{2})(B_1'(\sinh i(\overline{q'}\zeta - \overline{q'}))) \\
-\overline{\kappa}A &= B_1'(\overline{q'})(\cosh i(\overline{q'}\zeta - \overline{q'})) + (\overline{\Delta\beta} - i\frac{\overline{g_n}}{2})(B_1'(\sinh i(\overline{q'}\zeta - \overline{q'}))) \\
A(\zeta) &= \frac{-B_1'}{\overline{\kappa}}[\overline{q'}(\cosh i(\overline{q'}\zeta - \overline{q'})) + (\overline{\Delta\beta} - i\frac{\overline{g_n}}{2}) \sinh i(\overline{q'}\zeta - \overline{q'})]. \qquad (3.2.26)
\end{aligned}
$$

3.2.4 Reflectivity and Transmittivity

The reflectivity at out2 in Figure 2.3 of an active NIM-PIM DC can be expressed using equations (3.2.25) and (3.2.26) as:

$$R = \frac{|B(\zeta=0)|^2}{|A(\zeta=0)|^2} = \overline{\kappa}^2 \frac{|\sinh(-i\overline{q'})|^2}{|\overline{q'}\cosh(-i\overline{q'}) + (\overline{\Delta\beta} - i\overline{g_n}/2)\sinh(-i\overline{q'})|^2}.$$

Transmittivity at out1 in Figure 2.3 of an active NIM-PIM DC can be expressed using equations (3.2.25) and (3.2.26) as:

$$T = \frac{|A(\zeta=1)|^2}{|A(\zeta=0)|^2} = \frac{|\overline{q'}|^2}{|\overline{q'}\cosh(-i\overline{q'}) + (\overline{\Delta\beta} - i\overline{g_n}/2)\sinh(-i\overline{q'})|^2}. \quad (3.2.27)$$

The expressions obtained above are the general expressions for transmittivity T and reflectivity R of an active NIM-PIM DC. Note that the sign of $\overline{q'}$ does not affect R or T. Altering the values of optical gain in either one or both the waveguides of the NIM-PIM DC may result in a simplified form of these expressions. Such scenarios are discussed as follows:

Case: $\overline{\mathbf{g_p}} = \overline{\mathbf{g_n}} = \overline{\mathbf{g}}$:

Now we analyze the case when both PIM and NIM waveguides have the same amount of gain. 'H', the offset between $\overline{q}$ and $\overline{q'}$ is reduced to zero. This implies

that $\overline{q} = \overline{q'}$ in the case of equal gain.

$$H = \frac{(i\overline{g_p}/2 - i\overline{g_n}/2)}{(\overline{\Delta\beta} - i\overline{g_n}/2)}$$

$$H = \frac{(i\overline{g}/2 - i\overline{g}/2)}{(\overline{\Delta\beta} - i\overline{g}/2)}$$

$$\Rightarrow H = 0$$

$$\overline{q} = \overline{q'}(1 - H)$$

$$\Rightarrow \overline{q} = \overline{q'}.$$

The dispersion relation (3.2.23) boils down to an expression which is the equal to that of the active DFB resonator.

$$\overline{q'} = \pm\sqrt{\frac{(\overline{\Delta\beta})^2 - (\overline{\kappa})^2 - \overline{\Delta\beta}(i\overline{g_p}/2 + i\overline{g_n}/2) - (\overline{g_p g_n})/4]}{(1 - H)}}$$

$$\overline{q} = \pm\sqrt{(\overline{\Delta\beta})^2 - (\overline{\kappa})^2 - \overline{\Delta\beta}(i\overline{g}/2 + i\overline{g}/2) - (\overline{gg})/4}$$

$$\overline{q} = \pm\sqrt{(\overline{\Delta\beta})^2 - 2(\overline{\Delta\beta})(i\overline{g}/2) + (i\overline{g}/2)^2 - (\overline{\kappa})^2}$$

$$\overline{q} = \pm\sqrt{(\overline{\Delta\beta} - i\overline{g}/2)^2 - \overline{\kappa}^2}.$$

The transmittivity T for the equal gain case is:

$$T = \frac{|A(\zeta = 1)|^2}{|A(\zeta = 0)|^2} = \frac{|\overline{q}|^2}{|\overline{q}\cosh(-i\overline{q}) + (\overline{\Delta\beta} - i\overline{g}/2)\sinh(-i\overline{q})|^2}.$$

Using this simplified expression of 'T' and plotting the transmittivity versus the detuning results in Figure 3.3. T_{max} on the y-axis represent the highest peaks in the spectrum. For this plot, we have chosen coupling coefficient $\overline{\kappa} = 3$. It is interesting to note that with increasing levels of gain the peaks grow on both sides of the

stopband. At a certain detuning and optical gain, the peak may hit infinity even for a very small increase in gain and achieve a lasing action. This behavior is the same as that of an active DFB resonator. It is also observed that the identical levels of peaks result from the same values of $\overline{\Delta\beta}$ and $\overline{g}$ as those of the active DFB resonator in Figure 3.1. Hence, it is concluded that under equal gain circumstances, an active NIM-PIM DC acts like an active DFB resonator.

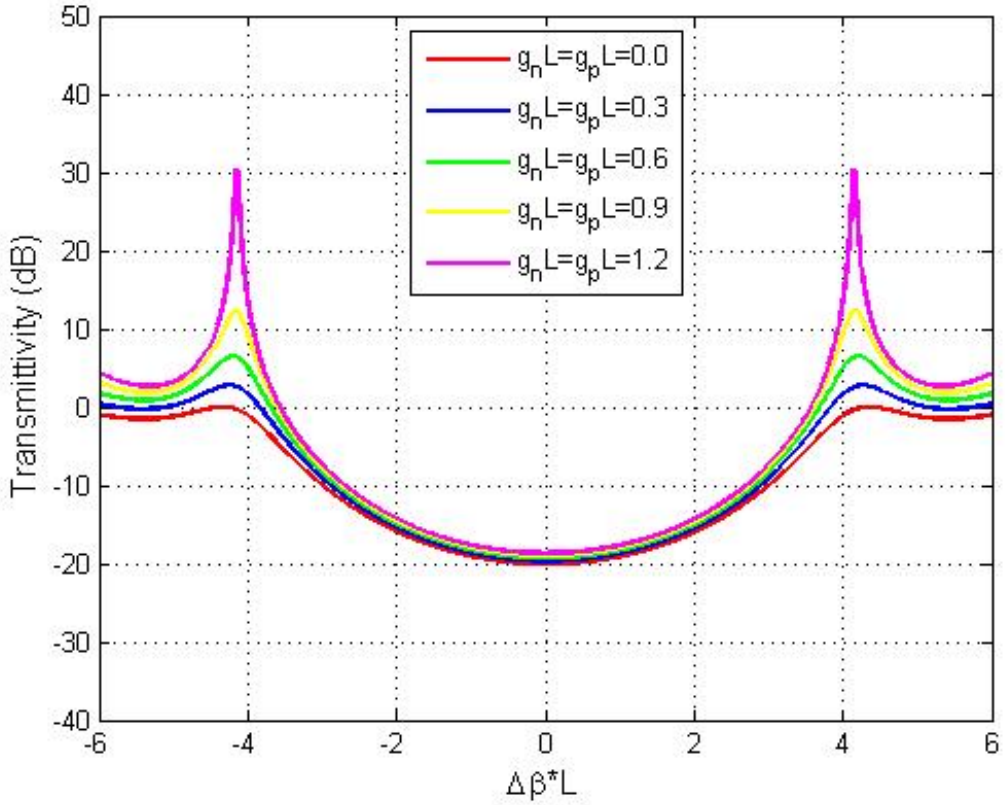

Figure 3.3: *Active NIM PIM DC - Transmittivity ($\overline{g_p} = \overline{g_n} = \overline{g}$) and $\overline{\kappa} = 3$.*

Figure 3.4 depicts the behavior of reflectivity peaks of an active NIM-PIM DC

with different levels of optical gain versus the normalized detuning. For this plot, we have chosen coupling coefficient $\overline{\kappa} = 3$. It is interesting to note that with lesser gain the reflectivity dips push downward while with increasing levels of optical gain these peaks grow upward. At a certain detuning and optical gain, the peak may push up and hit infinity even for a very small increase in gain and achieve a lasing action. It is also observed that the identical levels of peaks result from the same values of $\overline{\Delta\beta}$ and $\overline{g}$ as those of the active DFB resonator in Figure 3.2. Hence, it is concluded that under equal gain circumstances, an active NIM-PIM DC acts like an active DFB resonator.

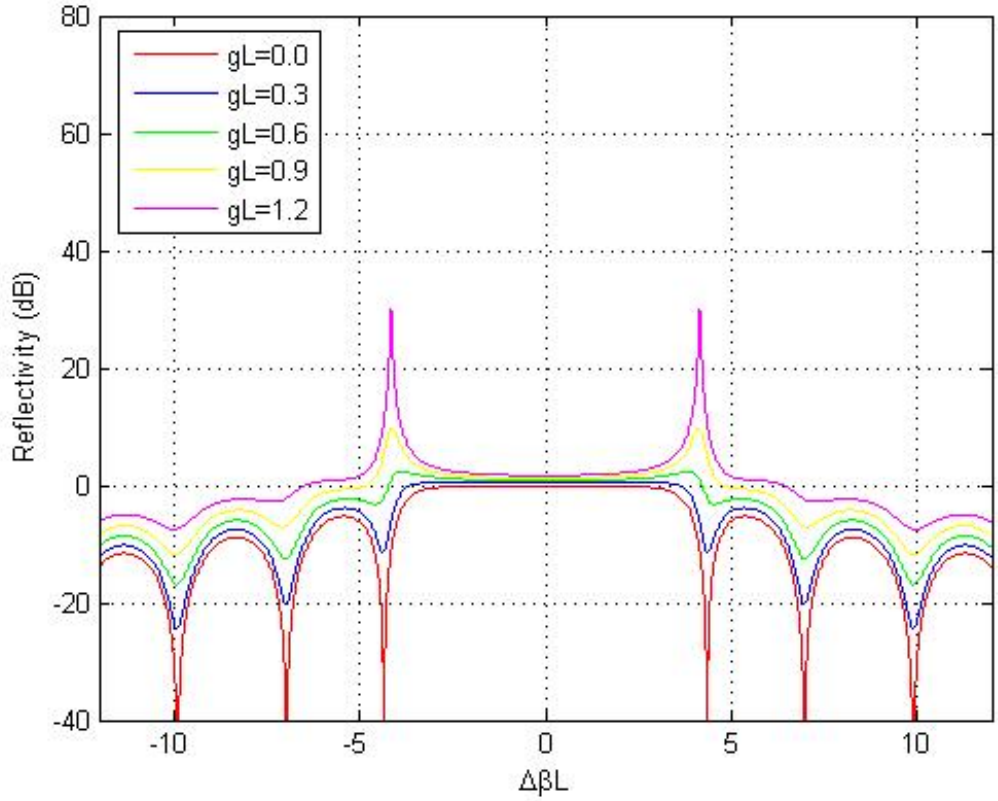

Figure 3.4: *Active DFB - Reflectivity ($\overline{g_p} = \overline{g_n} = \overline{g}$) and $\overline{\kappa} = 3$.*

Case: $\overline{g_p} = \overline{g}$ and $\overline{g_n} = 0$:

Next we analyze the case where we have introduced gain into the PIM waveguide while there is no such gain or loss in the NIM waveguide. 'H', the offset between

$\overline{q}$ and $\overline{q'}$ is reduced to:

$$H = \frac{(i\overline{g_p}/2 - i\overline{g_n}/2)}{(\overline{\Delta\beta} - i\overline{g_n}/2)}$$
$$H = \frac{(i\overline{g}/2 - 0)}{(\overline{\Delta\beta} - 0)}$$
$$H = \frac{i\overline{g}/2}{\overline{\Delta\beta}}.$$

The dispersion relation boils down to the following expression:

$$\overline{q'} = \pm\sqrt{\frac{(\overline{\Delta\beta})^2 - (\overline{\kappa})^2 - \overline{\Delta\beta}(i\frac{\overline{g_p}}{2} + i\frac{\overline{g_n}}{2}) - \frac{\overline{g_p g_n}}{4}}{(1-H)}}$$
$$\overline{q'} = \pm\sqrt{\frac{(\overline{\Delta\beta})^2 - (\overline{\kappa})^2 - \overline{\Delta\beta}(i\frac{\overline{g}}{2} + 0) - 0}{(1-H)}}$$
$$\overline{q'} = \pm\sqrt{\frac{\overline{\Delta\beta}^2 - \overline{\kappa}^2 - \overline{\Delta\beta}i\overline{g}/2}{(1-H)}}.$$

The transmittivity T in case of the above mentioned scenario is:

$$\frac{|A(\zeta=1)|^2}{|A(\zeta=0)|^2} = \frac{|\overline{q'}|^2}{|\overline{q'}\cosh(-i\overline{q'}) + \overline{\Delta\beta}\sinh(-i\overline{q'})|^2}.$$

We may now use the above simplified expression of 'T' for analyzing the transmission spectrum of an active NIM-PIM DC with gain in PIM only. Plotting transmittivity versus the detuning results in Figure 3.5 where T_{max} on the y-axis represent the highest peaks in the spectrum. For this plot, we have chosen coupling coefficient $\overline{\kappa} = 3$. It is interesting to note that similar to the case of equal optical gain in both waveguides, increasing levels of gain result in the growth of peaks on both sides of the stopband. At a certain detuning and optical gain, the peak may hit infinity even for a very small increase in gain and achieve a lasing action. However,

it is observed that much higher amounts of optical gain are required in the PIM to accomplish lasing.

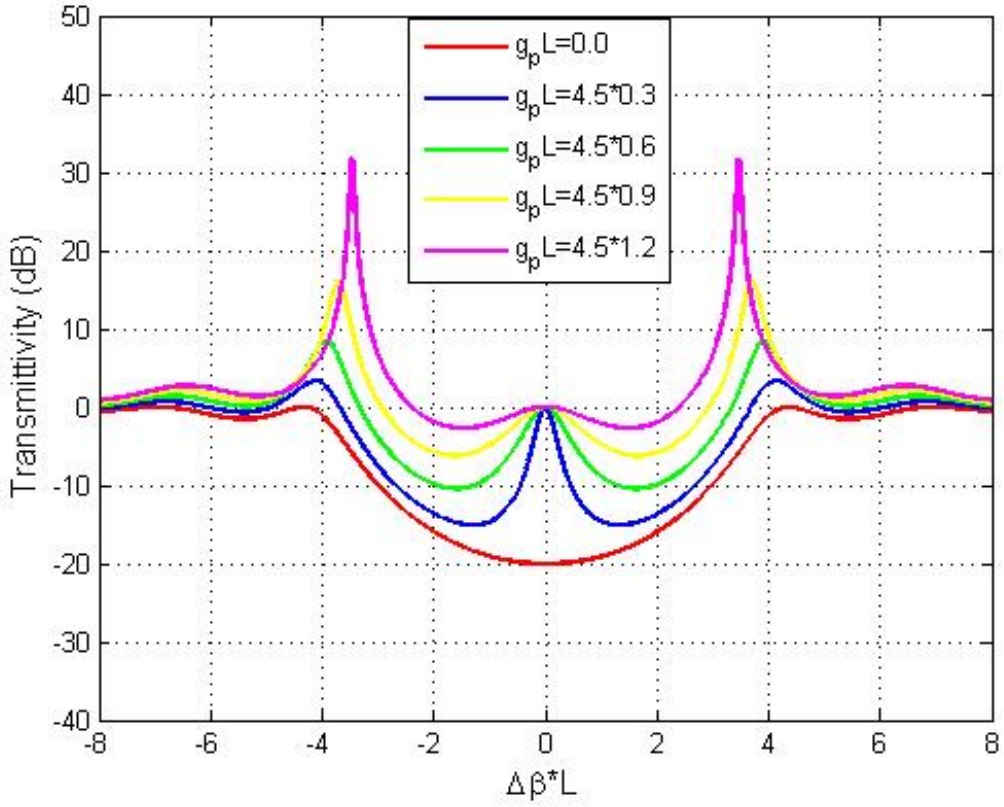

Figure 3.5: *Active NIM-PIM DC - Transmittivity ($\overline{g_p} = \overline{g}$ and $\overline{g_n} = 0$ and $\overline{\kappa} = 3$).*

Hence, it can be concluded that in the case where we have gain in the PIM waveguide and zero gain/loss in the NIM waveguide, more than twice the gain is required by the active NIM PIM DC to achieve the same levels of peaks as those of an active NIM-PIM DC with equal gain in each waveguide.

In Figure 3.5, we do notice a small hump in the middle and the transmittivity

seems to get clamped at zero at this point. The following mathematical reasoning may help explain this phenomena. The hump occurs at $\overline{\Delta\beta} = 0$ and for the case where $g_n = 0$. Plugging these values of $\overline{\Delta\beta}$ and g_n into equation (3.2.21), and calculating the offset H:

$$H = \frac{(i\overline{g_p}/2 - i\overline{g_n}/2)}{(\overline{\Delta\beta} - i\overline{g_n}/2)}$$
$$H = \frac{(i\overline{g}/2 - 0)}{0}$$
$$H = \infty.$$

Substituting $H = \infty$ in the dispersion relation (3.2.23) yields:

$$\overline{q'} = \pm\sqrt{\frac{(\overline{\Delta\beta})^2 - (\overline{\kappa})^2 - \overline{\Delta\beta}(i\overline{g_p}/2 + i\overline{g_n}/2) - (\overline{g_p g_n})/4}{(1-H)}}$$
$$\overline{q'} = \pm\sqrt{\frac{(\overline{\Delta\beta})^2 - (\overline{\kappa})^2 - \overline{\Delta\beta}(i\overline{g_p}/2)}{\infty}}$$
$$\overline{q'} = 0.$$

Substituting $\overline{q'} = 0$ in the expression for transmittivity T in equation (3.2.27) yields:

$$T = \frac{|A(\zeta=1)|^2}{|A(\zeta=0)|^2} = \frac{|\overline{q'}|^2}{|\overline{q'}\cosh(-i\overline{q'}) + (\overline{\Delta\beta} - i\overline{g_n}/2)\sinh(-i\overline{q'})|^2}$$
$$T = \frac{0}{|0+0|^2}.$$

From Figure 3.5, it is clear that $T = 0$. Thus at $\overline{g_n} = 0$ and $\overline{\Delta\beta} = 0$ for all values of $\overline{g}$ in PIM, $T = 0$.

Case: $\overline{\mathbf{g_p}} >= |\overline{\mathbf{g_n}}|$ and $\overline{\mathbf{g_n}} = -\overline{\mathbf{g}}$:

Next we analyze the case where we have introduced loss into the NIM waveguide and gain into the PIM waveguide. Here, we tried to model a more practical material where NIMs are usually marked by losses. This scenario is very interesting. It is observed in Figure 3.6 that peaks in the spectrum occur at $\overline{\Delta\beta} = 0$ i.e. in the middle of the stopband, with increasing values of optical gain in PIM. For this plot, we have chosen coupling coefficient $\overline{\kappa} = 3$. For a specific loss in NIM, the peak may hit infinity even for a very small increase in gain in the PIM and achieve a lasing action. Moreover, since there is a single strong resonance, the NIM-PIM DC exhibits a single lasing mode.

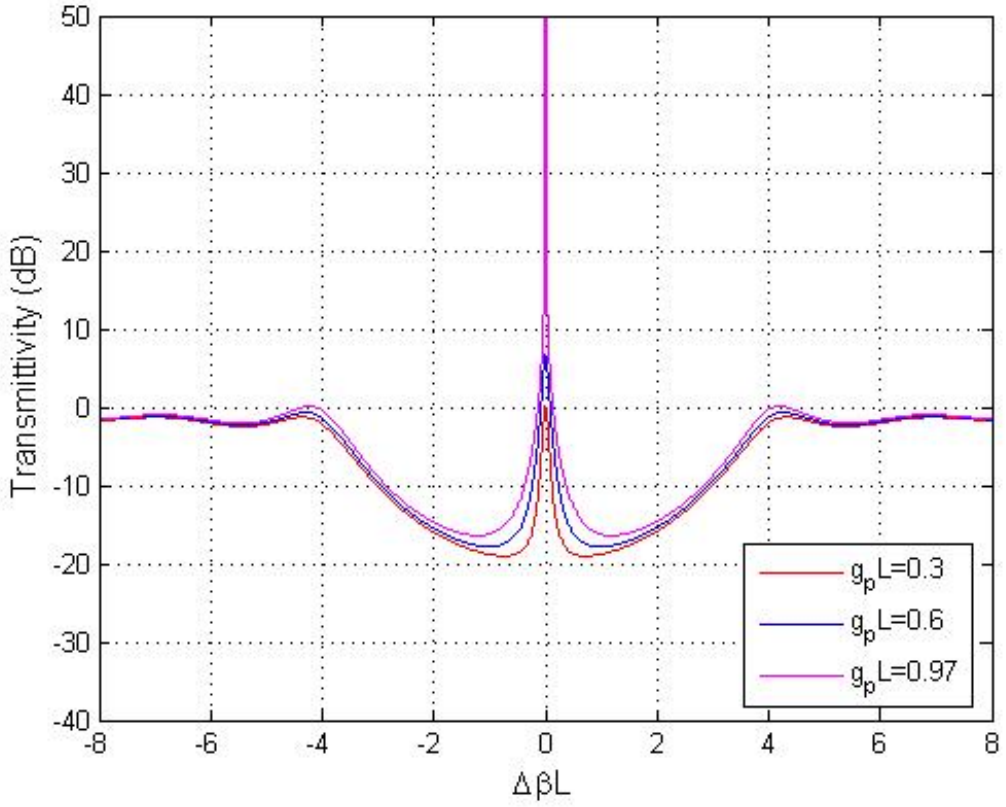

Figure 3.6: *Active NIM-PIM DC - Transmittivity* ($\overline{g_p} >= |\overline{g_n}|$, $\overline{g_n} = -0.3$) *and* $\overline{\kappa} = 3$.

3.3 SUMMARY OF STEPS

Active DFB Resonator

- The steps to follow in order to solve the coupled-mode equations of an active DFB resonator are the same as those carried out for the passive case. The only difference being the addition of g (gain) to the system.

Active NIM PIM DC - Deriving the Dispersion Relation

1. Consider the normalized asymmetric coupled-mode equations. e.g.equations (3.2.1) and (3.2.2).
2. Postulate the general solution e.g. equations (3.2.3) and (3.2.4).
3. Take one of the equations and plug in with the general solution e.g. equations (3.2.3) and (3.2.4) in (3.2.1).
4. Equate the coefficients of $e^{i\overline{q}\zeta}$ and those of $e^{i\overline{q'}\zeta}$ e.g. equations (3.2.5) and (3.2.7).
5. Add the two equations obtained above e.g. equation (3.2.13).
6. Equate the coefficients of $e^{-i\overline{q}\zeta}$ and those of $e^{-i\overline{q'}\zeta}$ e.g. equations (3.2.6) and (3.2.8).
7. Add the two equations obtained above e.g. equation (3.2.14).
8. Repeat the steps above for the second coupled-mode equation. This will also result in two equations. e.g. equations (3.2.3) and (3.2.4) in (3.2.2).
9. Thus, after carrying all these steps mentioned above, four equations are obtained e.g. e.g. equations (3.2.13), (3.2.14), (3.2.15) and (3.2.16).
10. Substitute for the value of B_1 in the first pair of equations, with the its value from the second pair of equations derived above e.g. equation (3.2.15) in (3.2.13).
11. Substitute for the value of B_2 in the first pair of equations, with the its value

from the second pair of equations derived above. e.g. equation (3.2.16) in (3.2.14).

12. Add these two equations and apply the quadratic formula to solve for $\overline{q'}$ i.e. equations (3.2.17) and (3.2.18). Dispersion Relation is obtained!
13. Subtract these two equations and an expression for the offset H is obtained i.e. i.e. equations (3.2.17) and (3.2.18)!

Active NIM-PIM DC - Solving for Transmittivity and Reflectivity

1. Consider the general solution e.g. equations (3.2.3) and (3.2.4).
2. Apply the boundary condition to the general solution to find B_2 e.g. equation (3.2.4).
3. Plug this value of B_2 in the original generalized solution and an expression for $B(\zeta)$ is obtained e.g. equations (3.2.24) and (3.2.4).
4. Consider the first coupled-mode equation and substitute for the value of B with the expression obtained above e.g. equation (3.2.25) in equation (3.2.2).
5. An expression for $A(\zeta)$ is derived e.g. equation (3.2.26).
6. Reflectivity is the ratio of power at $B(\zeta = 0)$ and input power i.e. $A(\zeta = 0)$.
7. Transmittivity is the ratio of power at $A(\zeta = 1)$ and input power i.e. $A(\zeta = 0)$.

CHAPTER 4

LASING BEHAVIOR

4.1 DFB RESONATOR

4.1.1 Lasing and Lasing Modes

Lasing Action

A laser generally consists of a gain medium and reflecting mirrors which provide the effective feedback. Once input light is generated by spontaneous emission, it passes through the gain medium and is amplified through stimulated emission. Since, the light travels back and forth through the laser cavity it undergoes repeated amplification before it is emitted.

The condition where gain equals the cavity losses is known as the lasing threshold. Once the gain overcomes the cavity losses, it results in an exponential increase in output photons, a sign of lasing action. The minimum gain required to achieve

lasing is known as lasing threshold gain [17].

Laser Modes

A resonant cavity consists of two types of spatial modes, the longitudinal modes and transverse modes. Transverse modes are perpendicular to the axis of the resonant cavity. By carefully analyzing a cross section of an output beam from a laser, a number of intensity distributions (patterns) are observed. These are the transverse modes referred to as TEM modes.

Longitudinal modes correspond to the standing waves formed by the waves travelling within the resonant cavity. The resonant cavity only supports waves with certain wavelengths. This can be explained with the help of the following figure:

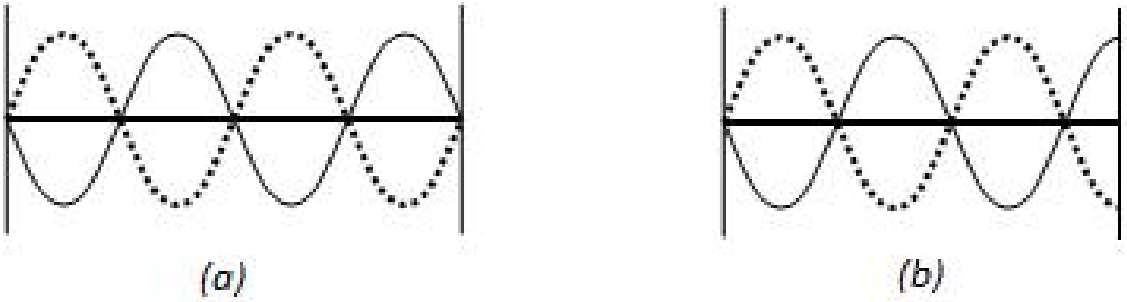

Figure 4.1: *Conditions to generate a standing wave.*

Stimulated light within the cavity travels in all directions and is reflected back after applying the boundary conditions as depicted in Figure 4.1. These reflected waves interfere with each other which may result in either constructive or destruc-

tive interference. Notice in (b), the wave is reflected back with a phase change of 180 degrees. However, this wave suffers a break in its phase. (a) depicts another wave which also suffers a phase change of 180 degrees but, with no break in its phase. Case (a) is the type of wave that results in a standing wave and is supported by the resonator. This condition can be expressed as $2d/\lambda = N$, where d is the distance between the reflecting surfaces, λ is the wavelength and N is an integer [17]. Hence it can be stated that in order to support the longitudinal mode pattern the length of the resonator should be equal to some integer multiple of half of the wavelength and that the resonant cavity's dimensions are very important in deciding the longitudinal laser modes [12]. A laser may support several longitudinal modes. However, only those standing mode patterns which occur in a spatial region of gain above the cavity losses are actually radiated out [17]. The number of longitudinal modes is proportional to the spectral width of a laser.

In the case of a DFB laser, grating perturbations provide the required feedback. The condition required to generate standing waves needs to be modified in terms of Bragg's grating condition expressed as $2\Lambda n_{eff} = \lambda$ where Λ is the grating period, n_{eff} is the refractive index of the medium. Two longitudinal modes are generated where one of them is suppressed in order to yield a single mode highly efficient narrow beam of light. These two modes correspond to the resonant peaks in figure 3.3. Our work on NIM-PIM DC is exciting in part because the spectra in

Figure 3.6 show one dominant mode. This may result in a naturally single-mode laser.

4.1.2 Transmittivity (Lasing Behavior with increasing gain)

Earlier in chapter three, we analyzed the transmission spectrum of an active DFB resonator. It was observed that with an increased gain in the medium, the transmittivity peaks at both ends of the stop band shoot up. At some point in the process, a very small increase in gain will result in very high peaks i.e. reaching infinity. This corresponds to the fact that a DFB resonator with an active gain medium can lase. The following plot depicts this behavior.

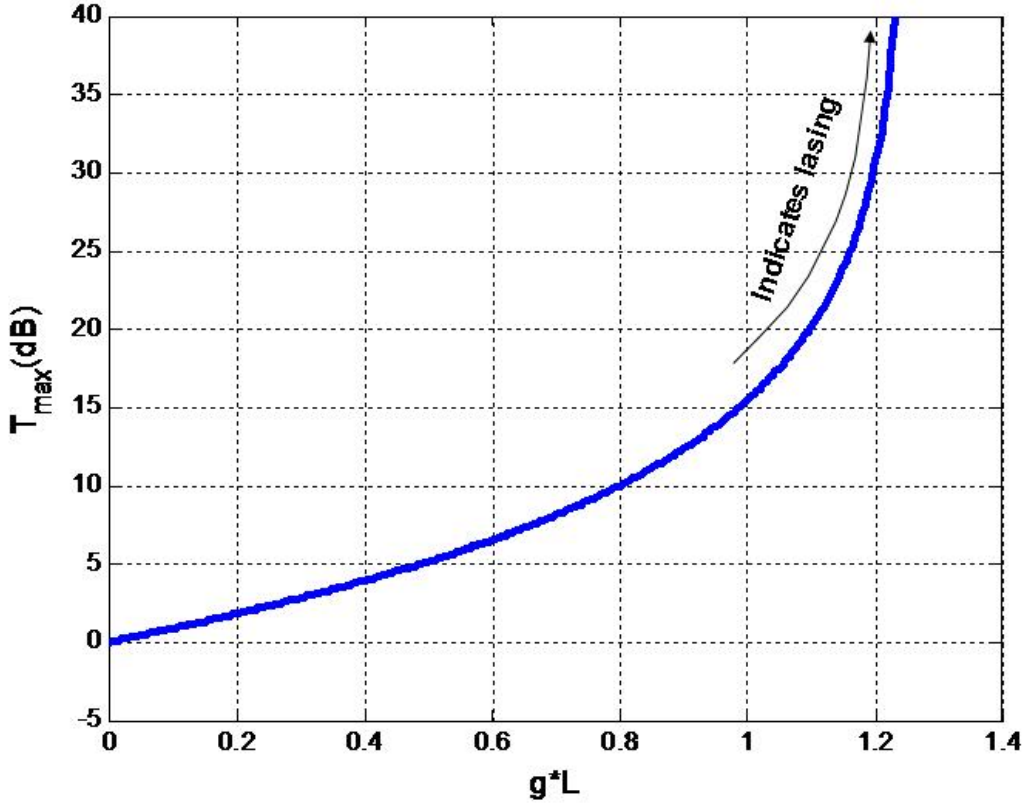

Figure 4.2: *Active DFB Resonator: Lasing Behavior - T_{max} vs Gain, $\overline{\kappa} = 3$.*

In Figure 4.2, the y-axis plots the maximum of the transmittivity spectrum obtained for a specific value of gain while the x-axis plots increasing values of normalized gain $\overline{g}$ for $\overline{\kappa} = 3$. It is observed that maximum transmittivity T_{max} exhibits an exponential increase with increasing values of gain $\overline{g}$. As more and more gain is added to the DFB structure, the transmittivity peaks grow and eventually a point is reached where a very small increase increase in gain would result in a very high peaks reaching infinity indicating the lasing behavior of an active DFB structure.

It is also observed from Figure 4.2 that a threshold gain ($\overline{g_{th}}$) of 1.25 is required to achieve lasing at $\overline{\Delta\beta} = 4.148$, and is termed as the corresponding threshold detuning ($\overline{\Delta\beta_{th}}$). We will be referring back to these threshold values later in section (4.1.5).

4.1.3 Lasing Boundary Conditions and Specific Solution

Boundary conditions for lasing assure that there is no light injected into the active structure:

$$A(\zeta = 0) = 0$$

$$B(\zeta = 1) = 0.$$

Applying the above lasing boundary conditions to the general solution yields:

$$A(\zeta) = A_1 e^{i\bar{q}\zeta} + A_2 e^{-i\bar{q}\zeta}$$

$$0 = A_1 + A_2$$

$$A_2 = -A_1.$$

$A(\zeta)$ can now be expressed as:

$$A(\zeta) = A_1 e^{i\bar{q}\zeta} - A_1 e^{-i\bar{q}\zeta}$$

$$A(\zeta) = A_1 (e^{i\bar{q}\zeta} - e^{-i\bar{q}\zeta}). \tag{4.1.1}$$

Similarly, applying the boundary conditions to $B(\zeta)$ yields:

$$B(\zeta) = B_1 e^{i\bar{q}\zeta} + B_2 e^{-i\bar{q}\zeta}$$

$$0 = B_1 e^{i\bar{q}} + B_2 e^{-i\bar{q}}$$

$$B_2 = -B_1 e^{2i\bar{q}}.$$

Substituting the above expression into the general expression for $B(\zeta)$ yields:

$$B(\zeta) = B_1 e^{i\bar{q}\zeta} + B_2 e^{-i\bar{q}\zeta}$$

$$B(\zeta) = B_1 e^{i\bar{q}\zeta} + (-B_1 e^{2i\bar{q}}) e^{-i\bar{q}\zeta}$$

$$B(\zeta) = B_1 (e^{i\bar{q}\zeta} - e^{2i\bar{q} - i\bar{q}\zeta})$$

$$B(\zeta) = B_1 e^{i\bar{q}} (e^{i\bar{q}\zeta - i\bar{q}} - e^{-i\bar{q}\zeta + i\bar{q}}). \tag{4.1.2}$$

4.1.4 Effective Reflectivity Coefficients

Expressions for the effective reflectivity coefficients encountered by the forward and backward propagating waves can be derived using the expressions derived

earlier in chapter three, i.e., (3.1.5), (3.1.6), (3.1.7) and (3.1.8):

$$r_a = \frac{B_1}{A_1} = \frac{\overline{q} - (\overline{\Delta\beta} - i\overline{g}/2)}{\overline{\kappa}}, \tag{4.1.3}$$

$$r_a = \frac{B_1}{A_1} = \frac{-\overline{\kappa}}{\overline{q} + (\overline{\Delta\beta} - i\overline{g}/2)}, \tag{4.1.4}$$

$$r_b = \frac{A_2}{B_2} = \frac{-\overline{\kappa}}{\overline{q} + (\overline{\Delta\beta} - i\overline{g}/2)}, \tag{4.1.5}$$

$$r_b = \frac{A_2}{B_2} = \frac{\overline{q} - (\overline{\Delta\beta} - i\overline{g}/2)}{\overline{\kappa}}. \tag{4.1.6}$$

From the above expressions, $r_a = r_b = r$, for an active DFB coupler. Expressing the general solution (3.2.3) and (3.2.4) in terms of the reflectivities r_a and r_b yields:

$$A(\zeta) = A_1 e^{i\overline{q}\zeta} + r_a B_2 e^{-i\overline{q}\zeta} \tag{4.1.7}$$

$$B(\zeta) = r_b A_1 e^{i\overline{q}\zeta} + B_2 e^{-i\overline{q}\zeta}. \tag{4.1.8}$$

Applying the lasing boundary conditions to (4.1.8) yields:

$$0 = r_b A_1 e^{i\overline{q}} + B_2 e^{-i\overline{q}}$$

$$B_2 = -r_b A_1 e^{2i\overline{q}}. \tag{4.1.9}$$

Applying lasing boundary conditions to (4.1.7) and using (4.1.9) yields:

$$\begin{aligned} 0 &= A_1 + r_a B_2 \\ 0 &= A_1 + r_a(-r_b A_1 e^{2i\overline{q}}) \\ 0 &= A_1(1 - r_a r_b e^{2i\overline{q}}) \\ r_a r_b e^{2i\overline{q}} &= 1. \end{aligned} \tag{4.1.10}$$

Since in the case of a DFB coupler, $r_a = r_b$, the above expression simplifies down to:

$$r^2 e^{2i\overline{q}} = 1. \tag{4.1.11}$$

This equation will be used later when deriving the trancendental eigenvalue equation for the active DFB resonator.

4.1.5 Transcendental Eigenvalue Equation

The coupled-mode equation for the forward propagating mode as mentioned previously, is expressed as:

$$\frac{dA}{d\zeta} = i(\overline{\Delta\beta} - i\overline{g}/2)A + i\overline{\kappa}B.$$

Applying the lasing boundary conditions to the general solution for these coupled-mode equations, and substituting the resulting expressions (4.1.1) and (4.1.2) in the

above coupled-mode equation:

$$\frac{d}{d\zeta}\{A_1(e^{i\overline{q}\zeta} - e^{-i\overline{q}\zeta})\} = i(\overline{\Delta\beta} - i\frac{\overline{g}}{2})\{A_1(e^{i\overline{q}\zeta} - e^{-i\overline{q}\zeta})\} + i\overline{\kappa}B_1 e^{i\overline{q}}(e^{i\overline{q'}\zeta - i\overline{q}} - e^{-i\overline{q}\zeta + i\overline{q}}).$$

Differentiating the above equation:

$$\begin{aligned}
i\overline{q}A_1\{e^{i\overline{q}\zeta} + e^{-i\overline{q}\zeta}\} + A_1(-i\overline{\Delta\beta} - \frac{\overline{g}}{2})\{e^{i\overline{q}\zeta} - e^{-i\overline{q}\zeta}\} \\
= i\overline{\kappa}B_1 e^{i\overline{q}}\{e^{i\overline{q}\zeta - i\overline{q}} - e^{-i\overline{q}\zeta + i\overline{q}}\} \\
i\overline{q}A_1\{e^{i\overline{q}\zeta} + e^{-i\overline{q}\zeta}\} + A_1(-i\overline{\Delta\beta} - \frac{\overline{g}}{2})\{e^{i\overline{q}\zeta} - e^{-i\overline{q}\zeta}\} \\
= i\overline{\kappa}(\pm A_1 e^{-i\overline{q}})e^{i\overline{q}}\{e^{i\overline{q}\zeta - i\overline{q}} - e^{-i\overline{q}\zeta + i\overline{q}}\} \\
i\overline{q}A_1\{e^{i\overline{q}\zeta} + e^{-i\overline{q}\zeta}\} + A_1(-i\overline{\Delta\beta} - \frac{\overline{g}}{2})\{e^{i\overline{q}\zeta} - e^{-i\overline{q}\zeta}\} \\
= i\overline{\kappa}(\pm A_1)\{e^{i\overline{q}\zeta - i\overline{q}} - e^{-i\overline{q}\zeta + i\overline{q}}\}.
\end{aligned}$$

Equating coefficients of $e^{i\overline{q}\zeta}$ and taking the positive value yields:

$$(i\overline{q})A_1 + (-i\overline{\Delta\beta} - \overline{g}/2)A_1 = \pm i\overline{\kappa}A_1 e^{-i\overline{q}}. \tag{4.1.12}$$

Equating coefficients of $e^{-i\overline{q}\zeta}$ and taking the negative value yields:

$$(i\overline{q})A_1 - (-i\overline{\Delta\beta} - \overline{g}/2)A_1 = \mp i\overline{\kappa}A_1 e^{-i\overline{q}}. \tag{4.1.13}$$

The coupled-mode equation for the backward propagating mode as mentioned previously, is expressed as:

$$\frac{-dB}{d\zeta} = i(\overline{\Delta\beta} - i\overline{g}/2)B + i\overline{\kappa}A.$$

Applying the lasing boundary conditions to the general solution for the coupled-mode equations, and substituting the resulting expressions (4.1.1) and (4.1.2) in the above equation yields:

$$\frac{-d}{d\zeta}B_1 e^{i\overline{q}}(e^{i\overline{q}\zeta - i\overline{q}} - e^{-i\overline{q}\zeta + i\overline{q}}) = i(\overline{\Delta\beta} - i\frac{\overline{g}}{2})B_1 e^{i\overline{q}}(e^{i\overline{q}\zeta - i\overline{q}} - e^{-i\overline{q}\zeta + i\overline{q}}) + i\overline{\kappa}A_1(e^{i\overline{q}\zeta} - e^{-i\overline{q}\zeta}).$$

Differentiating the above equation yields:

$$\begin{aligned}
-i\overline{q}B_1 e^{i\overline{q}}\{e^{i\overline{q}\zeta - i\overline{q}} + e^{-i\overline{q}\zeta + i\overline{q}}\} + (i\overline{\Delta\beta} - \frac{\overline{g}}{2})B_1 e^{i\overline{q}}\{e^{i\overline{q}\zeta - i\overline{q}} - e^{-i\overline{q}\zeta + i\overline{q}}\} \\
= i\overline{\kappa}A_1\{e^{i\overline{q}\zeta} - e^{-i\overline{q}\zeta}\} \\
-i\overline{q}B_1 e^{i\overline{q}}\{e^{i\overline{q}\zeta - i\overline{q}} + e^{-i\overline{q}\zeta + i\overline{q}}\} + (i\overline{\Delta\beta} - \frac{\overline{g}}{2})B_1 e^{i\overline{q}}\{e^{i\overline{q}\zeta - i\overline{q}} - e^{-i\overline{q}\zeta + i\overline{q}}\} \\
= i\overline{\kappa}(\pm B_1 e^{i\overline{q}})\{e^{i\overline{q}\zeta} - e^{-i\overline{q}\zeta}\} \\
-i\overline{q}B_1\{e^{i\overline{q}\zeta - i\overline{q}} + e^{-i\overline{q}\zeta + i\overline{q}}\} + (i\overline{\Delta\beta} - \frac{\overline{g}}{2})B_1\{e^{i\overline{q}\zeta - i\overline{q}} - e^{-i\overline{q}\zeta + i\overline{q}}\} \\
= \pm i\overline{\kappa}B_1\{e^{i\overline{q}\zeta} - e^{-i\overline{q}\zeta}\}.
\end{aligned}$$

Equating coefficients of $e^{i\overline{q}\zeta}$ and taking the positive value yields:

$$\begin{aligned}
(-i\overline{q})B_1\{e^{-i\overline{q}}\} + (i\overline{\Delta\beta} - \overline{g}/2)B_1\{e^{i\overline{q}}\} = \pm i\overline{\kappa}B_1 \\
(-i\overline{q})B_1 + (-i\overline{\Delta\beta} - \overline{g}/2)B_1 = \pm i\overline{\kappa}B_1\{e^{-i\overline{q}}.\}
\end{aligned} \tag{4.1.14}$$

Equating coefficients of $e^{-i\overline{q}\zeta}$ and taking the negative value yields:

$$\begin{aligned}
(-i\overline{q})B_1\{e^{i\overline{q}}\} + (-i\overline{\Delta\beta} - \overline{g}/2)B_1\{e^{i\overline{q}}\} = \mp i\overline{\kappa}B_1 \\
(-i\overline{q})B_1 + (-i\overline{\Delta\beta} - \overline{g}/2)B_1 = \mp i\overline{\kappa}B_1\{e^{-i\overline{q}}\}.
\end{aligned} \tag{4.1.15}$$

Adding equations (4.1.12) and (4.1.13) or (4.1.14) and (4.1.15) yields:

$$\begin{aligned} 2(i\overline{q})A_1 &= i\overline{\kappa}A_1\{e^{-i\overline{q}} - e^{i\overline{q}}\} \\ 2(i\overline{q}) &= -i\overline{\kappa}\{e^{i\overline{q}} - e^{-i\overline{q}}\} \\ (i\overline{q}) &= \overline{\kappa}\sin\overline{q}. \end{aligned} \tag{4.1.16}$$

The above transcendental equation provides a numerical solution for the threshold modes of a DFB structure; the solutions are known as transcendental eigenvalue solutions of the coupled-mode equations [18]. This expression relates gain and the corresponding detuning at threshold as depicted in the plot below:

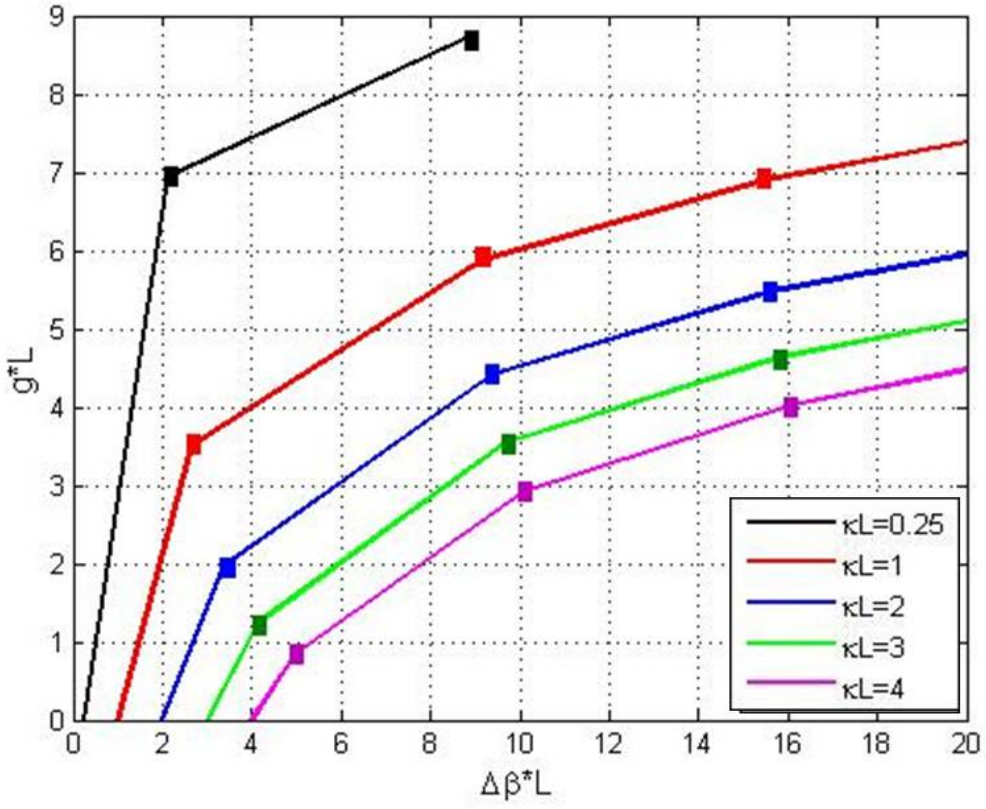

Figure 4.3: *Active DFB Resonator: Threshold gain vs Detuning.*

The longitudnal modes of an active DFB resonator can be obtained by a numerical solution of equation (4.1.16) which is explained in section three of this chapter. This solution results in the required threshold level gains and their respective detuning. Figure 4.3 depicts one side of the symmetric spectrum of the DFB structure with various modes obtained for different values of $\overline{\kappa}$. It is observed that in order to reach threshold the lowest amount of gain is required for the first mode followed by the higher modes. Thus we may conclude that modes closer to the

Bragg's wavelength are the first ones to lase. The threshold values of gain and detuning obtained from Figure 4.3 for $\overline{\kappa} = 3$ are 1.245 and 4.149 respectively. These are similar to the threshold values obtained using Figure 4.2 for $\overline{\kappa} = 3$. Hence it is possible to find the threshold values $\overline{g_{th}}$ and $\overline{\Delta\beta_{th}}$ using the T_{max} versus $\overline{g}$ plot. However, numerical solution of the transcendental eigenvalue equations makes life more easier.

4.2 NIM-PIM DC

4.2.1 Transmittivity (Lasing Behavior with increasing gain)

In this subsection, different scenarios of gain/loss based on equation (3.2.27) in one or both channels of a NIM-PIM DC are considered and their respective lasing behavior is analyzed.

Case: $\overline{\mathbf{g_p}} = \overline{\mathbf{g_n}} = \overline{\mathbf{g}}$

The first case to be analyzed includes gain in both the waveguides. We introduce equal amount of gain in both PIM and NIM channels. This case might not be practically viable but it acts as a good check for the model since the equations reduce to the expressions that govern active DFB structures.

The plot below shows behavior which matches that of a known DFB SOA.

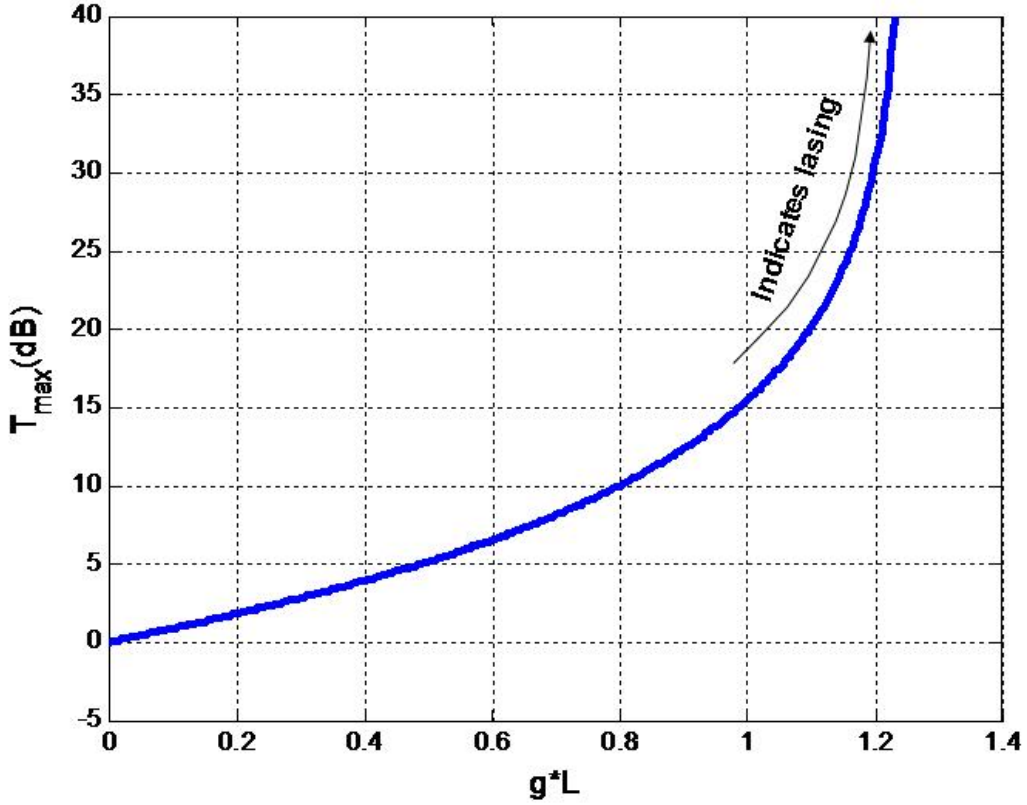

Figure 4.4: *Active NIM-PIM DC: Lasing Behavior - Same amount of gain in both PIM and NIM:* $\overline{g_p} = \overline{g_n}$, $\overline{\Delta\beta}$ *of maximum T,* $\overline{\kappa} = 3$.

In figure 4.4, the y-axis plots the maximum of transmittivity spectrum obtained for a specific value of gain while the x-axis plots increasing values of normalized gain $\overline{g}$ for $\overline{\kappa} = 3$. It is observed that maximum transmittivity T_{max} exhibits an exponential increase with increasing values of gain $\overline{g}$. As more and more gain is added to both NIM and PIM waveguides, the transmittivity peaks grow and eventually a point is reached where a very small increase increase in gain would result

in a very high peaks reaching infinity. Such behavior indicates that it is possible to achieve lasing with a NIM-PIM DC similar to that of an active DFB structure demonstrated previously in Figure 4.2. The difference being the fact that there is no grating structure and NIM provides the required feedback. It is also observed from Figure 4.4 that a threshold gain ($\overline{g_{th}}$) of 1.25 is required at $\overline{\Delta\beta} = 4.148$, and is termed as the corresponding threshold detuning ($\overline{\Delta\beta_{th}}$). We will be referring back to these threshold values in a later section.

Case: $\overline{\mathbf{g_n}} = 0$ and $\overline{\mathbf{g_p}} > 0$

Next, we consider the case where gain is introduced into the PIM waveguide only. NIM has zero gain. From Figure 3.5, it is clear that as we increase the gain, the transmittivity peaks shoot up, confirming the lasing action of a NIM-PIM DC. However, in this case more than twice the gain is required for the peaks to shoot up.

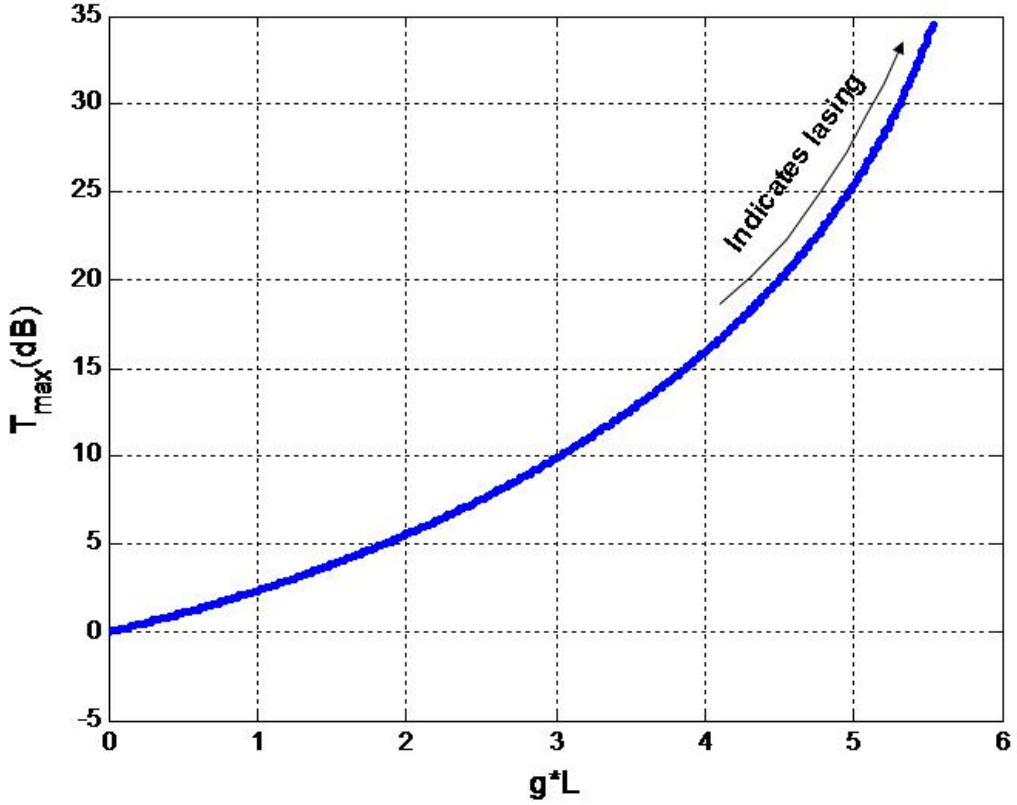

Figure 4.5: *Active NIM-PIM DC: Lasing Behavior - Gain in PIM ($\overline{g_p}$), $\overline{g_n} = 0$ and $\overline{\Delta\beta}$ of maximum T, $\overline{\kappa} = 3$.*

In Figure 4.5, the y-axis plots the maximum of transmittivity spectrum obtained for a specific value of gain while the x-axis plots increasing values of normalized gain $\overline{g}$ for $\overline{\kappa} = 3$. It is observed that maximum transmittivity T_{max} exhibits an exponential increase with increasing values of gain $\overline{g_p}$ in the PIM waveguide. As more and more gain is added, the transmittivity peaks grow and eventually a point is reached where a very small increase increase in gain would result in a very high

peaks reaching infinity. However, if we compare this case to the equal gain scenario in Figure 4.4, it is observed that a much higher amount of gain is required to reach the same level of T_{max}. Hence, we may conclude that it is possible to achieve lasing with a NIM-PIM DC where only the PIM waveguide has an increased gain. It is also observed from Figure 4.5 that a threshold gain ($\overline{g_{th}}$) of 5.625 is required at $\overline{\Delta\beta} = 3.419$, and is termed as the corresponding threshold detuning ($\overline{\Delta\beta_{th}}$). We will be referring back to these threshold values in a later section.

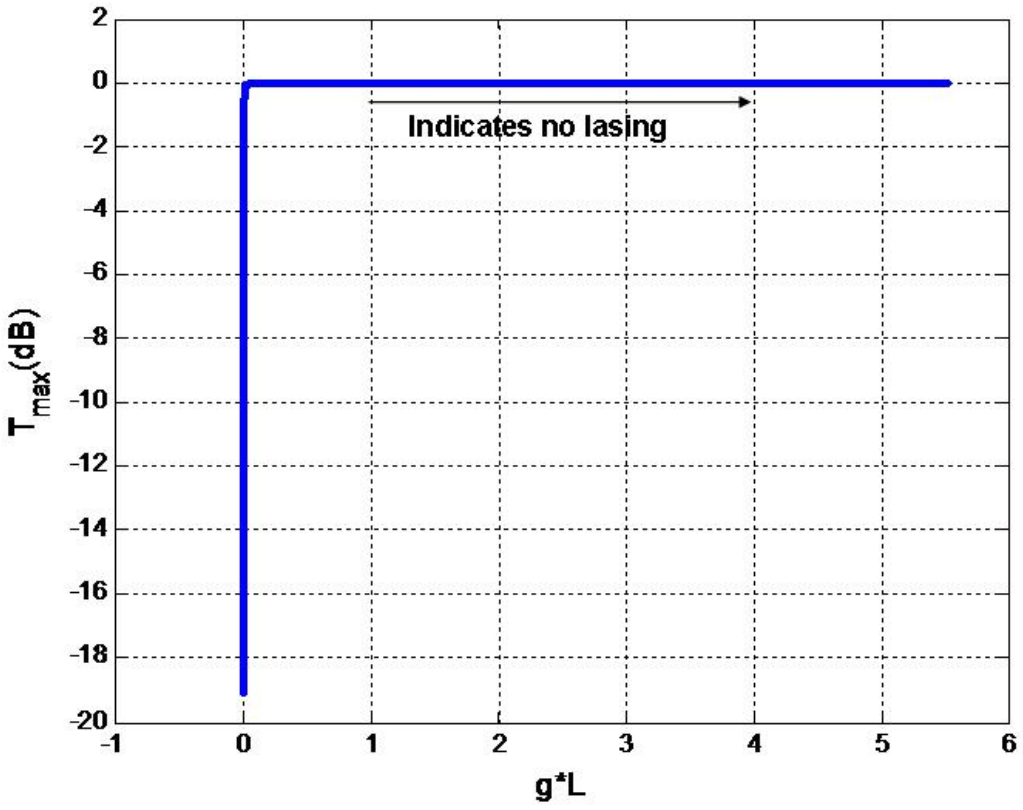

Figure 4.6: *Active NIM-PIM DC: Lasing Behavior - Gain in PIM ($\overline{g_p}$), $\overline{g_n = 0}$ and $\overline{\Delta\beta} = 0, \overline{\kappa} = 3$.*

In chapter three, Figure 3.5, a small hump was noticed at $\overline{\Delta\beta} = 0$. Here, we model this behavior for increasing values of gain and Figure 4.6 confirms the finding that no lasing is possible at $\overline{\Delta\beta} = 0$ where we have gain in PIM only and $\overline{g_n} = 0$ for $\overline{\kappa} = 3$.

Case: $\overline{g_n} < 0$, $\overline{g_p} >= |\overline{g_n}|$ and $\overline{\Delta\beta} = 0$

This scenario is very interesting. Here, we tried to model a more practical device having loss in the NIM waveguide and gain in the PIM waveguide. It was observed that a stable lasing action is achieved if the gain in PIM is equal to or greater than the absolute value of loss in NIM.

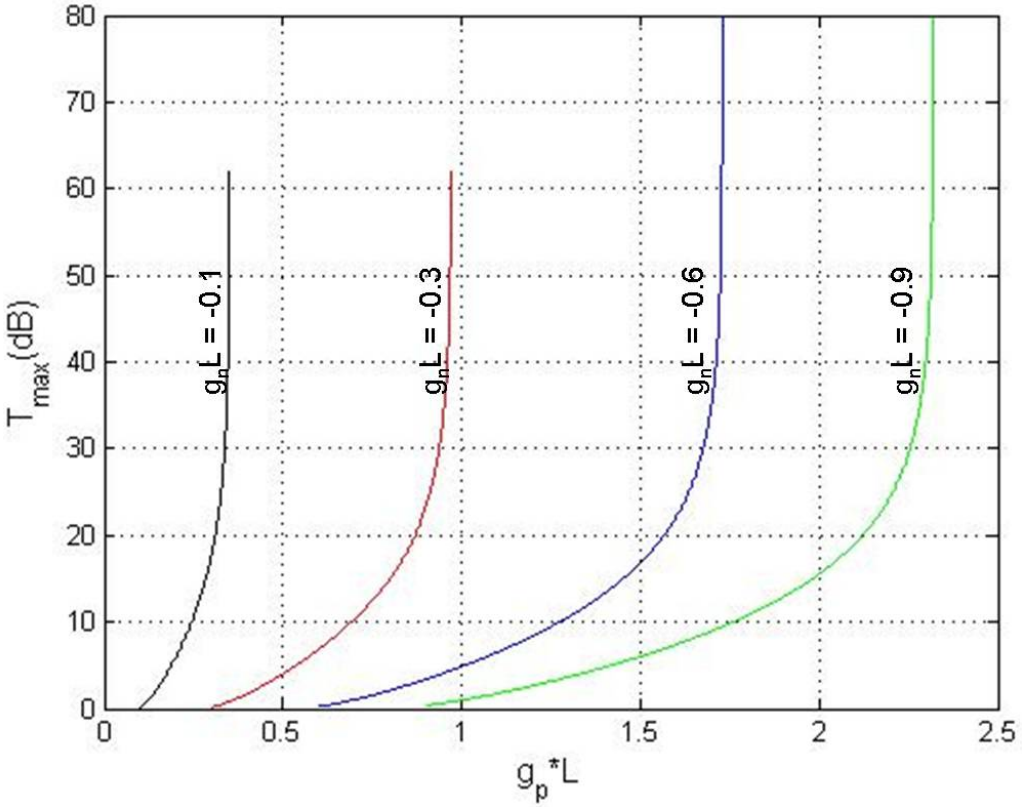

Figure 4.7: *Active NIM-PIM DC: Lasing Behavior - Losses in NIM with gain in PIM at* $\overline{\Delta\beta} = 0$ *and* $\overline{g_p} >= |\overline{g_n}|$, $\overline{\kappa} = 3$.

Figure 4.7 shows the T_{max} versus $\overline{g_p}$ for various values of $\overline{g_n}$ where $\overline{\kappa} = 3$. Notice how each curve on this plot starts off with $\overline{g_p} >= |\overline{g_n}|$ and grows upward with increasing values of $\overline{g_p}$ in the PIM waveguide. As more gain is added, the transmittivity peaks exhibit an exponential growth and eventually a point is reached where these peaks hit infinity indicating that such a device can lase. Hence, we may conclude that it is possible to achieve lasing with a NIM-PIM DC where we

have a lossy NIM while the PIM waveguide must posses gain which is either equal to or greater than the absolute value of losses in the NIM waveguide. It is also observed from Figure 4.7 that the required threshold gains ($\overline{g_{th}}$) to achieve lasing at $\overline{\Delta\beta} = 0$ for $\overline{g_n}$ = -0.1, -0.3, -0.6 and -0.9 are 0.35, 0.97, 1.73 and 2.32 respectively.

Case: $\overline{\mathbf{g_n}} < \mathbf{0}$, $\overline{\mathbf{g_p}} < |\overline{\mathbf{g_n}}|$ and $\overline{\Delta\beta} = 0$

This can be considered as an extension of the case discussed above. Here we studied what will happen if the gain in the PIM waveguide is lesser than the absolute value of loss in the NIM waveguide. A very peculiar behavior consisting of numerous longitudinal modes that can actually lase is observed.

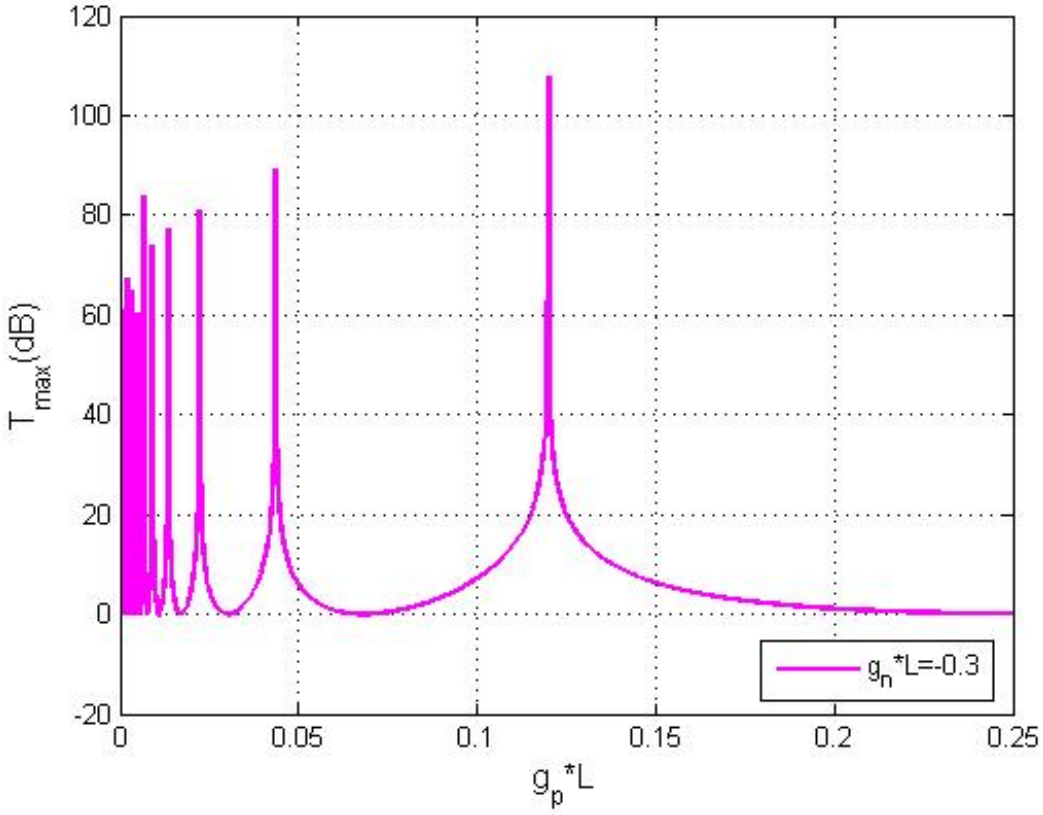

Figure 4.8: *Active NIM-PIM DC: Lasing Behavior - Losses in NIM with gain in PIM at* $\overline{\Delta\beta} = 0$ *and* $\overline{g_p} < |\overline{g_n}|$, $\overline{\kappa} = 3$.

Figure 4.8 shows the T_{max} versus $\overline{g_p}$ for various values of $\overline{g_n}$ where $\overline{\kappa} = 3$. Notice how the number of lasing modes decrease with higher values of gain $\overline{g_p}$ and the device achieves a stable lasing behavior once $\overline{g_p}$ is increased beyond $|\overline{g_n}|$.

The existence of multiple lasing modes when $\overline{\Delta\beta} = 0$ and $\overline{g_p} < |\overline{g_n}|$ can be explained by analyzing the behavior of $\overline{q'}$ at $\overline{\Delta\beta_{th}}$ for the cases where 1) $\overline{g_p} = \overline{g_n} = \overline{g}$ and $\overline{g_p} = \overline{g}$ and 2) $\overline{g_p} = \overline{g}$ and $\overline{g_n} = 0$. In the first case with equal gain in both the

waveguides, the behavior of $\overline{q'}$ at $\overline{\Delta\beta_{th}}$ with increasing values of gain is analyzed and the results are plotted in Figure 4.9. From Figure 4.9 it is observed that $\overline{q'}$ is always a complex quantity bearing both a real and imaginary part. Furthermore, $\overline{q'}$ varies over a small range.

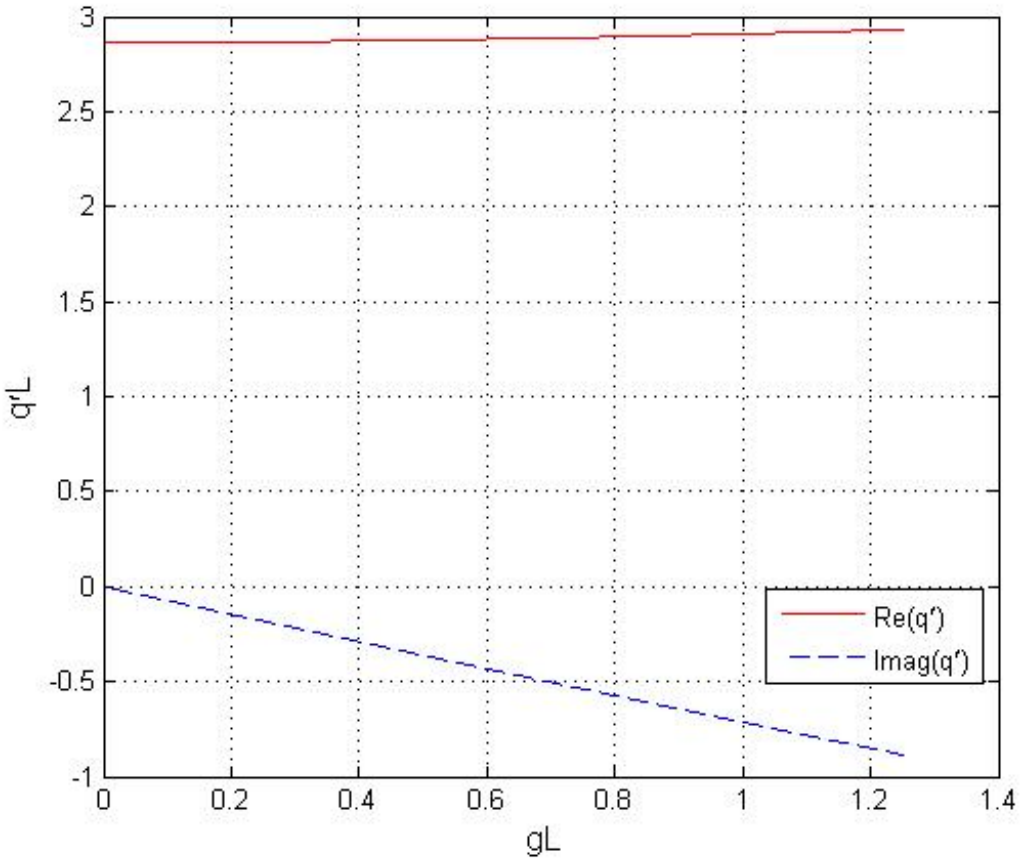

Figure 4.9: *Active NIM-PIM DC:* $\overline{q'}$ *versus increasing* $\overline{g}$ *at* $\overline{\Delta\beta_{th}} = 4.148$, $\overline{g_p} = \overline{g_n} = \overline{g}$, *and* $\overline{\kappa} = 3$.

Figure 4.10 depicts the behavior of $\overline{q'}$ at $\overline{\Delta\beta_{th}}$ when there is no gain or loss in the NIM waveguide. Notice that similar to the previous case, $\overline{q'}$ is always a complex

quantity bearing both a real and imaginary part. Furthermore, $\overline{q'}$ varies over a small range.

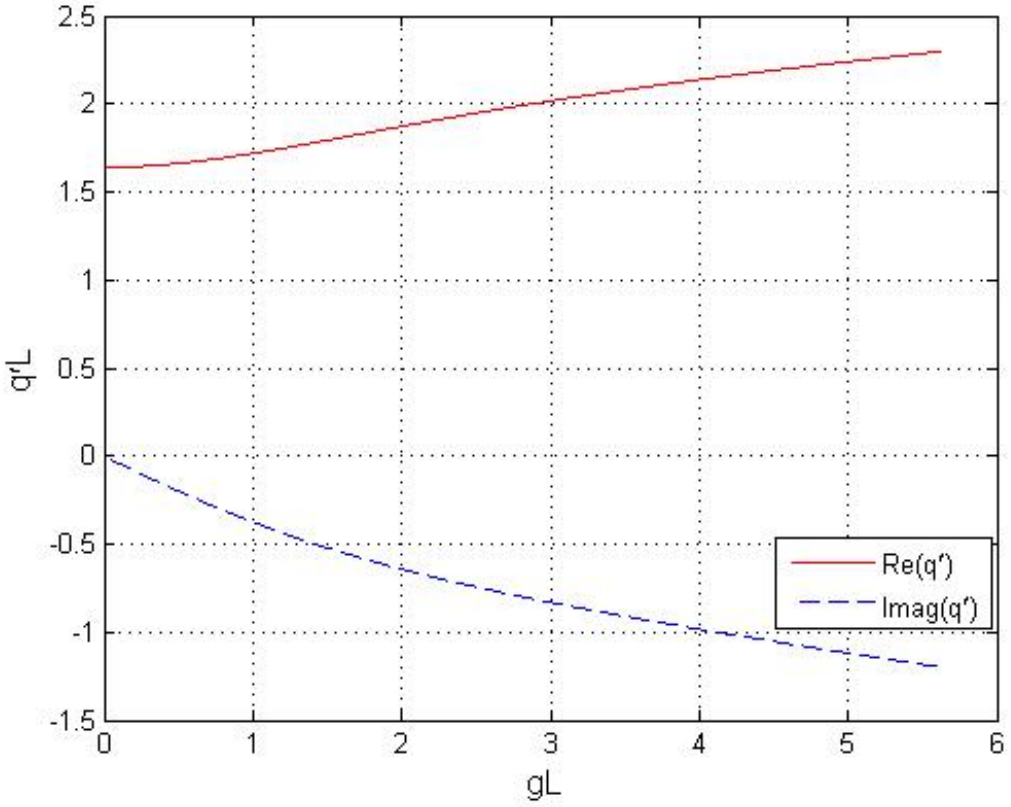

Figure 4.10: *Active NIM-PIM DC:* $\overline{q'}$ *versus increasing* $\overline{g}$ *at* $\overline{\Delta\beta_{th}} = 3.419$, $\overline{g_p} = \overline{g}$, $\overline{g_n} = 0$, *and* $\overline{\kappa} = 3$.

Figure 4.11 depicts the behavior of $\overline{q'}$ at $\overline{\Delta\beta_{th}} = 0$ when there are losses in the NIM waveguide. Figure 4.11 shows that $\overline{q'}$ is always a real quantity as opposed to the previous two cases. Besides $\overline{q'}$ being real, a huge variation is observed in its value. It is only at $\overline{g} >= |\overline{g_n}| = 0.3$ that this variation gets comparable to that of

the previous two cases and multiple lasing modes disappear.

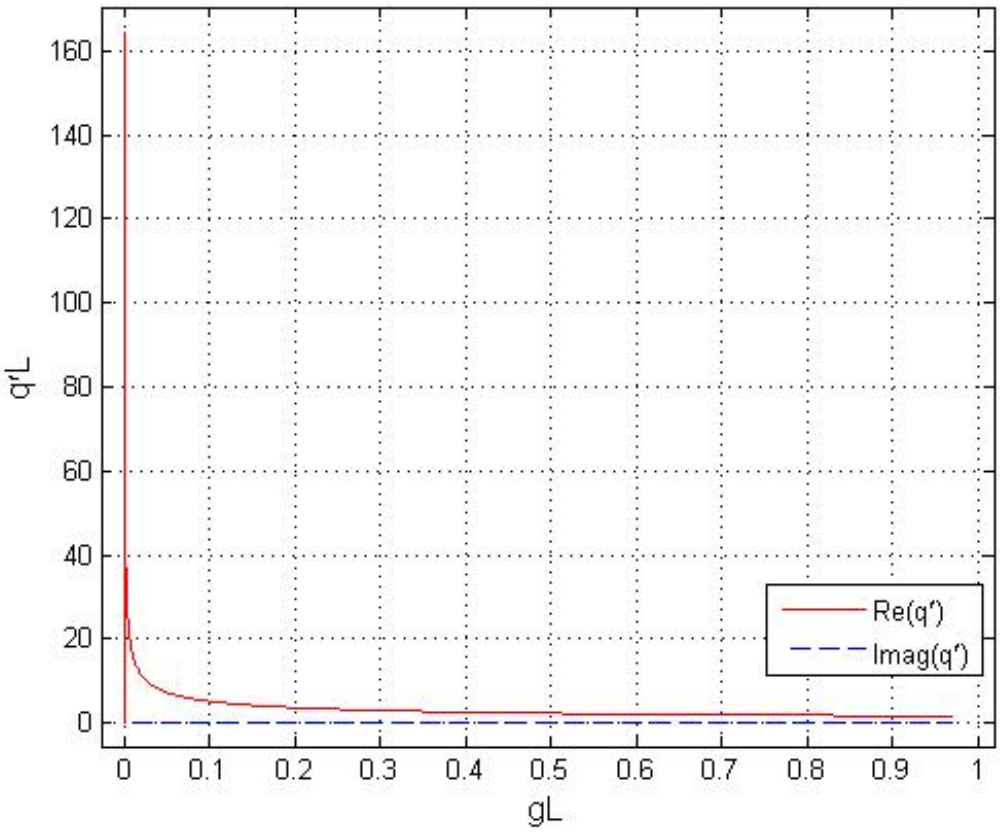

Figure 4.11: *Active NIM-PIM DC:* $\overline{q'}$ *versus increasing* $\overline{g}$ *at* $\overline{\Delta\beta_{th}} = 0$, $\overline{g_p} = \overline{g}$, $\overline{g_n} = -0.3$, *and* $\overline{\kappa} = 3$.

4.2.2 Lasing Boundary Conditions and Specific Solution

Boundary conditions for lasing a NIM PIM DC are the same as in case of a DFB structure, i.e. :

$$A(\zeta = 0) = 0$$

$$B(\zeta = 1) = 0.$$

Applying the above lasing boundary conditions to the general solution of the coupled-mode equations of a NIM-PIM DC yields:

$$A(\zeta) = A_1 e^{i\bar{q}\zeta} + A_2 e^{-i\bar{q}\zeta}$$

$$0 = A_1 + A_2$$

$$A_2 = -A_1.$$

$A(\zeta)$ can now be expressed as:

$$A(\zeta) = A_1 e^{i\bar{q}\zeta} - A_1 e^{-i\bar{q}\zeta}$$

$$A(\zeta) = A_1 (e^{i\bar{q}\zeta} - e^{-i\bar{q}\zeta}). \tag{4.2.1}$$

Similarly applying the boundary conditions to $B(\zeta)$ yields:

$$B(\zeta) = B_1 e^{i\overline{q'}\zeta} + B_2 e^{-i\overline{q'}\zeta}$$

$$0 = B_1 e^{i\overline{q'}} + B_2 e^{-i\overline{q'}}$$

$$B_2 = -B_1 e^{2i\overline{q'}}.$$

Substituting the above expression for B_2 into the general expression (3.2.4) for $B(\zeta)$ yields:

$$B(\zeta) = B_1 e^{i\overline{q'}\zeta} + B_2 e^{-i\overline{q'}\zeta}$$

$$B(\zeta) = B_1 e^{i\overline{q'}\zeta} + (-B_1 e^{2i\overline{q'}}) e^{-i\overline{q'}\zeta}$$

$$B(\zeta) = B_1 (e^{i\overline{q'}\zeta} - e^{2i\overline{q'} - i\overline{q'}\zeta})$$

$$B(\zeta) = B_1 e^{i\overline{q'}} (e^{i\overline{q'}\zeta - i\overline{q'}} - e^{-i\overline{q'}\zeta + i\overline{q'}}). \tag{4.2.2}$$

4.2.3 Effective Reflectivity Coefficients

Expressions for the reflectivities encountered by the forward and backward propagating waves can be derived using (3.2.13), (3.2.14), (3.2.15) and (3.2.16).

$$r_a = \frac{B_1}{A_1} = \frac{\overline{q} - \overline{\Delta\beta} + i\overline{g_p}/2}{\overline{\kappa}}. \tag{4.2.3}$$

$$r_a = \frac{B_1}{A_1} = \frac{-\overline{\kappa}}{\overline{q'} + \overline{\Delta\beta} - i\overline{g_n}/2}. \tag{4.2.4}$$

$$r_b = \frac{A_2}{B_2} = \frac{\overline{q'} - \overline{\Delta\beta} + i\overline{g_n}/2}{\overline{\kappa}}. \tag{4.2.5}$$

$$r_b = \frac{A_2}{B_2} = \frac{-\overline{\kappa}}{\overline{q} + \overline{\Delta\beta} - i\overline{g_p}/2}. \tag{4.2.6}$$

where r_a is the effective reflectivity of the forward-propagating mode while r_b indicates that of the backward-propagating mode.

Expressing the general solution in terms of the reflectivities r_a and r_b yields:

$$A(\zeta) = A_1 e^{i\overline{q}\zeta} + r_a B_2 e^{-i\overline{q}\zeta} \tag{4.2.7}$$

$$B(\zeta) = r_b A_1 e^{i\overline{q'}\zeta} + B_2 e^{-i\overline{q'}\zeta}. \tag{4.2.8}$$

Applying the above mentioned boundary condition to (4.2.8) yields:

$$0 = r_b A_1 e^{i\overline{q'}} + B_2 e^{-i\overline{q'}}$$

$$B_2 = -r_b A_1 e^{2i\overline{q'}}. \tag{4.2.9}$$

Applying boundary conditions to (4.2.7) and using (4.2.9) yields:

$$0 = A_1 + r_a B_2$$

$$0 = A_1 + r_a(-r_b A_1 e^{2i\overline{q'}})$$

$$0 = A_1(1 - r_a r_b e^{2i\overline{q'}})$$

$$r_a r_b e^{2i\overline{q'}} = 1. \tag{4.2.10}$$

Expression (4.2.10) is different from the one obtained for an active DFB structure (4.1.11). It involves r_a, r_b which are not always the same, and $\overline{q'}$ which is different from $\overline{q}$ for an asymmetric system. For an active NIM-PIM DC r_a is only equal to r_b when both NIM and PIM have the same amount of optical gain. The fact that r_a is not always equal to r_b lends a complexity to the process when we derive the transcendental eigenvalue equations for an active NIM-PIM DC in a later section of the chapter.

4.2.4 Transcendental Eigenvalue Equations

The coupled-mode equation for a PIM waveguide as mentioned previously, is expressed as:

$$\frac{dA}{d\zeta} = i(\overline{\Delta\beta} - i\overline{g_p}/2)A + i\overline{\kappa}B.$$

Applying the lasing boundary conditions to the general solution for the coupled mode equations of an active NIM-PIM DC, equations (4.2.1) and (4.2.2) are obtained. By substituting these two expressions in the above coupled-mode equation yields:

$$\frac{d}{d\zeta}\{A_1(e^{i\overline{q}\zeta} - e^{-i\overline{q}\zeta})\} = i(\overline{\Delta\beta} - i\frac{\overline{g_p}}{2})A_1(e^{i\overline{q}\zeta} - e^{-i\overline{q}\zeta}) + i\overline{\kappa}B_1e^{i\overline{q'}}(e^{i\overline{q'}\zeta - i\overline{q'}} - e^{-i\overline{q'}\zeta + i\overline{q'}})$$

$$(i\overline{q})A_1\{e^{i\overline{q}\zeta} + e^{-i\overline{q}\zeta}\} + A_1(-i\overline{\Delta\beta} - \frac{\overline{g_p}}{2})\{e^{i\overline{q}\zeta} - e^{-i\overline{q}\zeta}\} = i\overline{\kappa}B_1e^{i\overline{q'}}\{e^{i\overline{q'}\zeta - i\overline{q'}} - e^{-i\overline{q'}\zeta + i\overline{q'}}\}$$

$$(i\overline{q})A_1\{e^{i\overline{q'}\zeta - i\overline{q'}H\zeta} + e^{-i\overline{q'}\zeta + i\overline{q'}H\zeta}\} + A_1(-i\overline{\Delta\beta} - \frac{\overline{g_p}}{2})\{e^{i\overline{q'}\zeta - i\overline{q'}H\zeta} - e^{-i\overline{q'}\zeta + i\overline{q'}H\zeta}\}$$

$$= i\overline{\kappa}B_1e^{i\overline{q'}}\{e^{i\overline{q'}\zeta - i\overline{q'}} - e^{-i\overline{q'}\zeta + i\overline{q'}}\}.$$

Equating coefficients of $e^{i\overline{q'}\zeta}$ yields:

$$(i\overline{q})A_1\{e^{-i\overline{q'}H\zeta}\} + A_1(-i\overline{\Delta\beta} - \frac{\overline{g_p}}{2})\{e^{-i\overline{q'}H\zeta}\} = i\overline{\kappa}B_1e^{i\overline{q'}}\{e^{-i\overline{q'}}\}$$

$$(i\overline{q})A_1 + A_1(-i\overline{\Delta\beta} - \frac{\overline{g_p}}{2}) = i\overline{\kappa}B_1e^{i\overline{q'}}\{e^{-i\overline{q'} + i\overline{q'}H\zeta}\}. \quad (4.2.11)$$

Equating coefficients of $e^{-i\overline{q'}\zeta}$ yields:

$$(i\overline{q})A_1\{e^{i\overline{q'}H\zeta}\} - A_1(-i\overline{\Delta\beta} - \frac{\overline{g_p}}{2})\{e^{i\overline{q'}H\zeta}\} = -i\overline{\kappa}B_1e^{i\overline{q'}}\{e^{i\overline{q'}}\}$$

$$(i\overline{q})A_1 - A_1(-i\overline{\Delta\beta} - \frac{\overline{g_p}}{2}) = -i\overline{\kappa}B_1e^{i\overline{q'}}\{e^{i\overline{q'} - i\overline{q'}H\zeta}\}. \quad (4.2.12)$$

Adding equations (4.2.10) and (4.2.12) yields:

$$2(i\overline{q})A_1 = i\overline{\kappa}B_1 e^{i\overline{q'}}\{e^{-i\overline{q'}+i\overline{q'}H\zeta} - e^{i\overline{q'}-i\overline{q'}H\zeta}\}$$

$$2(i\overline{q})A_1 = -i\overline{\kappa}B_1 e^{i\overline{q'}}\{e^{i\overline{q'}-i\overline{q'}H\zeta} - e^{-i\overline{q'}+i\overline{q'}H\zeta}\}$$

$$(i\overline{q}) = \overline{\kappa}\frac{B_1}{A_1}e^{i\overline{q'}}\sin\{\overline{q'} - \overline{q'}H\zeta\}. \tag{4.2.13}$$

The coupled-mode equation for a NIM waveguide as mentioned previously is expressed as:

$$\frac{-dB}{d\zeta} = i(\overline{\Delta\beta} - i\overline{g_n}/2)B + i\overline{\kappa}A.$$

Applying the lasing boundary conditions to the general solution of an active NIM-PIM DC, equations (4.2.1) and (4.2.2) are obtained. By substituting these two expressions in the above coupled-mode equation for NIM yields:

$$\frac{-d}{d\zeta}B_1 e^{i\overline{q'}}(e^{i\overline{q'}\zeta - i\overline{q'}} - e^{-i\overline{q'}\zeta + i\overline{q'}}) = i(\overline{\Delta\beta} - i\frac{\overline{g_n}}{2})B_1 e^{i\overline{q'}}(e^{i\overline{q'}\zeta - i\overline{q'}} - e^{-i\overline{q'}\zeta + i\overline{q'}}) + i\overline{\kappa}A_1(e^{i\overline{q}\zeta} - e^{-i\overline{q}\zeta}).$$

Differentiating the above expression yields:

$$(-i\overline{q'})B_1 e^{i\overline{q'}}\{e^{i\overline{q'}\zeta - i\overline{q'}} + e^{-i\overline{q'}\zeta + i\overline{q'}}\} + (i\overline{\Delta\beta} - \frac{\overline{g_n}}{2})B_1 e^{i\overline{q'}}\{e^{i\overline{q'}\zeta - i\overline{q'}} - e^{-i\overline{q'}\zeta + i\overline{q'}}\}$$
$$= i\overline{\kappa}A_1\{e^{i\overline{q}\zeta} - e^{-i\overline{q}\zeta}\}$$

$$(-i\overline{q'})B_1 e^{i\overline{q'}}\{e^{i\overline{q'}\zeta - i\overline{q'}} + e^{-i\overline{q'}\zeta + i\overline{q'}}\} + (i\overline{\Delta\beta} - \frac{\overline{g_n}}{2})B_1 e^{i\overline{q'}}\{e^{i\overline{q'}\zeta - i\overline{q'}} - e^{-i\overline{q'}\zeta + i\overline{q'}}\}$$
$$= i\overline{\kappa}A_1\{e^{i\overline{q}\zeta} - e^{-i\overline{q}\zeta}\}$$

$$(-i\overline{q'})B_1 e^{i\overline{q'}}\{e^{i\overline{q'}\zeta - i\overline{q'}} + e^{-i\overline{q'}\zeta + i\overline{q'}}\} + (i\overline{\Delta\beta} - \frac{\overline{g_n}}{2})B_1 e^{i\overline{q'}}\{e^{i\overline{q'}\zeta - i\overline{q'}} - e^{-i\overline{q'}\zeta + i\overline{q'}}\}$$
$$= i\overline{\kappa}A_1\{e^{i\overline{q'}\zeta - i\overline{q'}H\zeta} - e^{-i\overline{q}\zeta + i\overline{q'}H\zeta}\}.$$

Equating coefficients of $e^{i\overline{q'}\zeta}$ yields:

$$\begin{aligned}
-i\overline{q'}B_1e^{i\overline{q'}}\{e^{-i\overline{q'}}\} + (i\overline{\Delta\beta} - \frac{\overline{g_n}}{2})B_1e^{i\overline{q'}}\{e^{-i\overline{q'}}\} &= i\overline{\kappa}A_1\{e^{-i\overline{q'}H\zeta}\} \\
-i\overline{q'}B_1e^{i\overline{q'}} + (i\overline{\Delta\beta} - \frac{\overline{g_n}}{2})B_1e^{i\overline{q'}} &= i\overline{\kappa}A_1\{e^{-i\overline{q'}H\zeta+i\overline{q'}}\} \\
-i\overline{q'}B_1 + (i\overline{\Delta\beta} - \frac{\overline{g_n}}{2})B_1 &= i\overline{\kappa}A_1e^{-i\overline{q'}}\{e^{-i\overline{q'}H\zeta+i\overline{q'}}\}. \quad (4.2.14)
\end{aligned}$$

Equating coefficients of $e^{-i\overline{q'}\zeta}$ yields:

$$\begin{aligned}
-i\overline{q'}B_1e^{i\overline{q'}}\{e^{i\overline{q'}}\} - (i\overline{\Delta\beta} - \frac{\overline{g_n}}{2})B_1e^{i\overline{q'}}\{e^{i\overline{q'}}\} &= -i\overline{\kappa}A_1\{e^{i\overline{q'}H\zeta}\} \\
-i\overline{q'}B_1e^{i\overline{q'}} - (i\overline{\Delta\beta} - \frac{\overline{g_n}}{2})B_1e^{i\overline{q'}} &= -i\overline{\kappa}A_1\{e^{i\overline{q'}H\zeta-i\overline{q'}}\} \\
-i\overline{q'}B_1 - (i\overline{\Delta\beta} - \frac{\overline{g_n}}{2})B_1 &= -i\overline{\kappa}A_1e^{i\overline{q'}}\{e^{-i\overline{q'}H\zeta+i\overline{q'}}\}. \quad (4.2.15)
\end{aligned}$$

Adding equations (4.2.14) and (4.2.15) yields:

$$\begin{aligned}
-2(i\overline{q'})B_1 &= i\overline{\kappa}A_1e^{-i\overline{q'}}\{e^{i\overline{q'}-i\overline{q'}H\zeta} - e^{-i\overline{q'}+i\overline{q'}H\zeta}\} \\
-\overline{q'}B_1 &= i\overline{\kappa}A_1e^{-i\overline{q'}}\sin\{\overline{q'} - \overline{q'}H\zeta\} \\
i\overline{q'} &= \overline{\kappa}\frac{A_1}{B_1}e^{-i\overline{q'}}\sin\{\overline{q'} - \overline{q'}H\zeta\}. \quad (4.2.16)
\end{aligned}$$

Equations (4.2.13) and (4.2.16) are the two transcendental eigenvalue equations for an active NIM-PIM DC.

The transcendental eigenvalue equations obtained for the DFB structure and NIM-PIM DC with equal gain in both waveguides can be solved using Matlab's root finding technique. However, in the case of varying gain in both waveguides it is not possible to use the mentioned routine since such a scenario involves more

than one unknown variable and no such routines are readily available for finding roots of equations with multiple unknowns. In order to overcome this problem, a technique is devised which involves the transmittivity equation (3.2.27) derived earlier in chapter three and the dispersion relation (3.2.23). The transcendental eigenvalue equation is solved numerically for the case where we have equal gain in both waveguides. This results in all possible values of $\overline{q'}$ along with the corresponding threshold values of $\overline{\Delta\beta}$ and $\overline{g_n}$. These values serve as the initial guess to our system. For lasing, the condition $T \to \infty$ or $1/T \to 0$ holds where T represents the transmittivity in equation (3.2.27). Find the minimum of $1/T$ using a matlab routine (fminsearch). The initial guess value is updated accordingly by the system with any variation in gain $(\overline{g_n})$ as it tries to find the lasing peak of the transmittivity spectrum using equation (3.2.27). The resulting modified values of $\overline{q'}$ along with the threshold values of $\overline{\Delta\beta}$ and $\overline{g_n}$ are then fed into the dispersion relation (3.2.23) for the active NIM-PIM DC and solved for threshold values of $\overline{g_p}$. Figure 4.12 indicates the threshold gain and detuning values for $\overline{g_p} = \overline{g_n}$ using the above mentioned technique. Note that the threshold values obtained for gain and detuning using this technique are the same as those obtained from Figure 4.4 indicating the accuracy of this method.

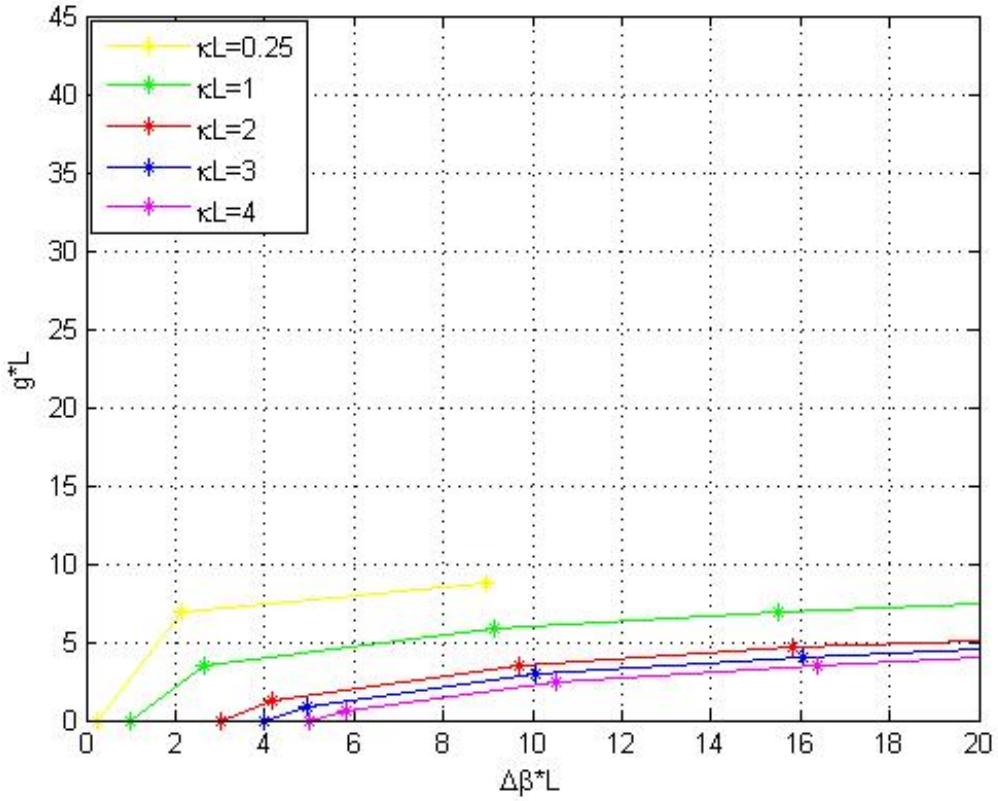

Figure 4.12: *Active NIM-PIM DC: Threshold gain vs detuning* $\overline{g_p} = \overline{g_n}$.

Figure 4.13 indicates the threshold gain and detuning values for $\overline{g_p} = \overline{g}$ and $\overline{g_n} = 0$ using the above mentioned technique. Note that the threshold values obtained for gain and detuning using this technique are similar to those obtained from Figure 4.5 indicating the accuracy of this method and that increased levels of $\overline{g_p}$ are required to achieve lasing in this case.

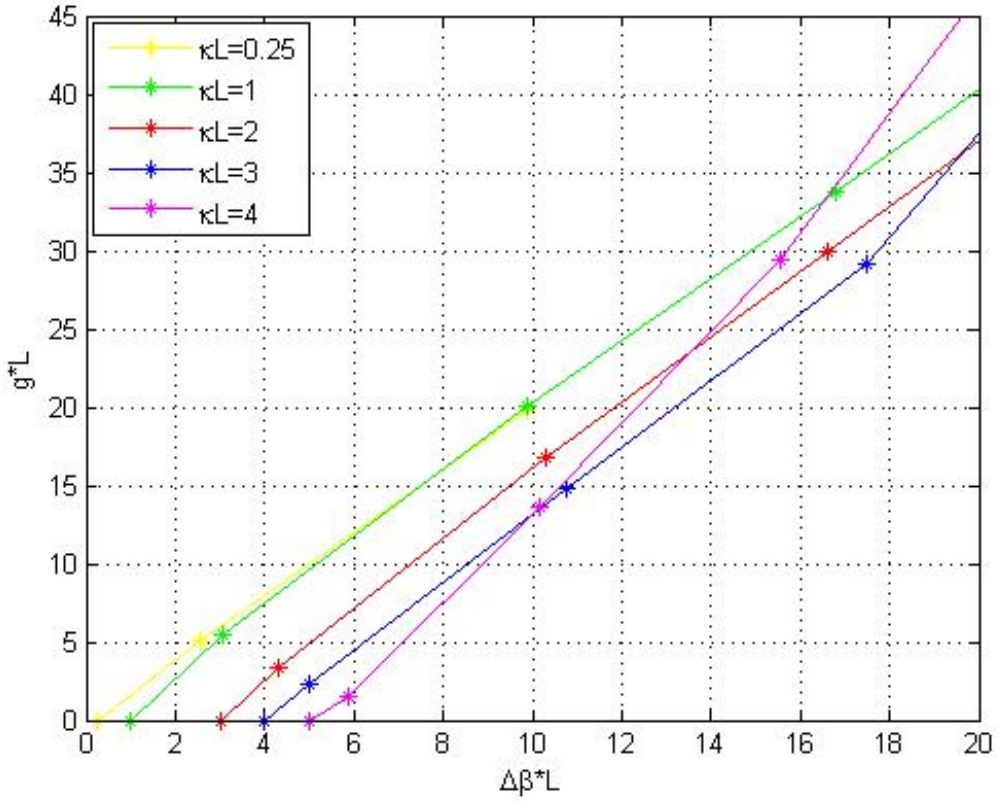

Figure 4.13: *Active NIM-PIM DC: Threshold gain vs detuning* $\overline{g_p} = \overline{g}$ *and* $\overline{g_n} = 0$.

The above technique however does not provide a feasible solution for the case where the NIM waveguide has losses. In this particular case, lasing occurs at $\overline{\Delta\beta} = 0$ and we have to manually assign $\overline{\Delta\beta} = 0$ in order for the system to converge at a correct solution.

4.3 SUMMARY OF STEPS

Active DFB Resonator - Effective Reflectivities

1. Define $r_a = \frac{B_1}{A_1}$ and $r_b = \frac{A_2}{B_2}$ (derived using expressions (3.1.5), (3.1.6), (3.1.7) and (3.1.8)).
2. Modify the general solution in terms of r_a and r_b e.g. equations (4.1.7) and (4.1.8).
3. Apply laser boundary conditions to the modified general solution and solve for B_2 e.g. equations (4.1.7), (4.1.8) and (4.1.9).
4. Plug in the value of B_2 in the modified solution for $A(\zeta)$ with boundary conditions applied and simplify to yield an expression for r_a and r_b. For a DFB resonator $r_a = r_b$ e.g. equation (4.1.11).

Active DFB Resonator - Transcendental Eigenvalue Equation

1. Apply the laser boundary conditions on both forward and backward traveling modes resulting in modified expression for $A(\zeta)$ and $B(\zeta)$ e.g. equations (4.1.1) and (4.1.2).
2. Plug this modified expression of A and B in the coupled-mode equation for the forward traveling mode e.g. equations (4.1.1) and (4.1.2) in (3.1.1).
3. Differentiate the resulting expression. Replace A_1 by $\pm B_1 e^{i\overline{q}}$ (obtained from effective reflectivity) and simplify accordingly.

4. Equate coefficients of $e^{i\overline{q}\zeta}$ and take the positive value e.g. equation (4.1.12).
5. Equate coefficients of $e^{-i\overline{q}\zeta}$ and take the negative value e.g. equation (4.1.13).
6. Add these two equations which results in required equation e.g. equation (4.1.16).
7. Repeat all of the above steps for coupled-mode equation of the backward traveling mode.
8. Similar results are obtained.

Active DFB Resonator - Lasing Thresolds (Numerical Solution)

1. Using root finding technique, find all possible roots of $\overline{q}$ for one fixed value of $\overline{\kappa}$.
2. Substitute each value of $\overline{q}$ in the dispersion relation to find $\overline{\Delta\beta}$ and $\overline{g}$.
3. The real part of this solution finds the threshold $\overline{g}$ while the imaginary part calculate the corresponding $\overline{\Delta\beta}$ at threshold.

Active NIM PIM DC - Effective Reflectivities

1. Define $r_a = \frac{B_1}{A_1}$ and $r_b = \frac{A_2}{B_2}$, using the relations obtained in chapter three while deriving the dispersion relation e.g. equations (3.2.13), (3.2.14), (3.2.15) and (3.2.16).
2. Modify the general solution in terms of r_a and r_b e.g. equations (4.2.7) and

(4.2.8).

3. Apply laser boundary conditions to the modified general solution and solve for B_2 e.g. equations (4.2.7), (4.2.8) and (4.2.10).
4. Plug in the value of B_2 and simplify to yield an expression for r_a and r_b e.g. (4.2.10). In this case $r_a = r_b$ only when the two waveguides have identical gain.

Active NIM PIM DC - Transcendental Eigenvalue Equation

1. Apply the laser boundary conditions to both forward and backward traveling modes resulting in modified expression for $A(\zeta)$ and $B(\zeta)$ e.g. equations (4.2.1) and (4.2.2).
2. Plug the modified expressions of A and B in the coupled-mode equation for PIM waveguide. e.g. equations (4.2.1) and (4.2.2) in (3.2.1).
3. Differentiate the resulting expression. Replace the exponentials involving $\overline{q}$ in terms of $\overline{q'}$.
4. Equate coefficients of $e^{i\overline{q'}\zeta}$ e.g. equation (4.2.10).
5. Equate coefficients of $e^{-i\overline{q'}\zeta}$ e.g. equations (4.2.12).
6. Add these two equations which results in a transcendental equation e.g. equations (4.2.10), (4.2.12) and (4.2.13).
7. Repeat all of the above steps for coupled-mode equation of the NIM waveg-

uide which results in equation (4.2.16).

References

[1] Evgenii E. Narimanov, Vladimir M. Shalaev, and Azriel Z. Genack, “Photonic Metamaterials: Introduction," J. Opt. Soc. Am. A 24, PM1-PM2 (2007)

[2] W. Cai and V. Shalaev, “Optical Metamaterials: Fundamentals and Applications," (Springer-2010), 2-3.

[3] M. Kafesaki, R. Penciu, Th. Koschny, N. H. Shen, D. Guney, J. Zhou, E. N. Economou and C. M. Soukoulis , “Optical metamaterials: Possibilities and limitations," Mesoscopic Physics in Complex Media 01011 (2010): 411, accessed March 20, 2011, doi:10.1051/iesc/2010mpcm01011.

[4] Alexander K. Popov and Vladimir M. Shalaev, “Compensating losses in negative-index metamaterials by optical parametric amplification," Opt. Lett. 31, 2169-2171 (2006).

[5] V. G. Veselago, “The electrodynamics of substances with simultaneously negative values of ϵ and μ," Sov. Phys. Usp. 10, 509 (1968).

[6] J. B. Pendry, “Negative refraction makes a perfect lens," Phys. Rev. Lett. 85, 3966 (2000).

[7] A. Alu and N. Engheta, in Negative-Refraction Metamaterials, edited by G.V. Eleftheriades and K. G. Balmain (Wiley, New York, 2005).

[8] M. Litchinitser, I. R. Gabitov, A. I. Maimistov, “Optical bistability in a nonlinear optical coupler with a negative-index channel," Physical Review Letters 99, pp 113902 (2007).

[9] A. K. Popov, S. A. Myslivets, and V. M. Shalaev, “Resonant nonlinear optics of backward waves in negative-index metamaterials," Appl. Phys. B: Photophys. Laser Chem. 96, 315 323 (2009).

[10] Gines Lifante, “Integrated Photonics: Fundamentals," (Wiley-2003), 52-60.

[11] Gines Lifante, “Integrated Photonics: Fundamentals," (Wiley-2003), 98-110.

[12] Mynbaev and Scheiner, “Fiber Optic Communications Technology," (Prentice Hall-2001), 586-589.

[13] G.P Agrawal, “Lightwave Technology," (Wiley-2004), Chapter 2.

[14] Alu and Engheta, “Negative-Refraction Metamaterials," (Wiley-2005), Chapter 9.

[15] N. M. Litchinitser, I. Gabitov, A. Maimistov, “Optical Bistability in a Nonlinear Optical Coupler with a Negative Index Channel," PRL 99 113902, (2007).

[16] G.P Agrawal and N.K. Dutta, “Semiconductor Lasers," (Springer-Verlag-1993), Chapter 7.

[17] Mynbaev and Scheiner, “Fiber Optic Communications Technology," (Prentice Hall-2001), 342-343.

[18] H. Kogelnik and C. V. Shank, “Coupled-wave theory of distributed feedback lasers," J. Appl. Phys. 43, 2327-2335 (1972).